Universidade de Lisboa

Faculdade de Farmácia

Departamento de Química Farmacêutica e Terapêutica

Development of new technoçogies for the selective removal of volatile compounds with applications in forensic science and natural aromas

José Augusto Faria Sineiro Restolho

Doutoramento em Farmácia

Especialidade em Química Farmacêutica e Terapêutica

2015

Universidade de Lisboa

Faculdade de Farmácia

Departamento de Química Farmacêutica e Terapêutica

Development of new technoçogies for the selective removal of volatile compounds with applications in forensic science and natural aromas

José Augusto Faria Sineiro Restolho

Tese orientada pelo Professor Doutor Carlos Alberto Mateus Afonso e coorientada pela Professora Doutora Benilde de Jesus Vieira Saramago e pelo Doutor Mário Jorge Dinis Barroso, especialmente elaborada para a obtenção do grau de doutor no ramo de Farmácia, especialidade de Química Farmacêutica e Terapêutica.

Deus quer, o homem sonha, a obra nasce…

In Mensagem, Fernando Pessoa

Um ponto que está no círculo e se coloca
no quadrado e no triângulo: conheces este ponto?
Tudo irá bem. Não o conheces? Tudo será em vão

Sobre o ponto de Bauhütte, Mössel

Resumo

O aumento da consciencialização sobre os problemas ambientais, levou a um aumento da procura por métodos mais "amigos" do ambiente nos diversos campos da ciência, estando focados sobretudo nos processos que dispensam a utilização de solventes. Nós encontramos dois bom exemplos nas áreas da toxicologia forense e da extração de compostos naturais, onde os solventes ainda são sobejamente utilizados.

Nos últimos vinte anos, o cabelo ganhou grande relevância enquanto amostra toxicológica, nomeadamente no campo das drogas de abuso. Ainda que esta matriz permita a detecção deste tipo de compostos após semanas, meses e até anos após o seu consumo, não dispensa um passo de pré lavagem (descontaminação) de forma a assegurar a ausência de drogas na superfície do cabelo. Apesar de existirem várias estratégias de descontaminação, nenhuma assegura a completa ausência de drogas da superfície do cabelo. Por outro lado, no campo da extração de compostos naturais, tem-se vindo a observar um aumento da procura de técnicas de extração mais seletivas, mais "amigas" do ambiente e com custos de operação menores e que possam ser aplicadas industrialmente.

Nestes contextos, a não volatilidade dos líquidos iónicos (ILs) tornam-nos sistemas quase ideias para a captura de diversos compostos. É possível encontrar na literatura algumas aplicações destes líquidos, nomeadamente na captura de dioxinas.

Neste trabalho apresenta-se o desenvolvimento de novas tecnologias para a remoção seletiva de compostos voláteis, com aplicação em ciências forenses (análise de cabelo, utilizando ILs) e em compostos naturais (óleos essenciais, sem utilização de ILs).

Começou-se por aplicar os ILs à descontaminação de amostras de cabelo contendo opiáceos na superfície. Testaram-se mais de quarenta ILs (100 ºC, 96 h) e o líquido tetrafluoroborato de 1-etanol-3-metilimidazólio, $[C_2OHMIM][BF_4]$, apresentou resultados bastante promissores (eficiência de extração > 80 %). De forma a reduzir o tempo de extração para menos de 24 h, o processo foi optimizado através da utilização do Desenho Experimental (DOE), e as condições finais foram 120 ºC, 16 h, e um conteúdo de água de 44 % (m/m). O método desenvolvido foi então comparado com o método proposto por Cairns e seus colaboradores (estratégia de descontaminação bastante utilizada e bastante morosa) e os resultados obtidos

mostraram que, em média, o método desenvolvido apresenta resultados ligeiramente melhores do que o outro método (% de diferença ~ 5 %). Este método foi então aplicado tanto à cocaína como aos canabinóides. No caso da cocaína, a temperatura utilizada levou à hidrólise espontânea deste composto para o seu metabolito benzoilecgonina (BZE). Infelizmente, para além de não nos ter sido possível remover a BZE da superfície do cabelo, também não conseguimos explicar o porquê deste comportamento. Quanto aos canabinóides, a triagem de ILs mostrou que estes apresentam uma elevada afinidade para os canabinóides (eficiência de extração > 90 %). Uma vez mais o líquido $[C_2OHMIM][BF_4]$ foi o IL de eleição, tendo-se optimizado o método através de DOE e as condições experimentais finais foram 100 ºC e 13 h. Quando este método foi comparado com o proposto por Cairns e os seus colaboradores, apresentou em média uma eficiência de extração superior (~20 %).

O método de descontaminação desenvolvido foi racionalizado de forma a compreender por completo o fenómeno. O estudo iniciou-se pela criação de um modelo hipotético de três fases: transporte das drogas para a interface gás – líquido do IL, adsorção na superfície livre do IL e absorção para o interior do líquido. De forma a avaliar a hipótese mencionada anteriormente, efetuaram-se experiências de microbalança de cristal de quartzo (QCM) e medidas de tensão superficial. As medidas de QCM permitiram-nos perceber os mecanismos de adsorção, seguida de absorção da água na superfície do IL, concluindo-se também que este influencia a cinética do processo. Adicionalmente, as medidas de tensão superficial permitiram-nos comprovar que o vapor de água ajuda a promover o transporte de drogas, devido à solubilização das mesmas. Mais ainda, através da utilização dos parâmetros de Kamlet – Taft para caracterizar a polaridade dos ILs, conclui-se que os catiões com maiores parâmetros de acidez e menores parâmetros de basicidade são os mais eficazes na remoção das drogas de abuso da superfície do cabelo.

A segunda parte deste trabalho envolveu o desenvolvimento de uma nova tecnologia para extrair seletivamente os compostos voláteis de plantas. Iniciou-se o desenvolvimento deste novo processo, utilizando folhas de eucalipto (*Eucalyptus Globulus*) como modelo. Salienta-se o facto de este novo método se basear nas pressões de vapor dos componentes voláteis. Neste caso particular, e tendo em conta a variabilidade intrínseca, decidiu-se dispensar o *screening* aquando da aplicação do DOE, passando-se diretamente para a aplicação do método da superfície de resposta

(RSM). Após a aplicação do RSM, conclui-se que as condições óptimas de extração para a obtenção do maior rendimento possível foram as seguintes: 50 °C, um caudal de azoto de 0.15 l/min durante 2.36 h. O vapor arrastado pelo azoto deve de ser condensado à temperatura de – 10 ºC. Aquando da aplicação destas condições às folhas de eucalipto, obteve-se um rendimento de extração de 6.11 %, o qual é bastante superior aos rendimentos obtidos por hidrodestilação. Este método foi ainda aplicado a outras duas espécies botânicas: à lavanda (*Lanvandula dentata*) e ao alecrim (*Rosmarius officinalis*). Os resultados mostraram uma vez mais, que apenas os componentes mais voláteis são extraídos. Esta característica confere ao método desenvolvido selectividade, a qual cremos que pode ser afinada para a extração de determinados compostos através da utilização de diferentes condições experimentais. Foram também obtidos rendimentos de extração superiores aos obtidos pela hidrodestilação: 7.23 % para a lavanda e 4.28 % para o alecrim.

Abstract

The increasing awareness on the environmental problems, led to an increasing demand of "greener" processes in the several fields of science, focusing mainly in solvent-free processes. We find two good examples in both forensic toxicology and natural compounds extraction fields, where solvents are still widely used.

In the last twenty years hair has gained great relevance as a toxicological sample, namely in the field of drugs of abuse. Although this matrix allows the detection of such compounds after weeks, months and even years (in same cases), it requires a pre-cleaning step (decontamination) in order to ensure the absence of drugs at the hair surface. Despite the existence of several decontamination strategies, none ensures the absence of drug at the hair surface. On the other, in the field of the extraction of natural compounds, it has been observed a rising demand for more selective, environmentally friendly, and cheaper extraction techniques that can be industrially applied.

In these contexts, the non-volatility of ionic liquids (ILs) makes them almost ideal systems for the sorption of compounds. In literature it is possible to find already some applications of these liquids, namely in the adsorption of dioxins.

We hereby present the development of new technologies for the selective removal of volatile compounds, applied to forensic toxicology (hair testing, using ILs) and to natural aromas (essential oils, without using ILs).

We started to apply the ILs to the decontamination of hair samples containing opiates at the surface. More than forty ILs were screened (100 ºC, 96h) and the liquid 1-ethanol-3-methylimidazolium tetrafluoroborate, $[C_2OHMIM][BF_4]$, showed very promising results (extraction efficiency > 80%). In order to reduce the extraction time to less than 24h, the process was optimized by means of *Design of Experiment* (DOE), and the final experimental conditions were 120 ºC, 16 h and a water content of 44% (w/w). The method was then compared with Cairns method (a common and very time-consuming decontamination strategy) and the results showed that the developed method yielded, in average, slightly better results (% difference ~5%). The method was then applied to both cocaine and cannabinoids. In the case of cocaine, the temperature led to the spontaneous hydrolysis of cocaine into its metabolite

benzoylecgonine (BZE). Unfortunately, we were not able to remove BZE from the hair surface and no explanation for this phenomenon was found. As for the cannabinoids, the ILs screening revealed a great affinity to these compound (extraction efficiency > 90%). Once more the liquid $[C_2OHMIM][BF_4]$ was chosen and the method was optimized for the cannabinoids extraction, and its final conditions were 100 ºC and 13 h. When compared with the Cairns decontamination, our method showed higher extraction efficiency.

The developed decontamination procedure was then rationalized in order to fully understand the phenomenon. A three steps model was assumed: transport of the drugs to IL gas-liquid interface, adsorption onto the liquid free surface and absorption into the bulk liquid. Quartz crystal microbalance (QCM) experiments, as well as surface tension measurements were performed to evaluate the proposed model. The results confirmed that the water vapor enhances the transport of the drugs (due to solubilization). Additionally, using Kamlet-Taft parameters to characterize the polarity of ILs, we concluded that the cations with the highest acidity and lowest basicity parameters are the most efficient in the removal of the drugs from hair.

The second part of the work involved the development of a new technology to selectively extract volatile compounds from botanicals. Using *Eucalyptus globulus* leafs as a model, a new extraction technique based on the vapor pressures was developed. In this particular case we found no need to use ILs. The method was optimized by mean of DOE and the optimum conditions were: 50 ºC, a nitrogen flow rate of 0.15 l/min , during 2.36 h. The vapor should be condensed at -10 ºC. Under these conditions the extraction yield was of 6.11 % (w/w). The method was further applied to both *Lavandula dentata* and *Rosmarinus officinalis.* The results showed not only the removal of the more volatile compounds (as expected), but also high extraction yields (7.23 % and 4.28 %, respectively).

Palavras-chave

Cabelo

Descontaminação

Drogas de abuso

Líquidos iónicos

Aromas naturais

Keywords

Hair

Decontamination

Drugs of abuse

Ionic liquids

Natural aromas

Essential oils

Abbreviations

6-MAM	6-Monoacetylmorphine
BZE	Benzoylecgonine
CCD	Central composite design
Coc	Cocaine
DOE	Design of experiment
EI	Electro ionization
EME	Ecgonine methyl ester
EO	Essential oil
EPA	US Environmental Protection Agency
FDA	Food and Drug Administration
GC	Gas chromatography
IL	Ionic liquid
Mor	Morphine
MS	Mass spectroscopy
NIDA	National Institute on Drug Abuse
RSM	Response surface method
SoHT	Society of Hair Testing
THC	Δ^9-Tetrahydrocannabinol
THCA	Tetrahydrocannabinolic acid
THCCOOH	11-Nor-9-carboxy- Δ^9-

	tetrahydrocannabinol
WHO	World Health Organization

Acknowledgements

I would like to thank Fundação para a Ciência e Tecnologia the financial support to this Ph.D. program with Ref. SFRH/BD/73228/2010.

I want to acknowledge my supervisors, Professor Carlos Afonso, Professor Benilde Saramago and PhD Mário Barroso, for all the guidance throughout this work.

I want to acknowledge Master Mário João Dias, director of the service of Forensic Toxicology of INMLCF, for allowing me to have access to lab.

I want to acknowledge Professor José Luis Mata, for all the help in the construction of custom equipments and for his friendship.

I would like to acknowledge PhD Virginia Hill, from Psychemedic, for the guidance in the validation of the developed decontamination method.

To Sandra, my wife, and Rafael, my son, my source of strength, to whom I acknowledge all the patience, love and support and simultaneously I dedicate this work. I would also like to acknowledge my parents for all the care and support

I would like to acknowledge to all my lab colleagues (to many persons to enumerate) for their collaboration and companionship and to my closest friends, some of which I'm proud to call brothers.

Table of Contents

Index

Chapter 1 – Introduction

This chapter provides a brief introduction on the role of hair analysis in toxicology, ionic liquids, extraction of essential oils, removal of harmful compounds from tobacco's mainstream smoke, and on the design of experiments as a process optimization tool.

Table of Contents

1.1. Drugs of abuse

The term "drug of abuse" refers to a wide spectrum of substances with effects on perception, reasoning, and mood, presenting different abilities to produce dependence in consumers. Speaking about the history of "drugs of abuse" is almost as speaking about Mankind's own history, since they were an integrant part of human culture, religious rituals, and have evolved simultaneously with humans [1]. Historical records show us that our ancestors from the Neolithic already consumed drugs, with a particular taste for the psychotropic ones (peyote, cannabis, poppy, coca, among others) [2].

In the following paragraphs, some relevant aspects from the drugs of abuse, particularly to this work, will be presented.

1.1.1. Opiates

The opiate group is constituted by the narcotic alkaloids found in the *Papaver somniferum* plant (opium poppy) (Figure 1). These compounds act on the nervous system receptors that are responsible for the pain regulation (opioid receptors). Opiates are extracted from the chalice of the opium poppy, in the latex form, which after oxidation originates the opium. In this complex alkaloid mixture, morphine and codeine are predominant. Morphine is extracted from opium and originates diacetylmorphine (heroin) by acetylation [3].

Heroin is largely consumed due to the euphoria effect (when administrated orally or intravenously), which is followed by a period of depression of the respiratory system. The main problem associated to this drug is the rapid onset of tolerance, resulting in the need of a continuous increase of the dosage for achieving the desired effect. The absence of consumption of this drug leads to hyperactivity of neurotransmitters, formerly inhibited by opiates. This situation leads to a massive adrenergic discharge [4,5], commonly known as withdrawal syndrome.

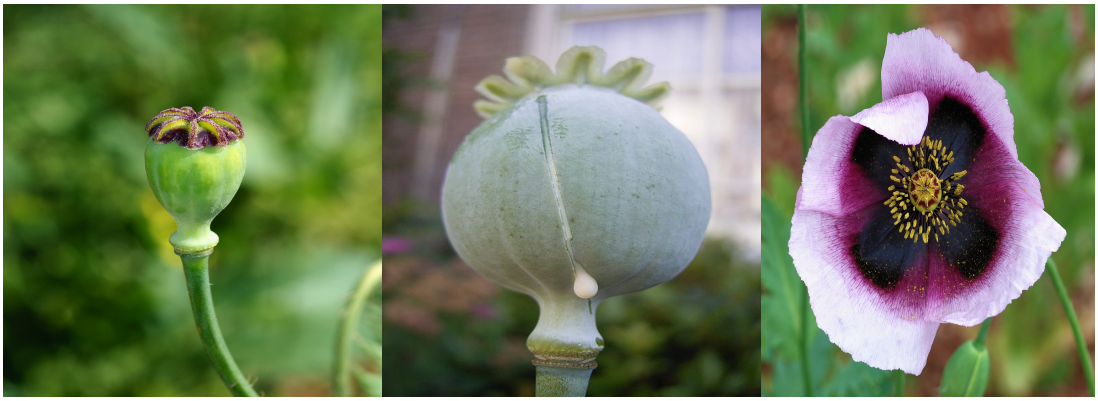

Figure 1 – *Opium poppy (Papaver somniferum;* retrieved from *Go Botany* [6]).

According to the United States' *National Institute on Drug Abuse* (NIDA), the most commonly used administration route for this drug is the intravenous injection (> 50%), and its effects are felt after 7 – 8 seconds [5]. After entering into the blood stream and passing through the liver, heroin is quickly metabolized into 6-monoacetylmorphine (6-MAM) and subsequently to morphine. Morphine is then conjugated with glucuronic acid originating two compounds: morphine-6-glucoronide (pharmacologically active) and morphine-3-glucoronide. The majority of heroin's metabolites (80%) are excreted in the urine during a period of 24h after consumption [7] (Figure 2).

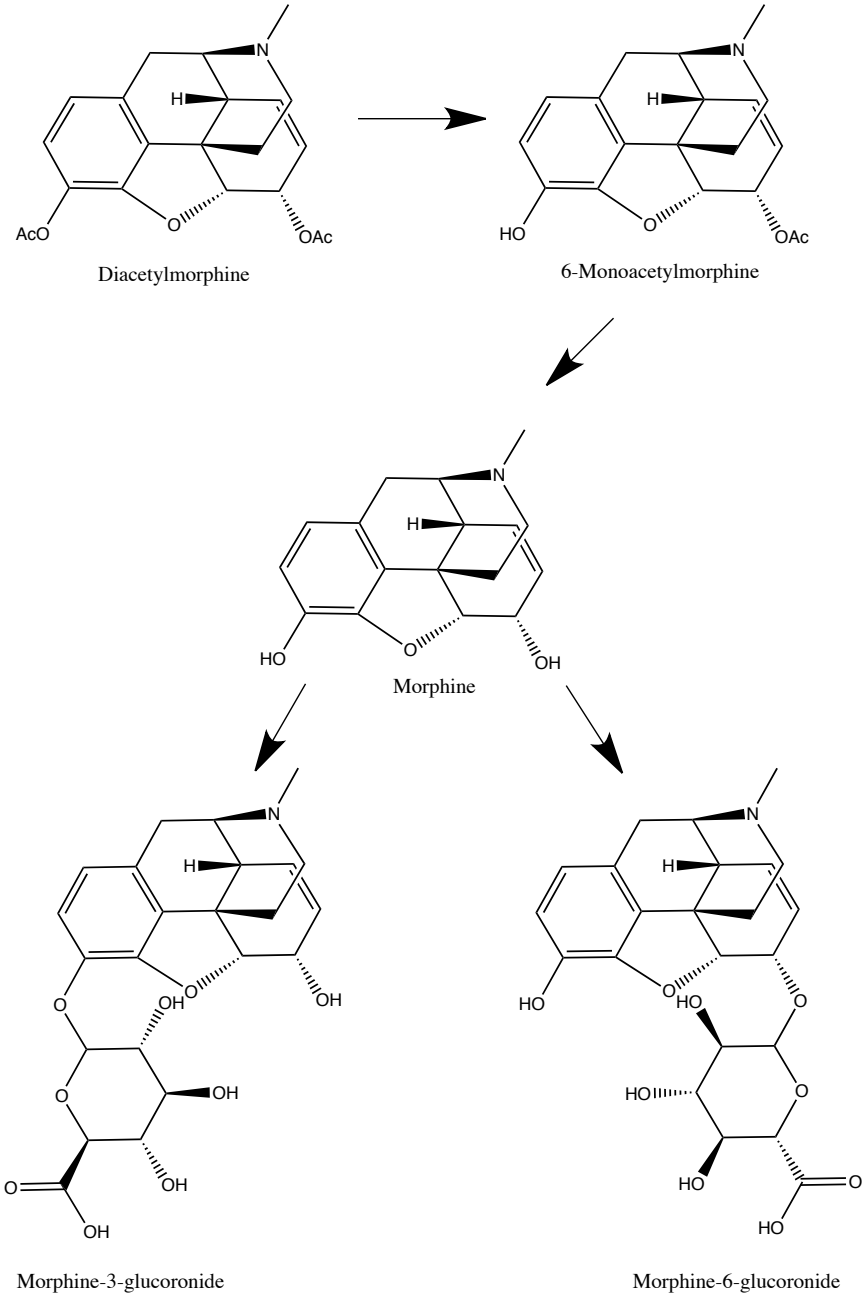

Figure 2 - Metabolic pathways of heroin [7].

1.1.2. Cocaine

Cocaine is one of the most powerful natural stimulants, having a quite long history of consumption and abuse [4]. This alkaloid is extracted from the leafs of *Erythroxylon coca* (Figure 3), a bush planted mainly in South America. Historical records state that the consumption of this alkaloid takes us at least to the year 2500 BC, to the Andes region, where miners consumed it as a stimulant, through the chewing of the coca

leafs. The Incas went further, since they believed that this substance was a gift from the gods [1,3,4].

Figure 3 - *Erythroxylon coca* (retrieved from *Go Botany* [6]).

Cocaine is a lipophilic alkaloid that crosses very easily the hematoencephalic barrier, accessing the central nervous system. There, it will inhibit monoamine oxidase (MAO), which is the enzyme responsible for the degradation of catecholamines (e.g. dopamine and noradrenalin). As consequence, the levels of these neurotransmitters will increase in the synaptic region, originating an increase on the heart rate, increase of both speed and clarity of reasoning, inhibition of pain and increase of blood pressure. The individual feels uncommonly aware, euphoric, excited, with a great clearness of mind, almost like if the time had stopped. This drug of abuse can be consumed through sniffing, smoking or even intravenous injection, entering very rapidly into the bloodstream despite the route of administration. Due to liver metabolism, cocaine is quickly metabolized to its major and inactive metabolite benzoylecgonine (BZE). There is, though, the possibility of formation of other metabolites, such as ecgonine methyl ester (EME) or ecgonine [4] (Figure 4). Like in the case of heroin, cocaine abuse can also give origin to withdrawal syndrome. In this particular case, the symptoms are characterized by insomnia, increased irritability and appetite, depression, fatigue, memory changes, paranoia, and the need for cocaine. However, this syndrome is not as painful as that observed after consumption of opiates.

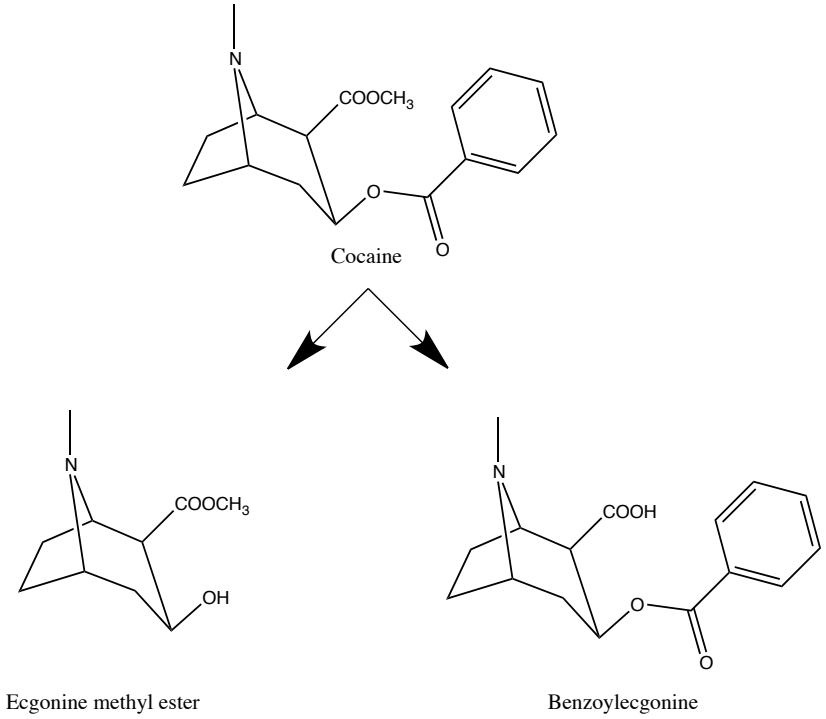

Figure 4 - Metabolic pathways of cocaine [7].

1.1.3. Cannabinoids

To speak about the cannabinoids history, we need to travel backwards 1200 years to China where the *Cannabis sativa* leafs (Figure 5) were used for paper production. Later, somewhere by the year 2700 BC, the emperor Shen-Nung specified the use of this plant for the treatment of beriberi, obstipation, gout and other diseases. Other medicinal applications of this plant didn't appear until the century II AC

Throughout history this plant was used, not only for its medicinal properties (as previously mentioned), but as well for religious purposes (psychotropic effects). The Hindu believed that the resin of this plant was part of the Shiva's saliva, and with it they produced the *ganja,* which was smoked. The Persians used this same resin (*hasheesh*), which was burned in religious ceremonies [8].

Figure 5 - *Cannabis sativa* (retrieved from *Go Botany* [6]).

The active compounds of this plant are found mainly in its resin and floral extremities.

From the pharmacological point of view, the active compound is the Δ^9-tetrahydrocannabinol (THC), which acts on specific receptors for endogenous cannabinoids (*N*-arachidonoylethanolamide and 2-arachidonoylglycerol). The different preparations of this drug (marihuana, hashish and cannabis essential oil) are usually smoked, alone or mixed with tobacco. The popularity of this drug is due to the fact that it promotes relaxation, euphoria and, at high doses, hallucinations. These effects are usually followed by a change in the notion of time and distance, increase of appetite, and of blood pressure and mood changes [3,7].

THC is mainly metabolized in the liver, firstly oxidized into the equally active 11-hydroxi-Δ^9-tetrahydrocannabinol (11-OH-THC). It is important to remark the production (in minor scale) of the 8-β-hidroxy-Δ^9-tetrahydrocannabinol (8-β-OH-THC) and of 8-α-hydroxiΔ^9-tetrahydrocannabinol (8-α-OH-THC). Afterwards, 11-OH-THC is oxidized to the inactive 11-nor-carboxy-Δ^9-tetrahydrocannabinol (THCCOOH). Both THCCOOH and its glucuronic conjugate are the main metabolites eliminated from the body (Figure 6).

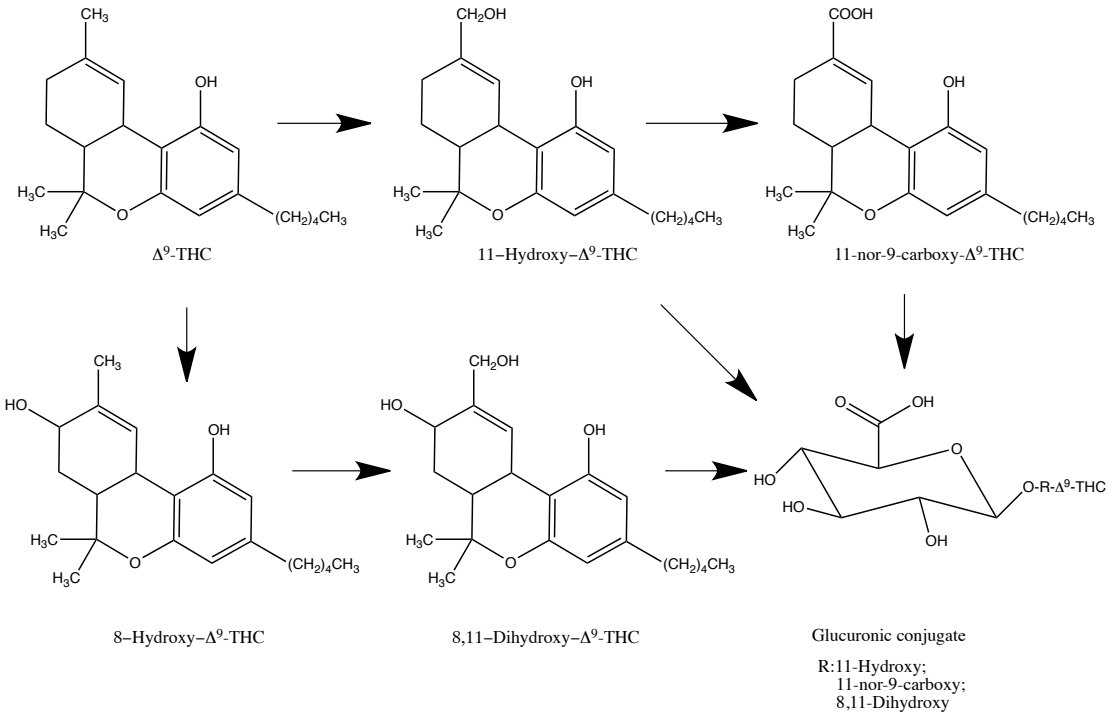

Figure 6 - Main metabolic routes of Δ^9-THC [7].

Contrary to heroin and cocaine, cannabinoids consumption has no associated withdrawal syndrome. The main reason for this is the fact that the majority of THC gets stored into the fatty tissue and, later, is slowly released into the bloodstream. About 80 to 90% of the consumed dose is excreted until five days after consumption (> 65% in feces and about 20% in urine), mainly in its carboxylated form [9].

1.2. Human hair

Human hair is a non-homogeneous fiber with a highly complex multi-layer structure, formed by keratinized cells that are agglomerated through the complex of cellular membranes. This set forms three concentric structures: cuticle, cortex and medulla (Figure 7). The cortex is responsible for the elasticity and color of hair, while the five to ten layers of cells that form the cuticle are responsible for its high physical and chemical resistance, as well as for its glow.

The hair is formed from the follicle (consisting in several layers of cells), located 3 to 5 mm below the skin. The high rate of mitotic activity in the follicle bulb produces an ascending flow of cells that will form the hair fiber. The melanocytes, which are located at the bottom of the papilla, synthesize melanin in specialized organelles

called melanossomes. The produced melanin is then transferred to the cells that migrate from the follicle [10,11].

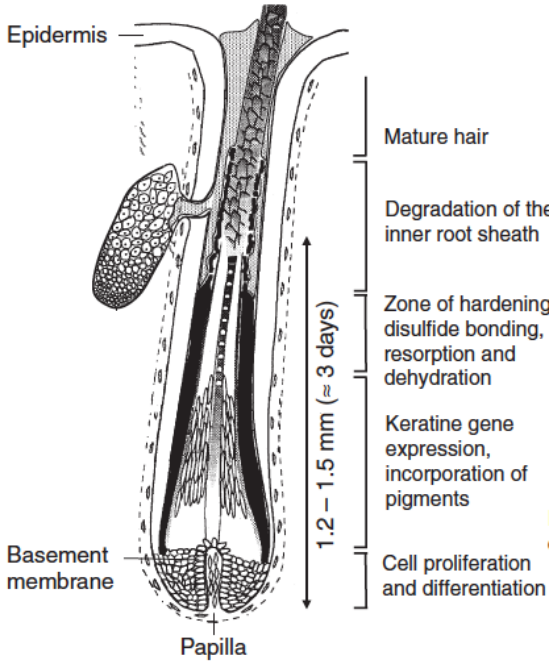

Figure 7 - Schematic representation of an hair follicle (modified from *State of the art in hair analysis for detection of drug and alcohol abuse* [11]).

The hair growth process occurs in cycles with periods of growth and latency. In the case of human hair, each follicle has a growth cycle independent of the adjacent follicles. The growth cycle begins with the anagen phase, during which the follicle develops itself and the hair is produced, being also in active growth. The anagen phase can last between 7 to 94 weeks, eventually reaching years (depending on the anatomic region). Then catagen phase follows. This phase (lasting about 2 – 3 weeks) is characterized by the ending of the follicle's activity and by the contraction of the papilla. After catagen, the follicle enters in a rest stage that lasts (telogen), in average, 100 days. After telogen another cycle begins (Figure 8) [4].

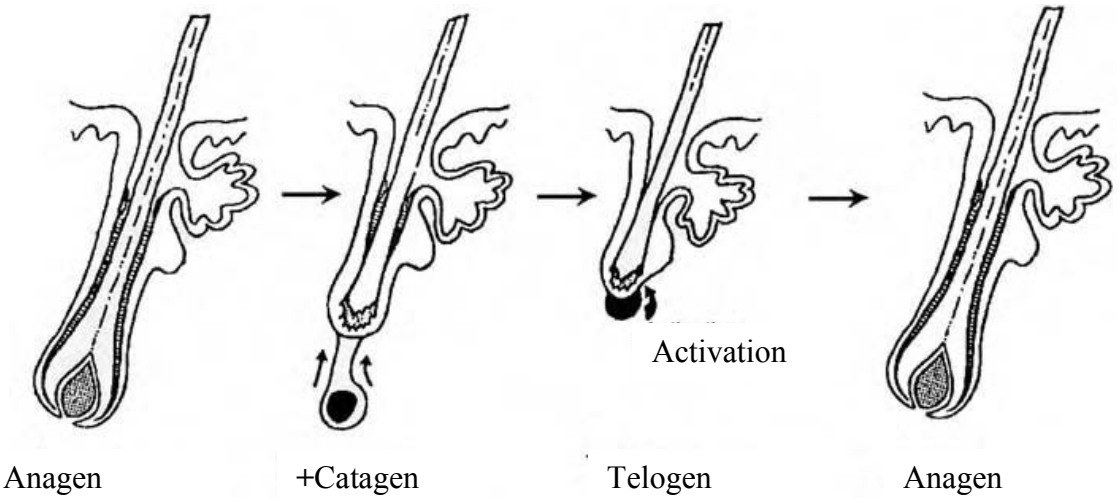

Figure 8 – Hair growing cycle (modified from *Analytical and Practical aspects of drug testing in hair* [4].

1.2.1. Mechanisms for drug incorporation

In 1954, Raymond Goldblum and collaborators [12] published a study about the relationship between barbiturates and drug dermatitis in guinea pigs. In this work they discovered that part of the barbiturates that were being administrated to the guinea pigs were incorporated in their hair. This fact was the starting point of new research trends in toxicology: hair testing to evaluate and report human exposure to xenobiotics.

The use of hair as a biological sample of toxicological interest for the detection and quantification of drugs of abuse has gained great relevance in the last twenty years for several reasons. The process involves a non-invasive collection, the sample is not easily adulterated or tampered, allows the detection of a large spectrum of drugs of abuse and a retrospective research on consumption as well [10,11,13].

The adoption of this new methodology brought the need to understand the mechanisms of incorporation of the substances into the hair. Typically, the drug incorporation models assume a passive diffusion of the compounds from the capillary vessels into the growing follicle in a time window of three days. According to these theoretical models, the concentration of the drug in the hair should be relate to its concentration in blood, but the experimental results do not agree with this assumption, which means that other incorporation mechanisms should be involved (Figure 9) [11].

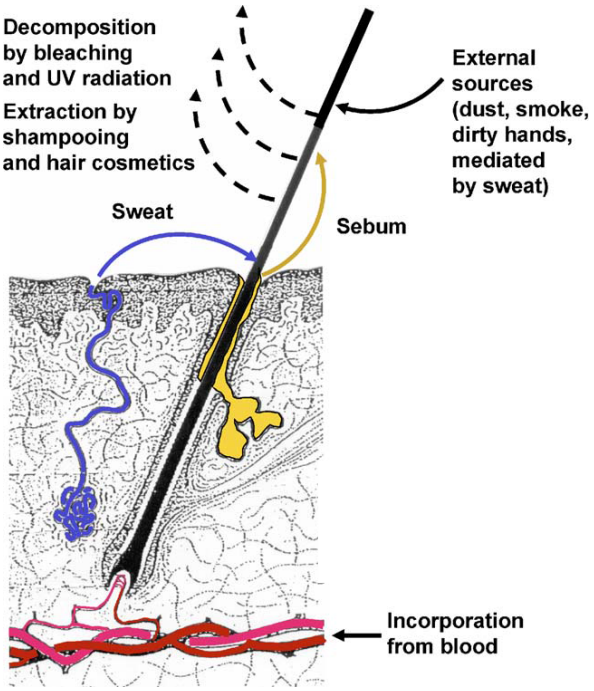

Figure 9 - Incorporation and elimination of drugs from hair (modified from *State of the art in hair analysis for detection of drug and alcohol abuse* [11]).

Henderson [14] demonstrated that substances can be incorporated in hair, not only through blood, but also from segregations coming from skin compartments (diffusion from sweat and sebum). One should also keep in mind the possibility of incorporation from the environment. Although this multi-compartment model [14] is generally well accepted, the incorporation mechanisms remain unclear and both the individual physical and physiological characteristics must be taken into account as well [11].

- **Drug incorporation from bloodstream**

As previously mentioned, the hair bulb, due to its structure, is highly irrigated. The incorporation of the drug into the hair will be strongly dependent of its own lipophilicity and basicity and also of the content of melanin in the hair follicle. In order to enter the cells of the growing matrix, the drug has to diffuse throughout the cellular membrane, which explains the importance of the lipophilicity. This consideration served as the cornerstone of the discussion reported by Nakahara and collaborators [15], in which they evaluated the incorporation of both cocaine and benzoylecgonine in mouse hair, after administration. These authors verified that the plasma concentration of benzoylecgonine was four times higher than that of cocaine,

while the opposite occurred in hair, where the concentration of benzoylecgonine was ten times lower than cocaine's. The main reason for this phenomenon lies in the concept of metabolism. The main goal of metabolism is to make the administered substances more hydrophilic, in order to facilitate their excretion (e.g. through urine). This means that the non-metabolized drug will be definitely more lipophilic than its metabolites, and so will cross much easily membrane barriers into the growing follicle. In the case of hydrophilic molecules or organic ions of medium molecular weight, the cellular membranes appear as insurmountable obstacles. In these cases, the pH gradient between plasma and hair cells, as well as the pKa of the substances, are critical factors for the transport. The plasma's pH is practically neutral (~7,3), while the melanocyte's pH is about 3 to 6 [16]. Therefore, basic drugs, such as cocaine, contrary to acidic ones (THC), accumulate very easily inside the hair (Figure 10). Once inside melanocytes, the basic drugs will be protonated, disabling them to diffuse again into the plasma [4,11]. This fact was proven by *in vitro* studies [17,18], where the authors demonstrated the affinity of melanin to bind basic drugs, being one of the strongest retention mechanisms of human body.

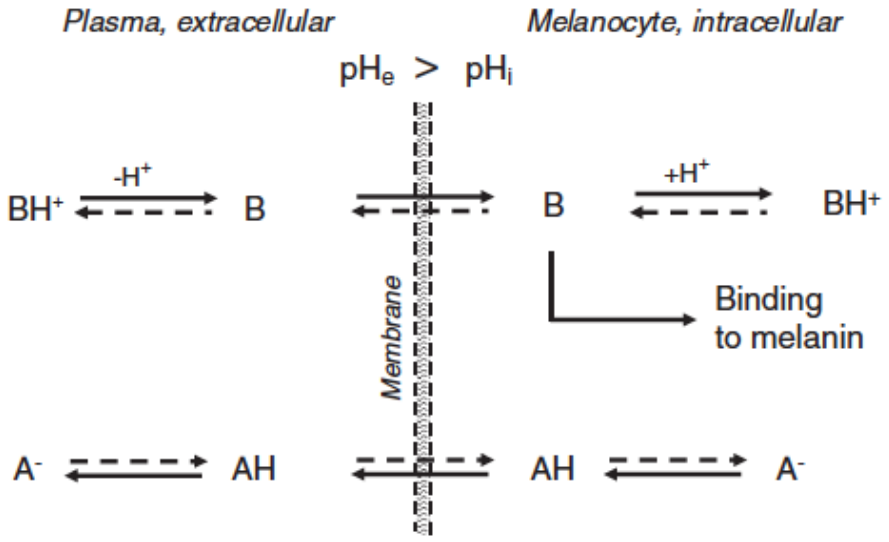

Figure 10 – Effect of both acidic and basic properties of drugs in its incorporation's rate in hair. A = acid drug; B = basic drug; e = extra-cellular space; i = intra-cellular space (modified from *State of the art in hair analysis for detection of drug and alcohol abuse* [11]).

- **Incorporation from sweat and sebum**

At this point, it is clear that the metabolites of drugs are water soluble, and therefore, one of the routes of excretion is through sweat [19–22]. This elimination enables the detection of such compounds in this toxicological sample. The hair is externally washed by sweat, enabling the metabolites present in this excretion to become initially deposited at the surface of hair and subsequently incorporated into its interior [4]. It is important to remark that, due to the presence of a significant amount of sebaceous glands near to the hair follicles, sebum plays also a significant role in terms of drugs and metabolites incorporation in hair.

- **External contamination**

Besides bloodstream, sweat and sebum incorporation, environmental contamination plays a role that cannot be neglected. In fact, this can be a serious problem for hair testing, given that the drugs can be present in the hair sample, even in the cases where there was no active consumption. The relevance of this problem increases when we are discussing about drugs of abuse that can be smoked or inhaled, as occurs in the cases of cannabis, cocaine and heroin. The contamination can occur by contact with contaminated hands and/or surfaces as well [23]. An interesting example of this problem is presented by some north-American authors [24–27] who claimed that significant traces of both cocaine and marihuana were found in US currency paper.

The possibility of an external contamination raises a huge problem in both legal and forensic levels. In fact, one of the major limitations of this matrix (hair) is the almost impossible distinction between a systemic incorporation (derived from consumption) and an external contamination [23]. The possibility of a false positive result can, not only deprive an innocent person from his or hers freedom, but also ruin the credibility of a hair-testing laboratory.

1.2.2. Decontamination processes

At this point, it is clear the existence of problems related to the possibility of an external contamination. In order to overcome this problem, the *Society of Hair Testing* proposed the need for a pre-cleaning step (or steps), which was called decontamination. According to this institution, this decontamination should comprise the following criteria [28]:

- Initial wash with an organic solvent (to remove possible traces of oils, hair care products, sebum and sweat);
- Wash with aqueous solutions (e.g. buffers);
- Store the washing solutions for later analysis.

Ideally, solvents used in the decontamination will extract exclusively the traces of sweat and sebum, as well as the drugs present in the surface of the hair. Unfortunately, there is no consensus in this theme [11], which results in several decontamination strategies published in scientific literature:

Table 1 - Decontamination strategies available in literature for cannabinoids, cocaine and opiates.

Class	Decontamination procedure	Reference
Cannabinoids	Dichloromethane	[29–35]
	Methanol	[36–39]
	2-Propanol	[40–42]
	Water, petrol ether, dichloromethane	[43,44]
	1M Phosphate buffer, water, methanol	[45]
	Acetone, petrol ether	[46]
	Dichloromethane, water, acetone (ultrasound bath)	[47]
	Ethanol	[48]
	Petrol ether, water dichloromethane	[49]
	Shampoo, deionized water, acetone, hair dried overnight	[50]
	Water, acetone	[51]
	Water, acetone, methanol, dichloromethane, phosphate buffer	[52]
	Water, petrol ether, acetone	[53]
	Water, petrol ether, methanol	[54]
Cocaine	Dichloromethane	[30,35,55–61]
	Methanol	[62–69]
	Water, acetone	[47,70,71]
	Dichloromethane, water, methanol	[13,72]
	0.1% aqueous solution of SDS, water, acetone	[73]

	0.1% aqueous solution of SDS, water, dichloromethane	[74]
	0.1% aqueous solution of SDS, water, methanol	[75]
	10% aqueous solution of SDS, water, acetone	[76]
	2-propanol, 0.01M phosphate buffer, 2-propanol	[77]
	2-Propanol, 5x 0.01M phosphate buffer/0.01% BSA, pH6	[78]
	2-Propanol, dichloromethane	[79]
	Dichloromethane, 2-propanol, acetone	[80]
	n-Hexane, acetone	[81]
	Shampoo, deionized water, acetone, hair dried overnight	[50]
	Tween 80, water	[82]
	Water	[83]
	Water, Petroleum benzine, dichloromethane	[84]
	Water, water/methanol/dichloromethane (50:50:50 v/v/v)	[85]
Opiates	Dichloromethane	[30,55–57,59,61,86,87]
	Methanol	[62,63,66,67,88,89]
	0.1% aqueous solution of SDS, water, acetone	[73]
	0.1% aqueous solution of SDS, water, dichloromethane	[74]
	1% aqueous solution of SDS, water, methanol	[90]
	10% aqueous solution of SDS, water, acetone	[76]
	2-propanol, 0.01M phosphate buffer, 2-propanol	[77]
	2-Propanol, 5x 0.01M phosphate buffer/0.01% BSA, pH6	[78]
	2-Propanol, dichloromethane	[79]
	Dichloromethane, 2-propanol, acetone	[80]
	Dichloromethane, water, methanol	[91]
	n-Hexane, acetone	[81]
	Shampoo deionized water, acetone, hair dried overnight	[50]
	Tween 80, water	[82]
	Water, acetone	[71]
	Water, Petroleum benzine, dichloromethane	[84]

From the analysis of the information present in table 1, it is easy to realize that the two main used decontamination procedures are the washings with only one solvent: dichloromethane or methanol. Non-protic solvents, such as dichloromethane or acetone, are advantageous because they do not swell the hair and thereby don't extract materials from inside the hair matrix. Though, their ability to dissolve the compounds

is moderate. In contrast, protic solvents, such as phosphate buffer or methanol, promote extraction in the washing step by swelling the hair [11]. Methanol, in particular, will not only promote hair swelling and extraction of drugs from the inside of the hair matrix, but will also damage the morphological structure of the hair, as reported by Stout and collaborators [10].

A more sophisticated approach is proposed by Cairns *et al.* [78]. The method of these authors consists in a wash with anhydrous isopropanol, followed by five sequential washings with phosphate buffer at 37 ºC. After this procedure, the hair sample is analyzed and two situations may occur: the amount of drug is < or > 0.2 ng/mg of hair. In the former case, the sample is considered to be negative; in the latter, application of a wash criterion is deemed necessary to determine whether the sample is positive or an eventually contaminated negative sample. The wash criterion is based on the comparison between the amount of drug per mg of hair in the washed hair sample and the amount of drug per mg of hair in the last washing solution. The amount in the last wash is multiplied by 5, and the result is subtracted from the amount in the hair. If the result is less than the cut-off for that particular drug, the hair may still be contaminated. If the result is above the cut-off, the sample is considered positive and, although some contamination could be present, it is not enough to transform a negative sample into a false positive; thus, no further washing would be required. Although this method is, to our knowledge, the only one that can give a reliable result regarding a possible contamination, it has as main drawbacks the human resources needed for its routinely application and the fact of being highly time-consuming (3h45). This justifies the demand for developing a more cost-effective decontamination method that can assure the absence of drug extraction from the inside of hair, maintaining its integrity.

1.3. Ionic liquids

1.3.1. Historical overview

Ionic liquids (ILs) have been accepted in the last ten years as new “green” chemicals, in both academic and industrial media.

In 1914, Sugden and Wilkins described for the first time an ionic liquid (ionic liquid stands for all salts, both organic and inorganic, with melting points below 100 ºC [92]), in this case, ethylammonium nitrate ($[EtNH_3][NO_3]$) [93].

In the beginning of the 70's, Wilkes tried to develop new batteries, to be used in nuclear warheads and in space probes, which need molten salts to work [94]. Nevertheless, the melting temperature for these salts was still too high, damaging the surrounding materials. The need to develop salts with even lower melting temperatures, led to the appearance of new ionic liquids. Wilkes and his collaborators continued the improvement of their ILs to be used as electrolytes in batteries, and this was the beginning of the production of ILs and of the discovery of their true potential [95,96].

At the end of the 90's, the ILs were already considered one of the most promising types of solvents [92]. The first ILs (e.g. organo-alluminates) were not stable in presence of air and water and reacted with several organic compounds. After the publication of both synthesis and application of the first known stable ILs (e.g. 1-*n*-butylimmidazolium tetrafluoroborate), the number of stable ILs grew at an almost exponential rate [97].

1.3.2. Properties

As any salt, the ILs are composed by a cation and an anion, though contrary to the common salts, the ILs melt at temperatures below 100 ºC [92]. In this group we find a sub-group called room temperature ionic liquids (RTILs), which are liquid at room temperature. This behavior is attributed to the inability of the ions to pack and it is favored by the use of big and asymmetric ions [92,98].

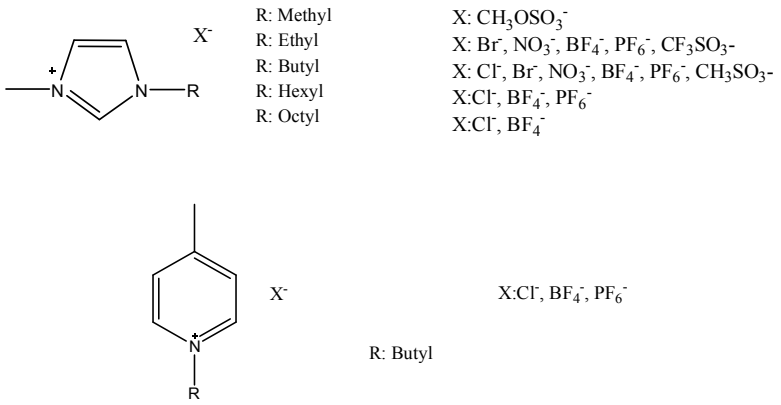

Figure 11 - Structures of imidazolium (upper scheme) and piridinium (lower scheme) based ionic liquids [92]

These liquids present uncommon properties, such as high thermal stability, low vapor pressure and high thermal conductivity [92,99–102], and, as a consequence, several applications have been discovered and studied. Some of these applications are briefly presented:

- Media in organic synthesis [94,99,100];
- Extracting agents in biphasic liquid systems [103–108];
- Catalysts in both homogenous and heterogeneous catalysis [99,100,104,109,110];
- Alternatives to common lubricants [111–115];
- Heat transfer fluids [116–119].

Another interesting feature of these liquids is their ability to capture compounds from atmosphere. Since 2002, scientists realized that ILs were able to dissolve both CO_2 and SO_2 gases [120–126] and hydrofluorocarbons [127]. These features were the starting point for the work of Kulkarni and his collaborators [128] In this work, they first report the ability of these liquids to adsorb organic compounds, such as 1,4-benzodioxane, biphenyl, xanthene and menthol, from the gas phase. One year later, the same authors have published a study where the same methodology was applied, but this time to ashes containing dioxin. In this study, both IL and ashes (containing dioxins) were heated together inside a closed chamber (Figure 12), proving that, if the solute can volatilize, than it is possible to capture it with an IL. At this point, it is important to remark that this study served as the starting point for the development of both a new decontamination procedure for hair testing and new filtration strategies to remove hazardous compounds from mainstream smoke of cigarettes.

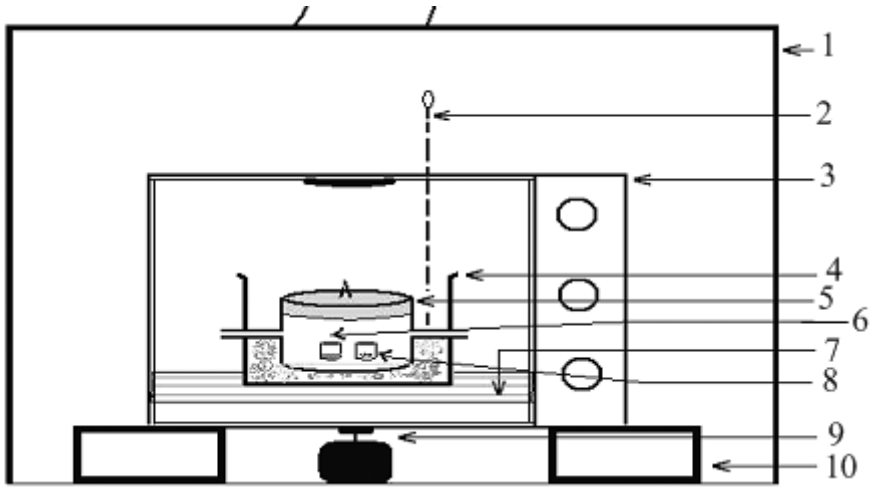

Figure 12 - Experimental setup used by Kulkarni, (modified from *Captures of Dioxins by Ionic Liquids* [129]). 1 – Fume Hood; 2 – Thermometer; 3- Owen; 4- Sand bath; 5 – closed glass chamber; 6 – Vial containing IL; 7 metal support; 8 – Vial with dioxins; 9 – magnetic stirrer; 10- solid support.

1.3.3. Toxicity

Since their very origin, that the ILs were considered as green solvents. Contrary to the common solvents (which are volatile), the ILs present an almost negligible vapor pressure and, therefore, will not contaminate the atmosphere. Nevertheless, this does not imply that they cannot pollute the environment through other routes. The majority of ILs are water soluble and can enter in the aqueous media through accidental spills, or through effluents discharges [92]. It is also of common knowledge that some of the most known and studied ILs, such as 1-*n*-Butyl-3-methylimidazolium hexafluorophosphate ([BMIM][PF_6]) and 1-*n*-Butyl-3-methylimidazolium tetrafluoroborate ([BMIM][BF_4]), quickly decompose in water, forming phosphoric or hydrofluoric acid, respectively [130]. Talking about ILs toxicity is always controversial. In 2008, Evans [131] reported the effects of some imidazolium and pyrrolidinium based ILs in phospholipidic bilayers, concluding that these ILs were not so "friendly" after all. Despite the results presented by Evans, research evolved towards the discovery of ILs based on biological molecules, such as choline and derivatives or aminoacids [132–139]. In a recent study [140], it was proven the low toxicity of choline based ILs, though we must stress that choline based ionic liquids are not necessarily of low toxicity, as stated by Ventura et al. [141], since it always depends on the cation-anion combination.

1.4. Essential oils (EO)

Essential oils (EOs), also called volatile or ethereal oils [142], are volatile, natural, complex systems, composed mainly of terpenes in addition to some other non-terpene components and are characterized by a strong odor. Typically, EOs are aromatic oily liquids, soluble in lipids, which are obtained from plant material (flowers, buds, seeds, leaves, twigs, bark, herbs, wood, fruits and roots) [143].

The EO compounds are formed by aromatic plants as secondary metabolites. In nature, essential oils play an important role in the protection of the plants, since they act as antibacterials, antivirals, antifungals, and insecticides. They also may attract some insects to favor the dispersion of pollens and seeds, or repel undesirable visitors [144].

1.4.1. Historical overview

Speaking about EOs across the ages almost like speaking of ancient civilizations, since they have evolved together with humanity. It is of common knowledge that spices were used in antiquity for their perfume, flavor and preservative properties. Nevertheless, Greek and Roman historic records already mention the use of turpentine oil (obtained from resins, mainly from pine). Although there are records related to the use of the distillation technique for the production of EOs in Egypt, Persia and India (> 2000 years ago), this technique was only precisely described in 13th century by a Catalan physician called Villanova [142]. During this century, EOs were produced by pharmacists in their pharmacies, and their pharmacological effects were described in pharmacopoeias. However, it was only during the 16th century that their use was widespread over Europe and their name was achieved. It is supposed that the name "essential oil" derived from the name coined by the Swiss reformer of medicine, Paracelsus von Hohenheim, who named the effective component of a drug *Quinta*

essentia. According to a French physician, Du Chesne (Quercetanus), in the 17th century the preparation of EOs was well known and pharmacies generally stocked 15–20 different oils which were used for medicinal purposes. Although in the 19th century De la Croix carried the first experimental measurement of the bactericidal properties of vapors of EO, during the course of the 19th and 20th centuries the use of Eos in medicine gradually became secondary to their use for flavor and aroma [142].

1.4.2. Application

As previously mentioned, the major current application of EOs is in the flavor and fragrance industries, in which they are used as flavoring agents (flavor industry) and as fragrance source in the fragrances market (perfumes, soaps, creams, lotions, shampoos, washing-up liquids, etc.) [145,146]. In these applications, there is an interesting trend called microencapsulation [146,147]. Typically, EOs are labile and volatile liquids, and the sensory perception can be changed as a result of heating, oxidation, chemical interactions or volatilization. Thus, the extent of these effects can be sufficient to dramatically alter the quality of products [148]. According to Poncelet [149], encapsulation is an effective way to minimize the harm of these problems and is essential from a scientific, industrial and economical point of view.

Regarding now the applications related to the biological activity of the EOs, we find them useful for several purposes: as dental root canal sealers [150], antiseptics [151], food preservatives [152], or even for the production of insect repellents [153].

1.4.3. Extraction processes

After understanding the basics about EOs and their use, it is important to understand how they are extracted from the plant material. The EOs can be extracted by the following methods: distillation, expression, *enfleurage*, solvent extraction and supercritical fluid extraction [142].

- **Distillation**

Distillation is undoubtedly the oldest method to extract essential oils. It can be of three different types: hydrodistillation, water and steam distillation and steam distillation.

In hydrodistillation, both plant material and water are boiled together, and the formed vapor (water and EO) is then cooled down (promoting condensation) and collected. This mixture quickly originates two phases, water and oil phases, which is separated through simple decantation.

In the case of the water and steam process, the water remains below the plant material, which has been placed on a grate while the steam is introduced from outside the main still (indirect steam). Then the procedure is similar to the one described for the hydrodistillation.

As for the steam distillation, steam is injected into the still, usually at slightly higher pressures and temperatures than the two methods described above.

Although both hydrodistillation and steam distillation are widely used in the flavor and fragrance industry, their main drawback is the high temperature (c.a. 100 ºC) that the plant material is submitted. This feature disables completely the possibility to apply this method to sensitive botanicals, such as jasmine or rose. Additionally, it is also important to take into account the high energy consumption of this process [142,145].

- **Expression**

The expression method (also known as cold pressing) consists basically in compressing fruit peels to extract their EO. It is important to remark that this technique is almost exclusive for citrus EOs. Although this method was applied manually, nowadays it was substituted by the *écuelle à piquer* process. This process consists in placing the fruit in a device with spikes on the side that puncture the oil cells in the skin of the fruit upon rotation. This causes the oil cells to rupture and the

essential oil, and other material such as pigments, to run down to the center of the device, which contains a collection area. The liquid is thereafter separated and the oil is removed from the water-based parts of the mixture and decanted [142,145].

- **Enfleurage**

Enfleurage is a traditional way to cold extract EOs from flowers, original from a southern region of France, called Grasse. In the early days of perfumery, many flower scents were extracted this way, now considered an ancient art that is passed down from father to son or from generation to generation. This process consisted in a cold-fat extraction process that is based upon the principles that fat possesses a high power of absorption, particularly animal fat. The fat used must be relatively stable against rancidity. It is a method used for flowers that continue developing and giving off their aroma even after harvesting (e.g., jasmine and tuberose). Today, Grasse continues to be one of the few areas in the world that continues to employ *enfleurage* as a method of extraction, though it has become a very rare technique [142].

- **Solvent extraction**

As previously mentioned, there are botanicals, such as jasmine or rose, which cannot be submitted to distillation. On the other hand, *enfleurage* does not enable industrial competitiveness. In this particular scenario, solvent extraction appears as good solution for these problems. This technique employs solvents, such as petrol ether, methanol, ethanol, or hexane, to extract the odoriferous lipophilic material from the plant. The solvent will also pull out chlorophyll and other plant tissues, resulting in a highly colored or thick/viscous extract. The first product made via solvent extraction is known as a concrete. A concrete is the concentrated extract that contains the waxes and/or fats as well as the odoriferous material from the plant. The concrete is then mixed with alcohol, which serves to extract the aromatic principle of the material. The final product is known as an absolute [142]. The solvent extraction can be sub-divided in three sub-groups:

- **Soxhlet extraction** (**see Figure 1 in** [154]**):** the plant material is placed inside a filter paper thimble-holder, and filled with condensed fresh solvent from a distillation flask. When the liquid reaches the overflow level, a siphon aspirates the solution of the thimble-holder and unloads it back into the distillation flask, carrying extracted solutes into the bulk liquid. In the solvent flask, solute is separated from the solvent using distillation. Solute is left in the flask and fresh solvent passes back into the plant solid bed. The operation is repeated until complete extraction is achieved [155]. Although this method offers a simple and cheap solution, it has as main disadvantages being too time-consuming, requires a large amount of solvents, which need an subsequent evaporation/concentration procedure and the possibility to promote thermal decomposition of some components of the EO cannot be neglected. It is also important to stress that one of the most used solvents is the *n*-hexane. Despite having a narrow boiling point range (approximately 63–69 ºC) and being an excellent oil solvent in terms of oil solubility and of easy recovery, it is also listed nº 1 on the list of 189 hazardous air pollutants by the US Environmental Protection Agency (EPA) [156].

- **Sonication-assisted extraction**: It is of common knowledge that sonic waves and consequent cavitation are of great utility in speeding dissolution, by breaking intermolecular interactions. This is the theory behind sonication-assisted extraction. In this process, both solvent (or mixture of solvents) and botanical are submitted to ultrasonic waves leading to the formation of a concrete [157]. This method is an inexpensive, simple and efficient alternative to conventional extraction techniques. The main benefits of use of ultrasound in solid–liquid extraction include the increase of extraction yield, faster kinetics and a possible reduction of the operating temperature allowing the extraction of thermolabile compounds. Furthermore, the ultrasound-assisted extraction, like Soxhlet extraction, can be used with any solvent for extracting a wide variety of natural compounds. However, the effects of ultrasound on extraction yield and kinetics may be linked to the nature of the plant matrix. The presence of a dispersed phase contributes to the ultrasound wave attenuation and the active part of ultrasound inside the extractor is restricted to a zone located in the vicinity of the ultrasonic emitter [154,157].

- **Microwave-assisted extraction:** Similar to the sonication-assisted extraction, this technique employs waves to increase both kinetics and yields of the extraction, though, instead of ultrasound waves, it is used electromagnetic waves (with wavelengths on the microwaves region). The efficiency of this method depends a lot of the microwave energy, thus, it is strongly dependent on the dielectric susceptibility of both the solvent and the solid plant matrix [158]. In spite of being considered an excellent alternative to the traditional solid-liquids extraction methods, this is a quite expensive technique that requires filtration or centrifugation to remove the solid residue. Furthermore, the efficiency of microwaves can be very poor when either the target compounds or the solvents are non-polar, or when they are volatile [154].

- **Accelerated solvent extraction (see Figure 3 in [154]:** This method consists in a solid–liquid extraction process performed at high temperatures, usually between 50 and 200 ºC and at pressures between 10 and 15 MPa. The main goal of the high pressure is to maintain the solvent physical state (liquid) at high temperature (but still below the supercritical conditions). The high temperature accelerates the extraction kinetics (enhances the diffusivity of the solvent) and the elevated pressure keeps the solvent in the liquid state, thus achieving safe and rapid extraction [159,160]. The main disadvantages are related to the amount of polar modifiers that need to be added, for example CO_2 to extract polar compounds. Special remark to the high temperatures that can degrade EO's compounds [159].

• Supercritical fluid extraction

Since gases and vapors have low solubilizing power, research has been carried out on gas-phase extractions performed at high pressures and temperatures. When a gas is compressed and heated, it can reach a state of aggregation at which no distinction between the gas and liquid can be observed (supercritical state). At these conditions the gas has improved solubilizing properties that are roughly comparable to those of liquids, yet it has an extremely high diffusion coefficient, resembling that of a natural

gas (substances that are in gaseous phase at SPT conditions) [161]. Compared with liquid solvents, supercritical fluids have several major advantages: the dissolving power of a supercritical fluid solvent depends on its density (highly adjustable by changing the pressure or/and temperature), the supercritical fluid has a higher diffusion coefficient and lower viscosity and surface tension than a liquid solvent, leading to more favorable mass transfer and can be highly selective [154,162–164]. However, the economics and onerous operating conditions of the SFE processes has restricted the applications to some very specialized fields such as essential oil extraction, coffee decaffeination and to university research [154].

1.5. Design of experiments (DOE): a multivariational approach towards process optimization

With the rapid growth of industries and industrial processes, the need for efficient optimization strategies of those processes grows as well. It is important to remark that the main goals of process optimization are: minimization of costs and time, maximization of efficiencies, product quality and productivity [165,166].

When optimizing a process involving *n* hypothetical factors there are three main strategies to achieve this optimization [166]:

- ***Best guess approach:*** An arbitrary set of factors are chosen and tested, maintaining the rest of factors at the same level. Based on the results, the operator will decide to perform or not another round of testing. The two main disadvantages of this method are the possibility of an incorrect initial guess, which implies choosing another set of factors to start testing and can take a long time to find the right combination.
- ***One-factor-at-a-time approach:*** This method consists on selecting a starting point or baseline set of levels for each factor. Then, each factor is varied over its range, maintaining the remaining ones constant at the baseline level. Besides being highly time-consuming, the major drawback of this method is the possibility of failing in taking into account the eventual existence of

interactions between factors. By interaction it is meant the failure of one factor to produce the same effect on the response at different levels of another factor.

- ***Design of experiments (DOE) or experimental design***: This strategy consists in a statistical tool (already used in chemometrics) that uses a multivariational approach (contrary to the previous univariational strategies) and allows the planning of the whole procedure thus minimizing the number of experiments needed. It aims at identifying and investigating the effect of the controlled factors on the response (result of an experiment) with simultaneous minimization of the effects of uncontrolled factors (noise factors) [167]. Additionally, this methodology takes into account the interactions between factors. When planning an experiment, it is important to have integration between process, statistics and good judgment (Figure 13) [165]. In the next paragraphs, two DOE designs (used in this work) will be addressed.

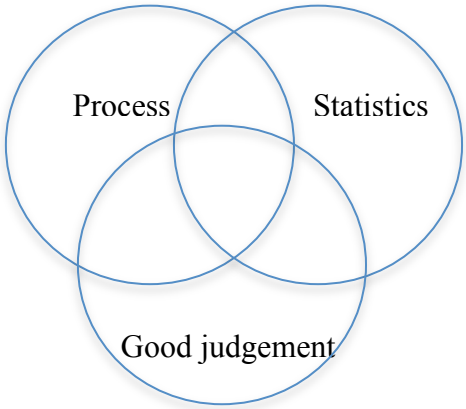

Figure 13 – Necessary interaction in experimental planning.

1.5.1. DOE factorial designs

A factorial design is a type of designed experiment that lets the operator to study the effects that several factors can have on a response. It also allows determining whether interactions between factors are present or not, as well as their statistical significance. This last feature comprises the main reason why the factorial designs are used as a screening method, as it allows the verification of both significance and testing range.

In the studies presented in this work, two-level full factorial designs were always used. In this type of design, 2^n experiments are conducted (where n stands for the number of factors in study), and each factor is tested for levels +1 and -1 (maximum and minimum value of each factor) (Figure 14).

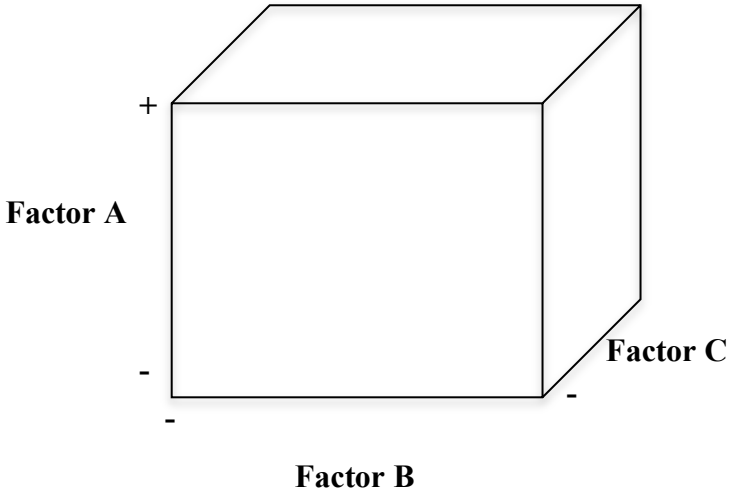

Figure 14 - Representation of a complete factorial design for three factors, each at two levels.

1.5.2. Response surface method (RSM) and Central composite design (CCD)

Although factorial design can be quite useful in terms of screening, its inability to predict the existence of curvature is its main flaw. Therefore, a response surface method (RSM) must be used for proper optimization. The main goal of a RSM design is to allow estimating interactions and even quadratic effects, and therefore, give an idea of the (local) shape of the response surface under investigation.

A central composite design, also known as Box-Wilson Central Composite Design, contains an imbedded factorial or fractional factorial design with center points that is augmented with a group of 'star points' that allow estimation of curvature (Figure 15) [166].

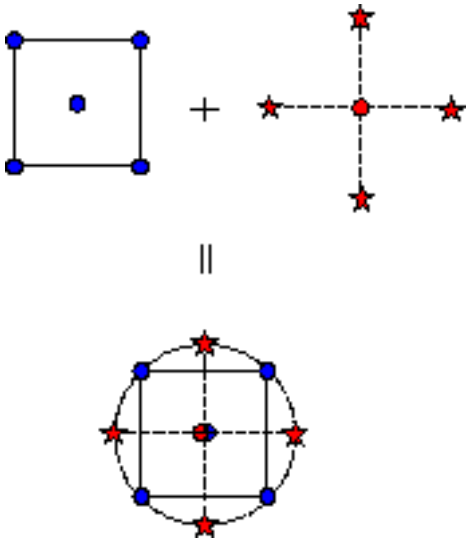

Figure 15 – Generation of a central composite design for two factors.

After the response surface is obtained, the experimental responses are then fitted to a second order model (eq. 2) whose solutions are the optimum conditions and desirability functions.

$$\hat{y}_i = \beta_0 + \sum_{i=1}^{n} \beta_i x_i + \sum_{i=1}^{n} \beta_{ii} x_i^2 + \sum_{i=1}^{n-1} \sum_{j=i+1}^{n} \beta_{ij} x_i x_j \quad (2)$$

where, $\hat{y}_i$ represents the predicted response, β_0 is the intercept coefficient (offset term), β_i is the regression coefficient of the linear effect, β_{ii} is the coefficient of the quadratic effect, β_{ij} represents the coefficient of the interaction effect, x_i and x_j are the independent variables (in coded values) and *n* represents the number of independent variables [166].

1.5.3. DOE applications

Although this methodology was developed in the 1950s, only in recent years it started to be used. Bibliographic data shows an almost exponential increase on its use (Figure 16), specially after 1980 which was possible due to the evolution of microcomputers and availability of statistical software [165]. Currently, DOE is applied all over industry and science, for example: in forensic applications [82,168,169], industrial processes [170] or supercritical extractions optimizations [171].

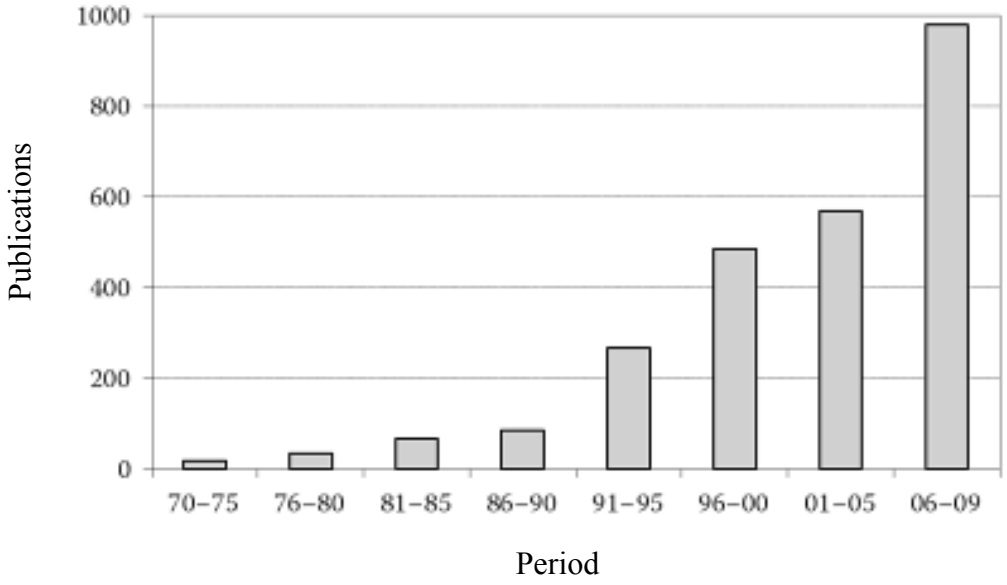

Figure 16 – Number of publications for each 5 years period, which used factorial design and/or response surface analysis (modified from *Experimental design and process optimization* [165]).

1.6. References

[1] "Serviço de Intervação nos Comportamentos Aditivos e nas Dependências," Available at: http://www.sicad.pt/, **n.d.**

[2] W. Sneader. *Drug Discovery: A History*, WILEY, West Sussex, **2005**.

[3] J. A. G. Calabuig. *Medicina Legal Y Toxicología*, Masson, Barcelona, **2005**.

[4] M. Yegles, R. Wenning. *Analytical and Practical Aspects of Drug Testing in Hair*, CRC Press, Boca Raton, **2007**.

[5] "National Institute on Drug Abuse," **n.d.**

[6] "Go Botany," Available at: https://gobotany.newenglandwild.org/species/papaver/somniferum/, **2014**.

[7] G. Cooper, A. Negrusz. *Clarke's Analytical Forensic Toxicology*, Pharmaceutical Press, **2013**.

[8] E. Abel. *Marihuana: The First Twelve Thousand Years*, **1980**.

[9] M. A. Huestis. Pharmacokinetics and Metabolism of the Plant Cannabinoids, Δ 9-Tetrahydrocannibinol, Cannabidiol and Cannabinol, in *Cannabinoids SE - 23*, (Ed: R. Pertwee), Springer Berlin Heidelberg, **2005**, pp. 657–690.

[10] P. R. Stout, J. D. Ropero-Miller, M. R. Baylor, J. M. Mitchell. Morphological changes in human head hair subjected to various drug testing decontamination strategies. *Forensic Sci. Int.*, **2007**, *172*, 164–70.

[11] F. Pragst, M. a Balikova. State of the art in hair analysis for detection of drug and alcohol abuse. *Clin. Chim. Acta.*, **2006**, *370*, 17–49.

[12] L. E. O. R. Goldbaum. BARBITURATE CONCENTRATIONS IN THE SKIN AND HAIR OF. **1953**, 121–129.

[13] M. Barroso, M. Dias, D. N. Vieira, J. A. Queiroz, M. López-Rivadulla, M. Lo. Development and validation of an analytical method for the simultaneous determination of cocaine and its main metabolite, benzoylecgonine, in human hair by gas chromatography/mass spectrometry. *Rapid Commun. Mass Spectrom.*, **2008**, *22*, 3320–6.

[14] G. L. Henderson. Mechanisms of drug incorporation into hair. *Forensic Sci. Int.*, **1993**, *63*, 19–29.

[15] Y. Nakahara, T. Ochiai, R. Kikura. Hair analysis for drugs of abuse. *Arch. Toxicol.*, **1994**, *68*, 54–59.

[16] C. R. Robbins. *Chemical and Physical Behavior of Human Hair*, Springer Berlin Heidelberg, Berlin, Heidelberg, **2012**.

[17] L. Pötsch, G. Skopp, G. Rippin. A comparison of 3 H-cocaine binding on melanin granules and human hair in vitro. *Int. J. Legal Med.*, **1997**, *110*, 55–62.

[18] D. J. Claffey, P. R. Stout, J. A. Ruth. 3H-Nicotine, 3H-Flunitrazepam, and 3H-Cocaine Incorporation Into Melanin: A Model for the Examination of Drug-Melanin Interactions. *J. Anal. Toxicol.*, **2001**, *25*, 607–611.

[19] E. J. Cone, M. J. Hillsgrove, A. J. Jenkins, R. M. Keenan, W. D. Darwin. Sweat Testing for Heroin, Cocaine, and Metabolites. *J. Anal. Toxicol.*, **1994**, *18*, 298–305.

[20] S. L. Kacinko, A. J. Barnes, E. W. Schwilke, E. J. Cone, E. T. Moolchan, M. A. Huestis. Disposition of cocaine and its metabolites in human sweat after controlled cocaine administration. *Clin. Chem.*, **2005**, *51*, 2085–94.

[21] P. Kintz. Excretion of MBDB and BDB in Urine, Saliva, and Sweat Following Single Oral Administration. *J. Anal. Toxicol.*, **1997**, *21*, 570–575.

[22] P. Kintz, A. Tracqui, P. Mangin. Sweat testing for benzodiazepines. *J. Forensic Sci.*, **1996**, *41*, 851–854.

[23] L. Tsanaclis, J. F. C. Wicks. Differentiation between drug use and environmental contamination when testing for drugs in hair. *Forensic Sci. Int.*, **2008**, *176*, 19–22.

[24] A. J. Jenkins. Drug contamination of US paper currency. *Forensic Sci. Int.*, **2001**, *121*, 189–193.

[25] E. S. Lavins, B. D. Lavins, A. J. Jenkins. Cannabis (marijuana) contamination of United States and foreign paper currency. *J. Anal. Toxicol.*, **2004**, *28*, 439–442.

[26] T. H. Jourdan, A. M. Veitenheimer, C. K. Murray, J. R. Wagner. The Quantitation of Cocaine on U.S. Currency: Survey and Significance of the Levels of Contamination. *J. Forensic Sci.*, **2013**, *58*, 616–624.

[27] J. Oyler, W. D. Darwin, E. J. Cone. Cocaine Contamination of United States Paper Currency. *J. Anal. Toxicol.*, **1996**, *20*, 213–216.

[28] U. Kingdom, S. D. Classes, I. Q. Control, E. Q. Control. Recommendations for Hair Testing in Forensic Cases Society of Hair Testing Criteria for mass spectrometric analysis. *Soc. Hair Test.*, **2004**.

[29] C. Moore, F. Guzaldo, T. Donahue. The determination of 11-nor-delta9-tetrahydrocannabinol-9-carboxylic acid (THC-COOH) in hair using negative ion gas chromatography-mass spectrometry and high-volume injection. *J. Anal. Toxicol.*, **2001**, *25*, 555–8.

[30] E. Lendoiro, O. Quintela, A. de Castro, A. Cruz, M. López-Rivadulla, M. Concheiro. Target screening and confirmation of 35 licit and illicit drugs and metabolites in hair by LC-MSMS. *Forensic Sci. Int.*, **2012**, *217*, 207–15.

[31] C. Moore, S. Rana, C. Coulter, F. Feyerherm, H. Prest. Application of Two-Dimensional Gas Chromatography with Electron Capture Chemical Ionization Mass Spectrometry to the Detection of 11-nor- 9-Tetrahydrocannabinol-9-carboxylic Acid (THC-COOH) in Hair. *J. Anal. Toxicol.*, **2006**, *30*, 171–177.

[32] J.-P. Selten, I. J. Bosman, D. de Boer, N. D. Veen, Y. van der Graaf, R. A. . Maes, R. S. Kahn. Hair analysis for cannabinoids and amphetamines in a psychosis incidence study. *Eur. Neuropsychopharmacol.*, **2002**, *12*, 27–30.

[33] G. Skopp, P. Strohbeck-Kuehner, K. Mann, D. Hermann. Deposition of cannabinoids in hair after long-term use of cannabis. *Forensic Sci. Int.*, **2007**, *170*, 46–50.

[34] R. Marsili, S. Martello, M. Felli, S. Fiorina, M. Chiarotti. Hair testing for delta9-THC-COOH by gas chromatography/tandem mass spectrometry in negative chemical ionization mode. *Rapid Commun. Mass Spectrom.*, **2005**, *19*, 1566–8.

[35] M.-L. Pujol, V. Cirimele, P. J. Tritsch, M. Villain, P. Kintz. Evaluation of the IDS One-Step ELISA kits for the detection of illicit drugs in hair. *Forensic Sci. Int.*, **2007**, *170*, 189–92.

[36] E. Han, H. Choi, S. Lee, H. Chung, J. M. Song. A study on the concentrations of 11-nor-Δ(9)-tetrahydrocannabinol-9-carboxylic acid (THCCOOH) in hair root and whole hair. *Forensic Sci. Int.*, **2011**, *210*, 201–5.

[37] E. Han, W. Yang, S. Lee, E. Kim, S. In, H. Choi, S. Lee, H. Chung, J. M. Song. Establishment of the measurement uncertainty of 11-nor-D9-tetrahydrocannabinol-9-carboxylic acid in hair. *Forensic Sci. Int.*, **2011**, *206*, e85–92.

[38] E. Han, H. Choi, S. Lee, H. Chung, J. M. Song. A comparative study on the concentrations of 11-nor-Δ9-tetrahydrocannabinol-9-carboxylic acid (THCCOOH) in head and pubic hair. *Forensic Sci. Int.*, **2011**, *212*, 238–41.

[39] E. Han, Y. Park, E. Kim, S. In, W. Yang, S. Lee, H. Choi, S. Lee, H. Chung, J. M. Song. Simultaneous analysis of Δ(9)-tetrahydrocannabinol and 11-nor-9-carboxy-tetrahydrocannabinol in hair without different sample preparation and derivatization by gas chromatography-tandem mass spectrometry. *J. Pharm. Biomed. Anal.*, **2011**, *55*, 1096–103.

[40] J. Y. Kim, S. Suh, M. K. In, K.-J. Paeng, B. C. Chung. Simultaneous determination of cannabidiol, cannabinol, and \gD9-tetrahydrocannabinol in human hair by gas chromatography-mass spectrometryin human hair by gas chromatography-mass spectrometry. *Arch. Pharm. Res.*, **2005**, *28*, 1086–1091.

[41] J. Y. Kim, J. C. Cheong, J. Il Lee, M. K. In. Improved gas chromatography-negative ion chemical ionization tandem mass spectrometric method for determination of 11-nor-Δ9-tetrahydrocannabinol-9-carboxylic acid in hair using mechanical pulverization and bead-assisted liquid-liquid extraction. *Forensic Sci. Int.*, **2011**, *206*, e99–102.

[42] J. Y. Kim, M. K. In. Determination of 11-nor-Delta(9)-tetrahydrocannabinol-9-carboxylic acid in hair using gas chromatography/tandem mass spectrometry in negative ion chemical ionization mode. *Rapid Commun. Mass Spectrom.*, **2007**, *21*, 1339–42.

[43] F. Musshoff, H. P. Junker, D. W. Lachenmeier, L. Kroener, B. Madea. Fully Automated Determination of Cannabinoids in Hair Samples using Headspace Solid-Phase Microextraction and Gas Chromatography-Mass Spectrometry. *J. Anal. Toxicol.*, **2002**, *26*, 554–560.

[44] F. Musshoff, D. W. Lachenmeier, L. Kroener, B. Madea. Automated headspace solid-phase dynamic extraction for the determination of cannabinoids in hair samples. *Forensic Sci. Int.*, **2003**, *133*, 32–38.

[45] M. A. Huestis, R. A. Gustafson, E. T. Moolchan, A. Barnes, J. a Bourland, S. A. Sweeney, E. F. Hayes, P. M. Carpenter, M. L. Smith. Cannabinoid concentrations in hair from documented cannabis users. *Forensic Sci. Int.*, **2007**, *169*, 129–36.

[46] U. Backofen, W. Hoffmann, F. M. Matysik. Determination of cannabinoids by capillary liquid chromatography with electrochemical detection. *Biomed. Chromatogr.*, **2000**, *14*, 49–52.

[47] G. Merola, S. Gentili, F. Tagliaro, T. Macchia. Determination of different recreational drugs in hair by HS-SPME and GC/MS. *Anal. Bioanal. Chem.*, **2010**, *397*, 2987–95.

[48] A. Pelander, J. Ristimaa, I. Rasanen, E. Vuori, I. Ojanperä. Screening for basic drugs in hair of drug addicts by liquid chromatography/time-of-flight mass spectrometry. *Ther. Drug Monit.*, **2008**, *30*, 717–24.

[49] E. S. Emídio, V. de Menezes Prata, F. J. M. de Santana, H. S. Dórea. Hollow fiber-based liquid phase microextraction with factorial design optimization and gas chromatography-tandem mass spectrometry for determination of cannabinoids in human hair. *J. Chromatogr. B. Analyt. Technol. Biomed. Life Sci.*, **2010**, *878*, 2175–83.

[50] J. C. Domínguez-Romero, J. F. García-Reyes, A. Molina-Díaz. Screening and quantitation of multiclass drugs of abuse and pharmaceuticals in hair by fast liquid chromatography electrospray time-of-flight mass spectrometry. *J. Chromatogr. B. Analyt. Technol. Biomed. Life Sci.*, **2011**, *879*, 2034–42.

[51] T. Nadulski, F. Pragst. Simple and sensitive determination of Delta(9)-tetrahydrocannabinol, cannabidiol and cannabinol in hair by combined silylation, headspace solid phase microextraction and gas chromatography-mass spectrometry. *J. Chromatogr. B. Analyt. Technol. Biomed. Life Sci.*, **2007**, *846*, 78–85.

[52] M. Conti, V. Tazzari, M. Bertona, M. Brambilla, P. Brambilla. Surface-activated chemical ionization combined with electrospray ionization and mass spectrometry for the analysis of cannabinoids in biological samples. Part I: analysis of 11-nor-9-carboxytetrahydro-cannabinol. *Rapid Commun. Mass Spectrom.*, **2011**, *25*, 1552–8.

[53] V. Auwärter, A. Wohlfarth, J. Traber, D. Thieme, W. Weinmann. Hair analysis for Delta9-tetrahydrocannabinolic acid A--new insights into the mechanism of drug incorporation of cannabinoids into hair. *Forensic Sci. Int.*, **2010**, *196*, 10–3.

[54] M. Uhl, H. Sachs. Cannabinoids in hair: strategy to prove marijuana/hashish consumption. *Forensic Sci. Int.*, **2004**, *145*, 143–7.

[55] L. Skender, V. Karačić, I. Brčić, A. Bagarić. Quantitative determination of amphetamines, cocaine, and opiates in human hair by gas chromatography/mass spectrometry. *Forensic Sci. Int.*, **2002**, *125*, 120–126.

[56] S. Paterson, N. McLachlan-Troup, R. Cordero, M. Dohnal, S. Carman. Qualitative Screening for Drugs of Abuse in Hair Using GC-MS. *J. Anal. Toxicol.*, **2001**, *25*, 203–208.

[57] K. Aleksa, P. Walasek, N. Fulga, B. Kapur, J. Gareri, G. Koren. Simultaneous detection of seventeen drugs of abuse and metabolites in hair using solid phase micro extraction (SPME) with GC/MS. *Forensic Sci. Int.*, **2012**, *218*, 31–6.

[58] S. Cristoni, E. Basso, P. Gerthoux, P. Mocarelli, E. Gonella, M. Brambilla, S. Crotti, L. R. Bernardi. Surface-activated chemical ionization ion trap mass spectrometry for the analysis of cocaine and benzoylecgonine in hair after extraction and sample dilution. *Rapid Commun. Mass Spectrom.*, **2007**, *21*, 2515–23.

[59] K. B. Scheidweiler, M. A. Huestis. Simultaneous quantification of opiates, cocaine, and metabolites in hair by LC-APCI-MS/MS. *Anal. Chem.*, **2004**, *76*, 4358–63.

[60] F. C. P. de Toledo, M. Yonamine, R. L. de Moraes Moreau, O. A. Silva. Determination of cocaine, benzoylecgonine and cocaethylene in human hair by solid-phase microextraction and gas chromatography–mass spectrometry. *J. Chromatogr. B*, **2003**, *798*, 361–365.

[61] D.-K. Huang, C. Liu, M.-K. Huang, C.-S. Chien. Simultaneous determination of morphine, codeine, 6-acetylmorphine, cocaine and benzoylecgonine in hair by liquid chromatography/electrospray ionization tandem mass spectrometry. *Rapid Commun. Mass Spectrom.*, **2009**, *23*, 957–62.

[62] M. Montagna, C. Stramesi, C. Vignali, A. Groppi, A. Polettini. Simultaneous hair testing for opiates, cocaine, and metabolites by GC–MS: a survey of applicants for driving licenses with a history of drug use. *Forensic Sci. Int.*, **2000**, *107*, 157–167.

[63] F. . Romolo, M. . Rotolo, I. Palmi, R. Pacifici, A. Lopez. Optimized conditions for simultaneous determination of opiates, cocaine and benzoylecgonine in hair samples by GC–MS. *Forensic Sci. Int.*, **2003**, *138*, 17–26.

[64] M. Felli, S. Martello, R. Marsili, M. Chiarotti. Disappearance of cocaine from human hair after abstinence. *Forensic Sci. Int.*, **2005**, *154*, 96–8.

[65] L. Mercolini, R. Mandrioli, B. Saladini, M. Conti, C. Baccini, M. A. Raggi. Quantitative analysis of cocaine in human hair by HPLC with fluorescence detection. *J. Pharm. Biomed. Anal.*, **2008**, *48*, 456–61.

[66] M. K. K. Nielsen, S. S. Johansen, P. W. Dalsgaard, K. Linnet. Simultaneous screening and quantification of 52 common pharmaceuticals and drugs of abuse in hair using UPLC-TOF-MS. *Forensic Sci. Int.*, **2010**, *196*, 85–92.

[67] M. Montagna, A. Polettini, C. Stramesi, A. Groppi, C. Vignali. Hair analysis for opiates, cocaine and metabolites. *Forensic Sci. Int.*, **2002**, *128*, 79–83.

[68] S. Vogliardi, D. Favretto, G. Frison, S. Maietti, G. Viel, R. Seraglia, P. Traldi, S. D. Ferrara. Validation of a fast screening method for the detection of cocaine in hair by MALDI-MS. *Anal. Bioanal. Chem.*, **2010**, *396*, 2435–40.

[69] W. E. Brewer, R. C. Galipo, K. W. Sellers, S. L. Morgan. Analysis of Cocaine, Benzoylecgonine, Codeine, and Morphine in Hair by Supercritical Fluid Extraction with Carbon Dioxide Modified with Methanol. *Anal. Chem.*, **2001**, *73*, 2371–2376.

[70] S. Gentili, M. Cornetta, T. Macchia. Rapid screening procedure based on headspace solid-phase microextraction and gas chromatography–mass spectrometry for the detection of many recreational drugs in hair. *J. Chromatogr. B*, **2004**, *801*, 289–296.

[71] S. Broecker, S. Herre, F. Pragst. General unknown screening in hair by liquid chromatography-hybrid quadrupole time-of-flight mass spectrometry (LC-QTOF-MS). *Forensic Sci. Int.*, **2012**, *218*, 68–81.

[72] E. Cognard, S. Rudaz, S. Bouchonnet, C. Staub. Analysis of cocaine and three of its metabolites in hair by gas chromatography-mass spectrometry using ion-trap detection for CI/MS/MS. *J. Chromatogr. B. Analyt. Technol. Biomed. Life Sci.*, **2005**, *826*, 17–25.

[73] K. Y. Zhu, K. W. Leung, A. K. L. Ting, Z. C. F. Wong, W. Y. Y. Ng, R. C. Y. Choi, T. T. X. Dong, T. Wang, D. T. W. Lau, K. W. K. Tsim. Microfluidic chip based nano liquid chromatography coupled to tandem mass spectrometry for the determination of abused drugs and metabolites in human hair. *Anal. Bioanal. Chem.*, **2012**, *402*, 2805–15.

[74] E. I. Miller, F. M. Wylie, J. S. Oliver. Simultaneous Detection and Quantification of Amphetamines, Diazepam and its Metabolites, Cocaine and its Metabolites, and Opiates in Hair by LC-ESI-MS-MS Using a Single Extraction Method. *J. Anal. Toxicol.*, **2008**, *32*, 457–469.

[75] H. Miyaguchi, H. Inoue. Determination of amphetamine-type stimulants, cocaine and ketamine in human hair by liquid chromatography/linear ion trap-Orbitrap hybrid mass spectrometry. *Analyst*, **2011**, *136*, 3503–11.

[76] D. Favretto, S. Vogliardi, G. Stocchero, A. Nalesso, M. Tucci, S. D. Ferrara. High performance liquid chromatography-high resolution mass spectrometry and micropulverized extraction for the quantification of amphetamines, cocaine, opioids, benzodiazepines, antidepressants and hallucinogens in 2.5 mg hair samples. *J. Chromatogr. A*, **2011**, *1218*, 6583–95.

[77] S. Hegstad, H. Z. Khiabani, L. Kristoffersen, N. Kunoe, P. P. Lobmaier, A. S. Christophersen. Drug Screening of Hair by Liquid Chromatography-Tandem Mass Spectrometry. *J. Anal. Toxicol.*, **2008**, *32*, 364–372.

[78] T. Cairns, V. Hill, M. Schaffer, W. Thistle. Removing and identifying drug contamination in the analysis of human hair. *Forensic Sci. Int.*, **2004**, *145*, 97–108.

[79] M. Sergi, S. Napoletano, C. Montesano, R. Iofrida, R. Curini, D. Compagnone. Pressurized-liquid extraction for determination of illicit drugs in hair by LC-MS-MS. *Anal. Bioanal. Chem.*, **2013**, *405*, 725–35.

[80] R. Cordero, S. Paterson. Simultaneous quantification of opiates, amphetamines, cocaine and metabolites and diazepam and metabolite in a single hair sample using GC-MS. *J. Chromatogr. B. Analyt. Technol. Biomed. Life Sci.*, **2007**, *850*, 423–31.

[81] M. Kłys, S. Rojek, J. Kulikowska, E. Bozek, M. Scisłowski. Usefulness of multi-parameter opiates-amphetamines-cocainics analysis in hair of drug users for the evaluation of an abuse profile by means of LC-APCI-MS-MS. *J. Chromatogr. B. Analyt. Technol. Biomed. Life Sci.*, **2007**, *854*, 299–307.

[82] P. Fernández, M. Lago, R. A. Lorenzo, A. M. Carro, A. M. Bermejo, M. J. Tabernero. Optimization of a rapid microwave-assisted extraction method for the simultaneous determination of opiates, cocaine and their metabolites in human hair. *J. Chromatogr. B. Analyt. Technol. Biomed. Life Sci.*, **2009**, *877*, 1743–50.

[83] F. Tagliaro, R. Valentini, G. Manetto, F. Crivellente, G. Carli, M. Marigo. Hair analysis by using radioimmunoassay, high-performance liquid chromatography and capillary electrophoresis to investigate chronic exposure to heroin, cocaine and/or ecstasy in applicants for driving licences. *Forensic Sci. Int.*, **2000**, *107*, 121–128.

[84] K. Lachenmeier, F. Musshoff, B. Madea. Determination of opiates and cocaine in hair using automated enzyme immunoassay screening methodologies followed by gas chromatographic-mass spectrometric (GC-MS) confirmation. *Forensic Sci. Int.*, **2006**, *159*, 189–99.

[85] V. Thibert, P. Legeay, F. Chapuis-Hugon, V. Pichon. Synthesis and characterization of molecularly imprinted polymers for the selective extraction of cocaine and its metabolite benzoylecgonine from hair extract before LC-MS analysis. *Talanta*, **2012**, *88*, 412–9.

[86] Y.-H. Wu, K.-L. Lin, S.-C. Chen, Y.-Z. Chang. Integration of GC/EI-MS and GC/NCI-MS for simultaneous quantitative determination of opiates, amphetamines, MDMA, ketamine, and metabolites in human hair. *J. Chromatogr. B. Analyt. Technol. Biomed. Life Sci.*, **2008**, *870*, 192–202.

[87] Y.-H. Wu, K.-L. Lin, S.-C. Chen, Y.-Z. Chang. Simultaneous quantitative determination of amphetamines, ketamine, opiates and metabolites in human hair by gas chromatography/mass spectrometry. *Rapid Commun. Mass Spectrom.*, **2008**, *22*, 887–97.

[88] B. Guthery, T. Bassindale, A. Bassindale, C. T. Pillinger, G. H. Morgan. Qualitative drug analysis of hair extracts by comprehensive two-dimensional gas chromatography/time-of-flight mass spectrometry. *J. Chromatogr. A*, **2010**, *1217*, 4402–10.

[89] L. Tsanaclis, J. Nutt, K. Bagley, S. Bevan, J. Wicks. Differentiation between consumption and external contamination when testing for cocaine and cannabis in hair samples. *Drug Test. Anal.*, **2014**, *6 Suppl 1*, 37–41.

[90] Y.-H. Lin, M.-R. Lee, R.-J. Lee, W.-K. Ko, S.-M. Wu. Hair analysis for methamphetamine, ketamine, morphine and codeine by cation-selective exhaustive injection and sweeping micellar electrokinetic chromatography. *J. Chromatogr. A*, **2007**, *1145*, 234–40.

[91] M. Barroso, M. Dias, D. N. Vieira, M. López-Rivadulla, J. a Queiroz. Simultaneous quantitation of morphine, 6-acetylmorphine, codeine, 6-acetylcodeine and tramadol in hair using mixed-mode solid-phase extraction and gas chromatography-mass spectrometry. *Anal. Bioanal. Chem.*, **2010**, *396*, 3059–69.

[92] S. Keskin, D. Kayrak-Talay, U. Akman, Ö. Hortaçsu. A review of ionic liquids towards supercritical fluid applications. *J. Supercrit. Fluids*, **2007**, *43*, 150–180.

[93] S. Sugden, H. Wilkins. CLXVII.?The parachor and chemical constitution. Part XII. Fused metals and salts. *J. Chem. Soc.*, **1929**, 1291.

[94] J. Gorman. Faster, Better, Cleaner? *Sci. News*, **2001**, *160*, 156.

[95] A. A. Fannin, D. A. Floreani, L. A. King, J. S. Landers, B. J. Piersma, D. J. Stech, R. L. Vaughn, J. S. Wilkes. Properties of 1,3-dialkylimidazolium chloride-aluminum chloride ionic liquids. 2. Phase transitions, densities, electrical conductivities, and viscosities. *J. Phys. Chem.*, **1984**, *88*, 2614–2621.

[96] J. S. Wilkes, J. A. Levisky, R. A. Wilson, C. L. Hussey. Dialkylimidazolium chloroaluminate melts: a new class of room-temperature ionic liquids for electrochemistry, spectroscopy and synthesis. *Inorg. Chem.*, **1982**, *21*, 1263–1264.

[97] J. Dupont. On the solid, liquid and solution structural organization of imidazolium ionic liquids. *J. Braz. Chem. Soc.*, **2004**, *15*, 341–350.

[98] R. Renner. Ionic liquids: An industrial cleanup solution. *Environ. Sci. Technol.*, **2001**, *35*, 410A–413A.

[99] T. Welton. Room-Temperature Ionic Liquids. Solvents for Synthesis and Catalysis. *Chem. Rev.*, **1999**, *99*, 2071–2084.

[100] J. P. Hallett, T. Welton. Room-temperature ionic liquids: solvents for synthesis and catalysis. 2. *Chem. Rev.*, **2011**, *111*, 3508–76.

[101] J. Restolho, J. L. Mata, B. Saramago. On the interfacial behavior of ionic liquids: surface tensions and contact angles. *J. Colloid Interface Sci.*, **2009**, *340*, 82–86.

[102] J. Restolho, A. P. Serro, J. L. Mata, B. Saramago. Viscosity and Surface Tension of 1-Ethanol-3-methylimidazolium Tetrafluoroborate and 1-Methyl-3-octylimidazolium Tetrafluoroborate over a Wide Temperature Range. *J. Chem. Eng. Data*, **2009**, *54*, 950–955.

[103] K. E. Gutowski, G. A. Broker, H. D. Willauer, J. G. Huddleston, R. P. Swatloski, R. D. Rogers. Controlling the aqueous miscibility of ionic liquids: Aqueous biphasic systems of water-miscible ionic liquids and water structuring salts for recycle, metathesis, and separations. **2000**, 2000–2001.

[104] C. Liu, X. Li, Z. Jin. Progress in thermoregulated liquid/liquid biphasic catalysis. *Catal. Today*, **2014**, DOI 10.1016/j.cattod.2014.07.060.

[105] M. Domínguez-Pérez, L. Tomé. Extraction of biomolecules using aqueous biphasic systems formed by ionic liquids and aminoacids. *Sep. ...*, **2010**, *72*, 85–91.

[106] J. H. Santos, F. A. E Silva, S. P. M. Ventura, J. A. P. Coutinho, R. L. de Souza, C. M. F. Soares, A. S. Lima. Ionic liquid-based aqueous biphasic systems as a versatile tool for the recovery of antioxidant compounds. *Biotechnol. Prog.*, **2014**, DOI 10.1002/btpr.2000.

[107] K. E. Gutowski, G. G. A. Broker, H. D. Willauer, J. G. Huddleston, R. P. Swatloski, J. D. Holbrey, R. D. Rogers. Controlling the aqueous miscibility of ionic liquids: aqueous biphasic systems of water-miscible ionic liquids and water-structuring salts for recycle, metathesis, and separations. *J. Am. Chem. Soc.*, **2003**, *125*, 6632–3.

[108] C. F. Poole, S. K. Poole. Extraction of organic compounds with room temperature ionic liquids. *J. Chromatogr. A*, **2010**, *1217*, 2268–86.

[109] C. Hardacre, V. Parvulescu. *Catalysis in Ionic Liquirds: From Catalyst Synthesis to Application*, Royal Society Of Chemistry, **2014**.

[110] J. Estager, J. D. Holbrey, M. Swadźba-Kwaśny. Halometallate ionic liquids--revisited. *Chem. Soc. Rev.*, **2014**, *43*, 847–86.

[111] M.-D. Bermúdez, A.-E. Jiménez, J. Sanes, F.-J. Carrión. Ionic liquids as advanced lubricant fluids. *Molecules*, **2009**, *14*, 2888–908.

[112] F. Zhou, Y. Liang, W. Liu. Ionic liquid lubricants: designed chemistry for engineering applications. *Chem. Soc. Rev.*, **2009**, *38*, 2590–9.

[113] A. García, R. González, A. Hernández Battez, J. L. Viesca, R. Monge, A. Fernández-González, M. Hadfield. Ionic liquids as a neat lubricant applied to steel–steel contacts. *Tribol. Int.*, **2014**, *72*, 42–50.

[114] A. M. Cione, O. a Mazyar, B. D. Booth, C. McCabe, G. K. Jennings. Deposition and Wettability of [bmim][triflate] on Self-Assembled Monolayers. *J. Phys. Chem. C*, **2009**, *113*, 2384–2392.

[115] I. Minami. Ionic liquids in tribology. *Molecules*, **2009**, *14*, 2286–305.

[116] I. M. Shahrul, I. M. Mahbubul, S. S. Khaleduzzaman, R. Saidur, M. F. M. Sabri. A comparative review on the specific heat of nanofluids for energy perspective. *Renew. Sustain. Energy Rev.*, **2014**, *38*, 88–98.

[117] J. Liu, F. Wang, L. Zhang, X. Fang, Z. Zhang. Thermodynamic properties and thermal stability of ionic liquid-based nanofluids containing graphene as advanced heat transfer fluids for medium-to-high-temperature applications. *Renew. Energy*, **2014**, *63*, 519–523.

[118] A. Heintz. Recent developments in thermodynamics and thermophysics of non-aqueous mixtures containing ionic liquids. A review. *J. Chem. Thermodyn.*, **2005**, *37*, 525–535.

[119] C. P. Fredlake, J. M. Crosthwaite, D. G. Hert, S. N. V. K. Aki, J. F. Brennecke. Thermophysical Properties of Imidazolium-Based Ionic Liquids. *J. Chem. Eng. Data*, **2004**, *49*, 954–964.

[120] J. L. Anderson, J. K. Dixon, E. J. Maginn, J. F. Brennecke. Measurement of SO2 solubility in ionic liquids. *J. Phys. Chem. B*, **2006**, *110*, 15059–62.

[121] J. Huang, A. Riisager, P. Wasserscheid, R. Fehrmann. Reversible physical absorption of SO2 by ionic liquids. *Chem. Commun. (Camb).*, **2006**, 4027–9.

[122] W. Wu, B. Han, H. Gao, Z. Liu, T. Jiang, J. Huang. Desulfurization of Flue Gas: SO2 Absorption by an Ionic Liquid. *Angew. Chemie*, **2004**, *116*, 2469–2471.

[123] W. Wu, B. Han, H. Gao, Z. Liu, T. Jiang, J. Huang. Desulfurization of flue gas: SO(2) absorption by an ionic liquid. *Angew. Chem. Int. Ed. Engl.*, **2004**, *43*, 2415–7.

[124] J. Tang, H. Tang, W. Sun, H. Plancher, M. Radosz, Y. Shen. Poly(ionic liquid)s: a new material with enhanced and fast CO2 absorption. *Chem. Commun. (Camb).*, **2005**, 3325–7.

[125] J. Zhang, S. Zhang, K. Dong, Y. Zhang, Y. Shen, X. Lv. Supported absorption of CO2 by tetrabutylphosphonium amino acid ionic liquids. *Chemistry*, **2006**, *12*, 4021–6.

[126] E. D. Bates, R. D. Mayton, I. Ntai, J. H. Davis. CO 2 Capture by a Task-Specific Ionic Liquid. *J. Am. Chem. Soc.*, **2002**, *124*, 926–927.

[127] M. B. Shiflett, A. Yokozeki. Solubility and diffusivity of hydrofluorocarbons in room-temperature ionic liquids. *AIChE J.*, **2006**, *52*, 1205–1219.

[128] P. S. Kulkarni, L. C. Branco, J. G. Crespo, C. a M. Afonso. A comparative study on absorption and selectivity of organic vapors by using ionic liquids based on imidazolium, quaternary ammonium, and guanidinium cations. *Chem. - A Eur. J.*, **2007**, *13*, 8470–7.

[129] P. S. Kulkarni, L. C. Branco, J. G. Crespo, C. A. M. Afonso. Capture of dioxins by ionic liquids. *Environ. Sci. Technol.*, **2008**, *42*, 2570–4.

[130] L. Cammarata, S. G. Kazarian, P. a. Salter, T. Welton. Molecular states of water in room temperature ionic liquidsElectronic Supplementary Information available. See http://www.rsc.org/suppdata/cp/b1/b106900d/. *Phys. Chem. Chem. Phys.*, **2001**, *3*, 5192–5200.

[131] K. O. Evans. Supported phospholipid bilayer interaction with components found in typical room-temperature ionic liquids - a QCM-D and AFM Study. *Int. J. Mol. Sci.*, **2008**, *9*, 498–511.

[132] J. Restolho, J. L. Mata, B. Saramago. Choline based ionic liquids: Interfacial properties of RTILs with strong hydrogen bonding. *Fluid Phase Equilib.*, **2012**, *322-323*, 142–147.

[133] J. Pernak, A. Syguda, I. Mirska, A. Pernak, J. Nawrot, A. Pradzyńska, S. T. Griffin, R. D. Rogers. Choline-derivative-based ionic liquids. *Chem. - A Eur. J.*, **2007**, *13*, 6817–27.

[134] M. Zakrewsky, K. S. Lovejoy, T. L. Kern, T. E. Miller, V. Le, A. Nagy, A. M. Goumas, R. S. Iyer, R. E. Del Sesto, A. T. Koppisch, D. T. Fox, S. Mitragotri. Ionic liquids as a class of materials for transdermal delivery and pathogen neutralization. *Proc. Natl. Acad. Sci.*, **2014**, *111*, 13313–13318.

[135] F. a E Silva, F. Siopa, B. F. H. T. Figueiredo, A. M. M. Gonçalves, J. L. Pereira, F. Gonçalves, J. a P. Coutinho, C. a M. Afonso, S. P. M. Ventura. Sustainable design for environment-friendly mono and dicationic cholinium-based ionic liquids. *Ecotoxicol. Environ. Saf.*, **2014**, *108*, 302–10.

[136] G. Tao, L. He, W. Liu, L. Xu, W. Xiong, T. Wang, Y. Kou. Preparation, characterization and application of amino acid-based green ionic liquids. *Green Chem.*, **2006**, *8*, 639.

[137] K. Fukumoto, M. Yoshizawa, H. Ohno. Room temperature ionic liquids from 20 natural amino acids. *J. Am. Chem. Soc.*, **2005**, *127*, 2398–9.

[138] G. Tao, L. He, N. Sun, Y. Kou. New generation ionic liquids: cations derived from amino acids. *Chem. Commun.*, **2005**, 3562–4.

[139] H. Ohno, K. Fukumoto. Amino acid ionic liquids. *Acc. Chem. Res.*, **2007**, *40*, 1122–9.

[140] W. Gouveia, T. F. Jorge, S. Martins, M. Meireles, M. Carolino, C. Cruz, T. V Almeida, M. E. M. Araújo. Toxicity of ionic liquids prepared from biomaterials. *Chemosphere*, **2014**, *104*, 51–6.

[141] S. P. M. Ventura, F. a e Silva, A. M. M. Gonçalves, J. L. Pereira, F. Gonçalves, J. a P. Coutinho. Ecotoxicity analysis of cholinium-based ionic liquids to Vibrio fischeri marine bacteria. *Ecotoxicol. Environ. Saf.*, **2014**, *102*, 48–54.

[142] E. Guenther. *The Essential Oils*, D. Van Nostrand Company, Inc., New York, **1952**.

[143] S. A. A. J. van de Braak, G. C. J. J. Leijten, A. Institute. *Essential Oils and Oleoresins : A Survey in the Netherlands and Other Major Markets in the European Union*, CBI, Centre For The Promotion Of Imports From Developing Countries, Rotterdam, **1994**.

[144] F. Bakkali, S. Averbeck, D. Averbeck, M. Idaomar. Biological effects of essential oils--a review. *Food Chem. Toxicol.*, **2008**, *46*, 446–75.

[145] H. Surburg, J. Panten. *Common Fragrance and Flavor Materials*, Wiley-VCH Verlag GmbH & Co. KGaA, Weinheim, FRG, **2006**.

[146] Z. Xiao, W. Liu, G. Zhu, R. Zhou, Y. Niu. A review of the preparation and application of flavour and essential oils microcapsules based on complex coacervation technology. *J. Sci. Food Agric.*, **2014**, *94*, 1482–94.

[147] I. M. Martins, M. F. Barreiro, M. Coelho, A. E. Rodrigues. Microencapsulation of essential oils with biodegradable polymeric carriers for cosmetic applications. *Chem. Eng. J.*, **2014**, *245*, 191–200.

[148] G. Y. Zhu, Z. B. Xiao, R. J. Zhou, F. P. Yi. Fragrance and Flavor Microencapsulation Technology. *Adv. Mater. Res.*, **2012**, *535-537*, 440–445.

[149] D. Poncelet. Microencapsulation: fundamentals, methods and applications, in *Surf. Chem. Biomed. Environ. Sci.*, (Eds: J. Blitz, V. Gun'ko), Springer, Heidelberg, **2006**, pp. 23–34.

[150] A. MANABE, S. NAKAYAMA, K. SAKAMOTO. Effects of essential oils on erythrocytes and hepatocytes from rats and dipalmitoyl phosphatidylcholine-liposomes. *Jpn. J. Pharmacol.*, **1987**, *44*, 77–84.

[151] S. D. Cox, C. M. Mann, J. L. Markham, H. C. Bell, J. E. Gustafson, J. R. Warmington, S. G. Wyllie. The mode of antimicrobial action of the essential oil of Melaleuca alternifolia (tea tree oil). *J. Appl. Microbiol.*, **2001**, *88*, 170–175.

[152] M. J. MENDOZA-YEPES, L. E. SANCHEZ-HIDALGO, G. MAERTENS, F. MARIN-INIESTA. INHIBITION OF LISTERIA MONOCYTOGENES AND OTHER BACTERIA BY A PLANT ESSENTIAL OIL (DMC) IN SPANISH SOFT CHEESE. *J. Food Saf.*, **1997**, *17*, 47–55.

[153] L. S. Nerio, J. Olivero-Verbel, E. Stashenko. Repellent activity of essential oils: a review. *Bioresour. Technol.*, **2010**, *101*, 372–8.

[154] L. Wang, C. L. Weller. Recent advances in extraction of nutraceuticals from plants. *Trends Food Sci. Technol.*, **2006**, *17*, 300–312.

[155] M. . Luque de Castro, L. . García-Ayuso. Soxhlet extraction of solid materials: an outdated technique with a promising innovative future. *Anal. Chim. Acta*, **1998**, *369*, 1–10.

[156] "List of hazardous air pollutants," Available at: http://www.epa.gov/ttnatw01/188polls.html, **2014**.

[157] J. . Luque-García, M. . Luque de Castro. Ultrasound: a powerful tool for leaching. *Trends Anal. Chem.*, **2003**, *22*, 41–47.

[158] C. Sparr Eskilsson, E. Björklund. Analytical-scale microwave-assisted extraction. *J. Chromatogr. A*, **2000**, *902*, 227–250.

[159] A. Brachet, S. Rudaz, L. Mateus, P. Christen, J.-L. Veuthey. Optimisation of accelerated solvent extraction of cocaine and benzoylecgonine from coca leaves. *J. Sep. Sci.*, **2001**, *24*, 865–873.

[160] B. Kaufmann, P. Christen. Recent extraction techniques for natural products: microwave-assisted extraction and pressurised solvent extraction. *Phytochem. Anal.*, **2002**, *13*, 105–13.

[161] I. D. A. J. Starmans, H. H. Nijhuis. metabolites from plant material : A review. *Trends Food Sci. Technol.*, **1996**, *7*, 191–197.

[162] E. Reverchon. Supercritical fluid extraction and fractionation related products. *J. Supercrit. Fluids*, **1997**, *10*, 1–37.

[163] S. M. Pourmortazavi, S. S. Hajimirsadeghi. Supercritical fluid extraction in plant essential and volatile oil analysis. *J. Chromatogr. A*, **2007**, *1163*, 2–24.

[164] M. Lo Presti, S. Ragusa, A. Trozzi, P. Dugo, F. Visinoni, A. Fazio, G. Dugo, L. Mondello. A comparison between different techniques for the isolation of rosemary essential oil. *J. Sep. Sci.*, **2005**, *28*, 273–80.

[165] M. I. Rodrigues, A. F. Iemma. *Experimental Design and Process Optimization*, Taylor & Francis, Boca Raton, **2014**.

[166] D. C. Montgomery. *Design and Analysis of Experiments*, John Whiley & Sons, Inc, New York, **2001**.

[167] J. N. Miller, J. C. Miller. *Statistics and Chemometrics for Analytical Chemistry*, Pearson / Prentice Hall, Harlow, **2000**.

[168] S. Costa, M. Barroso, a Castañera, M. Dias. Design of experiments, a powerful tool for method development in forensic toxicology: application to the optimization of urinary morphine 3-glucuronide acid hydrolysis. *Anal. Bioanal. Chem.*, **2010**, *396*, 2533–42.

[169] L. Kristoffersen, L.-E. Stormyhr, A. Smith-Kielland. Headspace gas chromatographic determination of ethanol: the use of factorial design to study effects of blood storage and headspace conditions on ethanol stability and acetaldehyde formation in whole blood and plasma. *Forensic Sci. Int.*, **2006**, *161*, 151–7.

[170] N. Alagumurthi, K. Palaniradja, V. Soundararajan. Optimization of Grinding Process Through Design of Experiment (DOE)—A Comparative Study. *Mater. Manuf. Process.*, **2006**, *21*, 19–21.

[171] K. M. Sharif, M. M. Rahman, J. Azmir, A. Mohamed, M. H. a. Jahurul, F. Sahena, I. S. M. Zaidul. Experimental design of supercritical fluid extraction – A review. *J. Food Eng.*, **2014**, *124*, 105–116.

Chapter 2 – Hair decontamination: opiates

This chapter describes the development and optimization of a contactless hair decontamination procedure and its application to opiates.

The presented results were published in the peer-reviewed international journal Drug Testing and Analysis DOI: 10.1002/dta.1695 (in press) and in the patent application PCT/IB2012/051125

Table of contents

2.1. Decontamination process for the removal of opiates contamination

As mentioned in Chapter 1, hair has assumed a very important role in terms of toxicological research, mainly because of its large detection window (allowing drug detection for months or even years after consumption) for a large spectrum of drugs of abuse (e.g. opiates, cocaine, cannabinoids, etc.). Nevertheless, a cleaning pre-step is usually needed prior to analysis to ensure that the hair's surface is free of externally deposited contaminants (particularly in the case of smoked drugs), which are not derived from active consumption [1]. This pre-cleaning or decontamination step is determinant, because of the legal implications that a positive result may have on the individual's life or freedom. So far, and to our knowledge, the only published method that seems to fully fulfill the Society for Hair Testing requirements is that proposed by Cairns et al. [2] and routinely used for the analysis of thousands of samples each year (see section 1.2.2 in Chapter 1). The main disadvantages of this method are the number of human resources needed and the fact that it is time consuming (at least, 3 h 45 min).

In this work, the authors proved the ability of the ILs to adsorb compounds from the surrounding atmosphere. Based on this ability, we decided to use a Y-shaped glass flask (Figure 2.1) that would prevent physical contact between the hair and the IL, preserving sample integrity. It is important to stress that this contact between the IL and the hair at the tested temperatures would result in the dissolution of the hair matrix, impairing its further usage.

Bearing this is in mind and taking the work of Kulkarni *et al.* [3] as the starting point, we developed a novel process in which a small amount of IL (ca. 100 mg) is used to efficiently remove low volatile compounds, in this case opiates, from the surface of hair samples (ca. 100 mg), without any physical contact between the IL and the hair, which is the key feature of the process. Figure 2.1 shows the Y-shaped glass flask that

was used in this work. Furthermore, the whole process was optimized by means of the DOE approach and validated according to the procedure presented by Cairns et al [2].

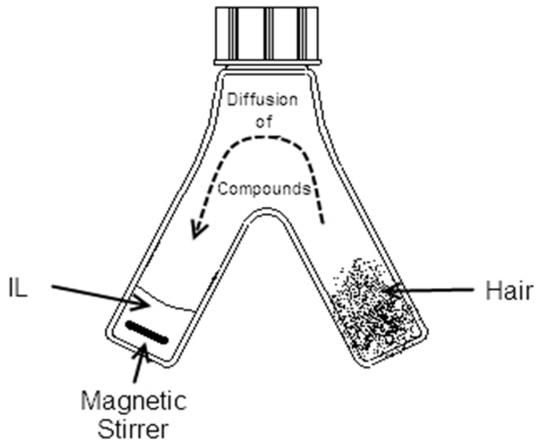

Figure 2.1 - Schematic representation of the proposed decontamination.

2.2. Results and discussion

2.2.1. Hair contamination

Contaminated hair samples are not easily obtained, and therefore we have chosen to prepare "positive" externally contaminated hair samples. These "positive" hair samples were prepared using the method described by Cairns et al. [2]. Briefly, blab la bla…

The sample SH0, whose analyte concentrations were 1 $ng.mg^{-1}$ of morphine and 0.52 $ng.mg^{-1}$ of 6-MAM (coefficient of variation of 10.00 and 13.46 %, respectively), was considered suitable for the decontamination experiments, since it mimics well an authentic contamination situation (> 0.5 $ng.mg^{-1}$ of 6-MAM and a 6-MAM to morphine ratio below 1.3). Thus, when submitted to the wash criterion proposed by Cairns et al. [2], this sample batch failed to be considered as positive.

2.2.2. Screening of ILs

Forty ILs with different cations and anions were tested at 100 ºC for 96 h to decontaminate SH0 samples. This temperature was selected in order to ensure the absence of decomposition (> 130 ºC) of both ILs [4] and hair [5].

A first trial involving six ionic liquids with different cations and anions was carried out at 100 ºC for 96 h. These first experiments revealed that it was actually possible to remove opiates (low volatile compounds) from the hair surface. Furthermore, different behaviors were observed: some of the tested ILs yielded high extraction efficiencies[1] for all analytes (e.g. $[C_2OHMIM][BF_4]$ and [P(6,6,6,14)][Cl]), while others (e.g. Aliquat 338 and $[OMIM][BF_4]$) showed analyte-selectivity (Figure 2.2).

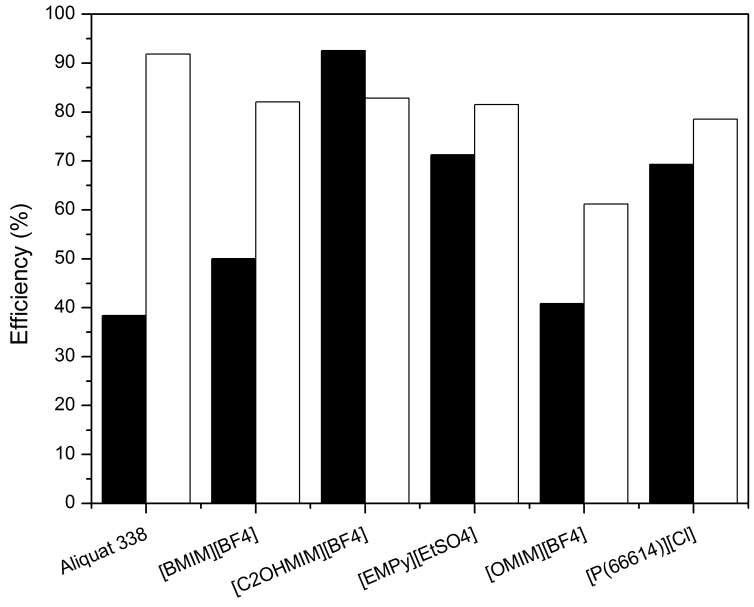

Figure 2.2. First ILs screening trial (96 h, 100 ºC). Morphine (■), 6-MAM (□).

These results were definitely encouraging and led us to test a large and diversified group of ILs, which were as representative as possible of the most common IL families [6]. These results were grouped in terms of the cation type and will be discussed below.

[1] $\text{Efficiency } (\%) = \frac{[\text{contaminated hair}] - [\text{decontaminated hair}]}{[\text{contaminated hair}]} \times 100$

- **Phosphonium based ILs**

In this group, only three ILs with the same cation were studied (Figure 2.3). All liquids, despite the differences in terms of the anion, seemed to have a high affinity for the studied opiates (efficiency > 70 %).

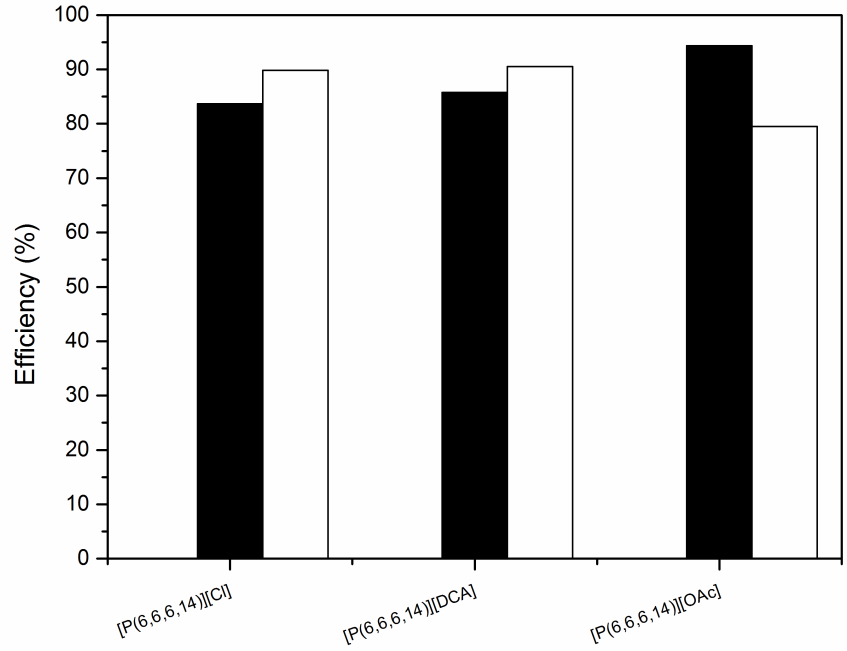

Figure 2.3. Decontamination efficiencies obtained for the tested phosphonium based ILs (96 h, 100 ^{o}C). Morphine (■), 6-MAM (□).

- **1-Methyl-3-alkylimidazolium based ILs**

1-Alkyl-3-methylimidazolium based ILs are probably the most investigated group of ILs and the largest one in this study. Results obtained for this group are depicted in Figure 2.4. Some promising ILs were found, such as $[C_2OHMIM][BF_4]$, $[C_3OMIM][OTf]$, $[C_3MIM][Cl]$, $[BzMIM][NTf_2]$ and [OMIM][TSA]. A deeper analysis of the results seems to reveal a certain trend within the liquids varying in the alky chain length, i.e. an increase in the number of carbons of the side chain led to a

decrease in the extraction efficiency (e.g. [BMIM][OAc] < [EMIM][OAc]; [OMIM][BF_4] < [BMIM][BF_4] in this case only for 6-MAM).

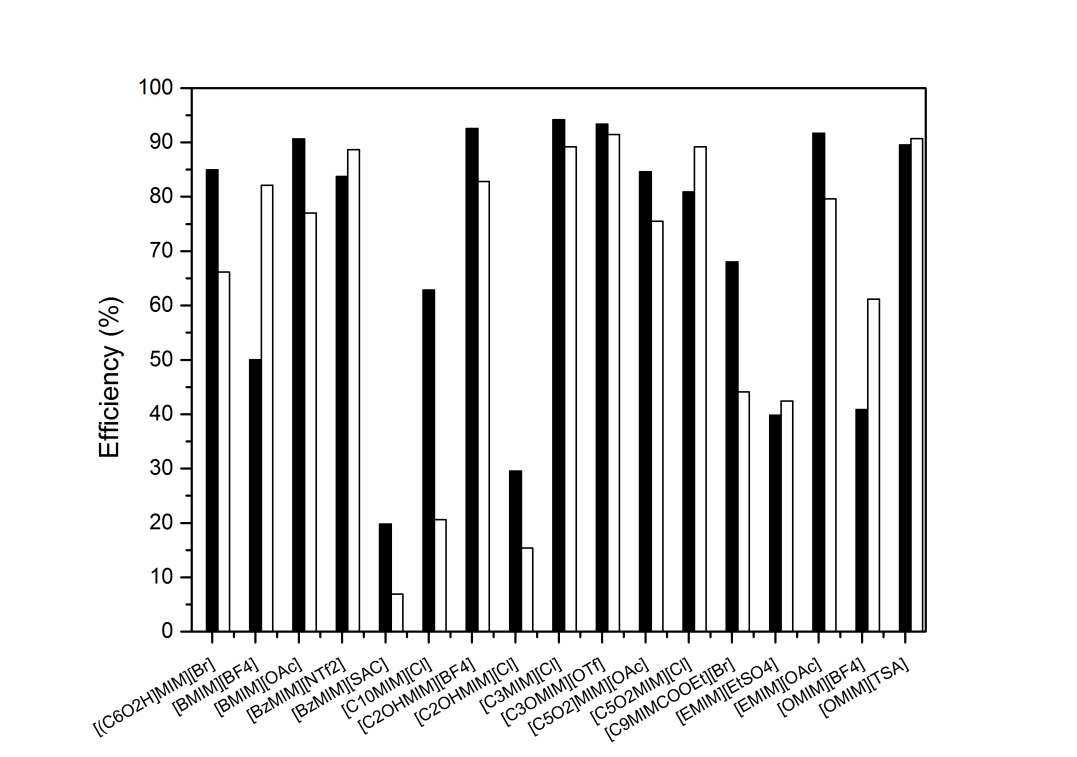

Figure 2.4. Decontamination efficiencies obtained for the tested 1-methyl-3-alkylimidazolium based ILs (96 h, 100 ^{o}C). Morphine (■), 6-MAM (□).

• 1,3 - Dibenzylimidazolium based ILs

For the group of 1,3-Dibenzylimidazolium based ILs (Figure 2.5), only the anion was changed. The good affinity of these ILs for codeine (with the exception of [Bz_2IM][DCA]) should be highlighted. In general terms, [Bz_2IM][TSA] presented extraction efficiencies above 70% for the two studied opiates.

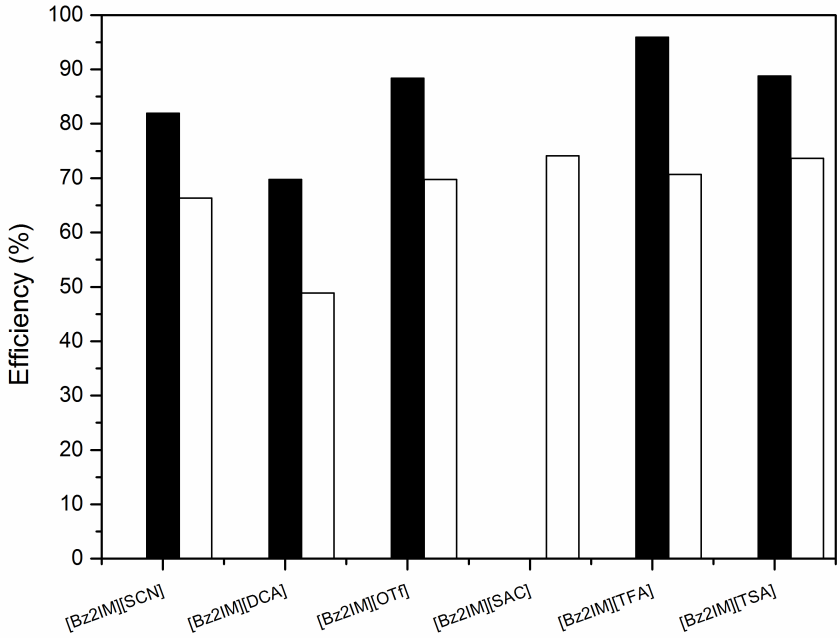

Figure 2.5. Decontamination efficiencies obtained for the tested 1,3-dibenzylimidazolium based ILs (96 h, 100 ^{o}C). Morphine (■), 6-MAM (□).

- **1-Alkyl-3-methylpyridinium based ILs**

In the case of 1-Alkyl-3-methylpyridinium based ILs (Figure 2.6), two ILs were tested, and the results were not very promising. [EMPy][$EtSO_4$] worked reasonably well for the extraction of both morphine and 6-MAM.

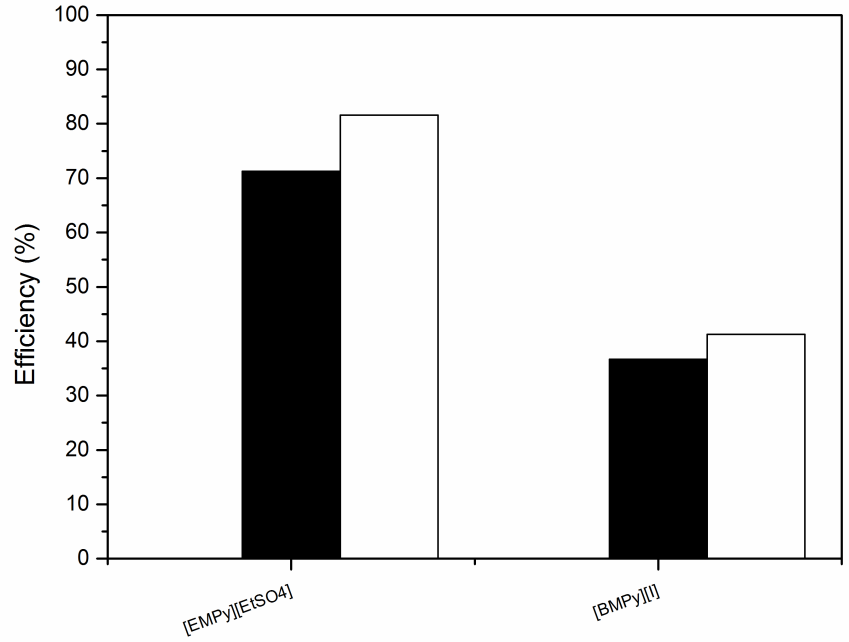

Figure 2.6. Decontamination efficiencies obtained for the tested 1-methylpyridinium based ILs (96 h, 100 ^{o}C). Morphine (■), 6-MAM (□).

- **Quaternary ammonium based ILs**

In the quaternary ammonium based ILs, both guanidinium (Figure 2.7) and trialkylammonium based ILs (Figure 2.8) were included. For the guanidinium group, besides the high efficiencies presented by [$TMGC_7$][I], we want to highlight the evidence of analyte selectivity presented by this method, since [dHDMG][OAc] extracts only 6-MAM and [$(C_3O)_4$DMG][Cl] does not extract 6-MAM at all. These results are definitely encouraging and create the opportunity for the development of new analytical processes outside the field of hair decontamination. Concerning trialkylammonium based ILs, the results were satisfactory in general but [PhTMEA][OTf] stands out with extraction efficiencies above 90% for the studied opiates.

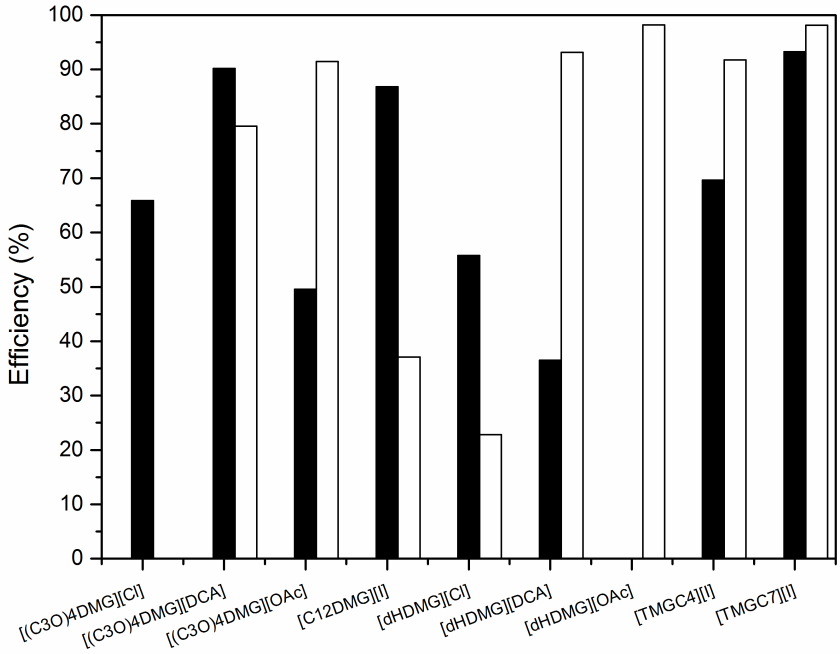

Figure 2.7. Decontamination efficiencies obtained for the tested guanidinium based ILs (96 h, 100 ^{o}C). Morphine (■), 6-MAM (□).

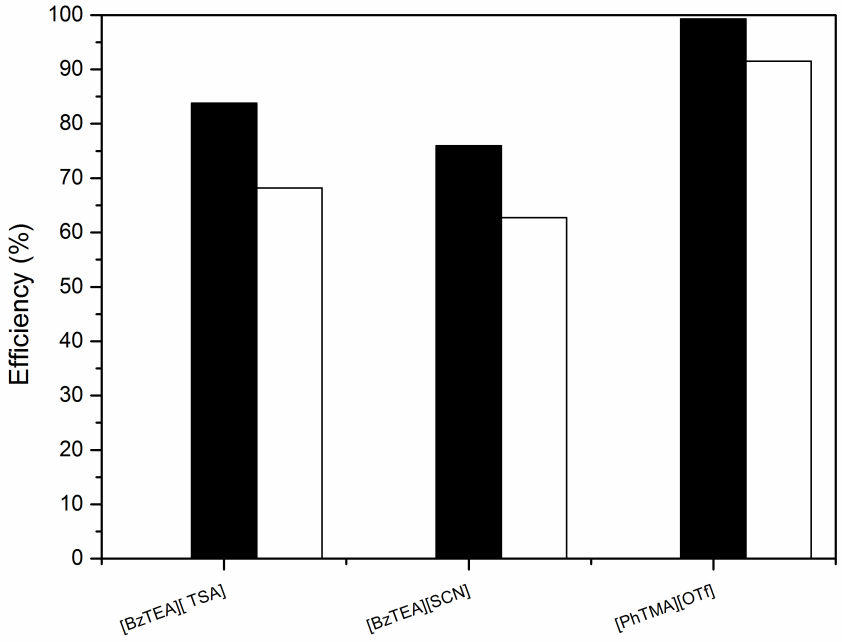

Figure 2.8. Decontamination efficiencies obtained for the tested quaternary ammonium based ILs (96 h, 100 ^{o}C). Morphine (■), 6-MAM (□).

- **Equimolar mixtures of some of the most promising ILs**

The results presented above show that some ILs presented very high extraction efficiencies for only one or two of the studied analytes. In order to check if the combination of ILs with different specificities could yield a mixture with high efficiencies for all analytes, several binary mixtures were prepared. Equimolar proportions were used (in the case of aliquat containing mixtures, the aliquat average molecular weight was considered). The results that are presented in Figure 2.9 show that the mixtures have lower values for the extraction efficiencies than the pure compounds.

So far, no attempt to correlate structural properties of the ILs with the correspondent extraction efficiencies was successful. At this point, our claim is that each combination cation/anion has unique properties.

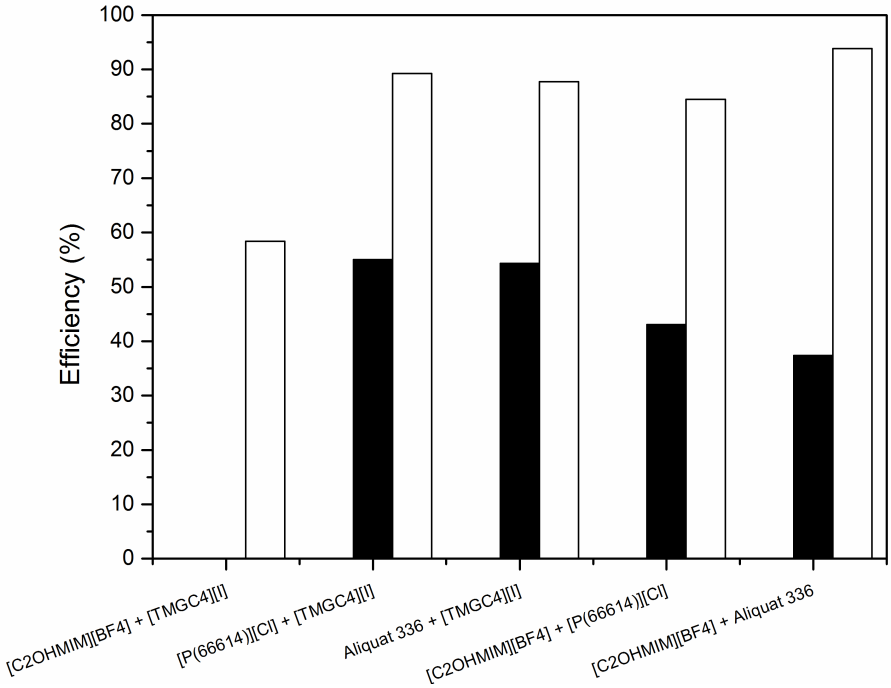

Figure 2.9. Decontamination efficiencies obtained for the tested equimolar mixtures of some of the most promising ILs (96 h, 100 ^{o}C). Morphine (■), 6-MAM (□).

2.2.3. Experiments performed in the absence of ILs

In order to evaluate the true influence of the IL, experiments in which the hair was simply heated for 96 h with, and without vacuum were made (Table 2.1 and 2.2), and the extraction efficiencies were always below 40% for all compounds

Table 2.1. Decontamination efficiencies for *in vitro* contaminated samples obtained for the experiments, where the hair was heated at 100 ºC, for 96 h, under vacuum (0.1 mBar) and without any IL (average values for three independent experiments).

	Morphine	6-MAM
Efficiency (%)	24.26	12.14
Standard deviation	7.68	6.19
CV (%)	31.66	50.74

Table 2.2. Decontamination efficiencies for *in vitro* contaminated samples obtained for the experiments, where the hair was heated at 100 ºC, for 96 h, at atmospheric pressure and without any IL (average values for three independent experiments). Quer dizer, sem vácuo deu melhor do que com?

	Morphine	6-MAM
Efficiency (%)	38.88	38.56
Standard deviation	8.77	4.35
CV (%)	22.56	11.28

2.2.4. Screening summary

The overall results demonstrated that each ion pair combination is unique (which probably explains the disappointing results obtained for the ILs mixtures and the lack of correlation between ILs). In addition, the comparison of both methanolic and Cairns et al. [2] washing procedures showed that ILs removed almost twice more contaminants (Figure 2.10).

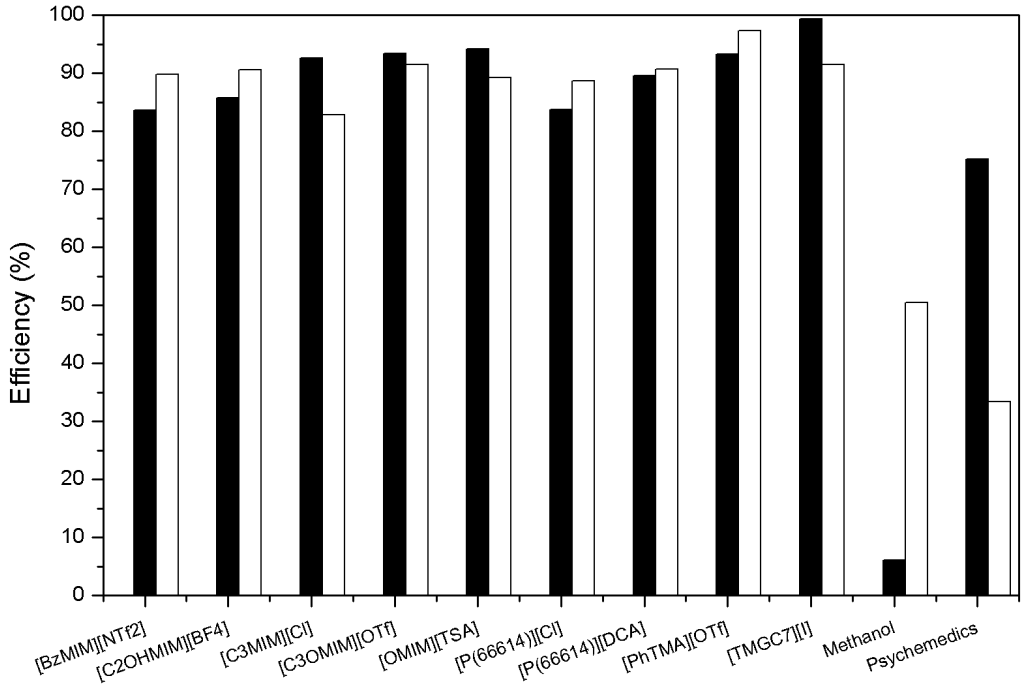

Figure 2.10. Efficiencies of the more promising ILs, and their comparison with both methanolic and Cairns et al. washings (Psychemedics), for Morphine (▪) and 6-MAM (□) extraction from the

surface of externally contaminated hair (96 h, 100 ºC for ILs and room temperature for methanol).

2.2.5. Morphological changes in hair

One of the problems associated to the conventional methanolic decontamination, is the production of morphological changes in the hair structure [7] In order to assess the effect of the IL treatment on the hair surface, scanning electron microscopy (SEM) analysis was performed, and the images showed that no morphological changes were visible in the hair's structure after treatment with the IL (Figure 2.11B), when compared both to untreated hair (Figure 2.11A) and to contaminated hair heated for 16 h at 120 ºC in the absence of IL (Figure 2.11C).

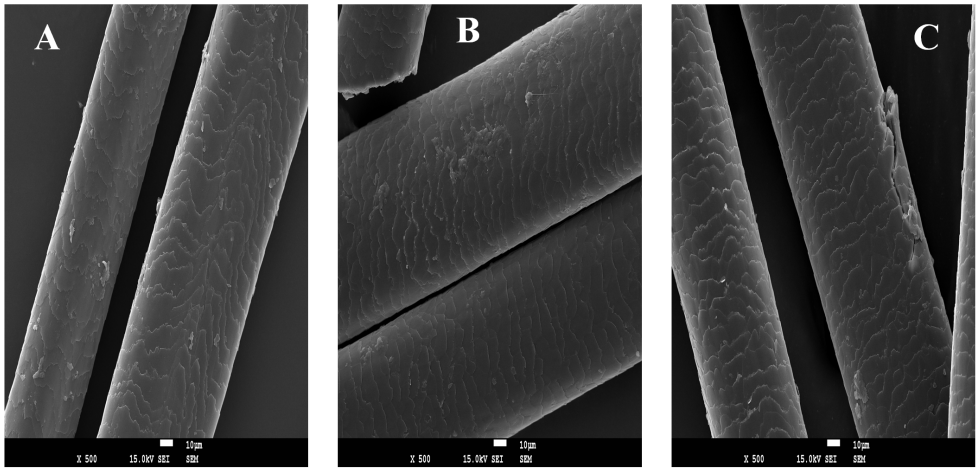

Figure 2.11. SEM images of: (A) Untreated contaminated hair; (B) Contaminated hair treated for 96 h at 100 ºC in the presence of IL; (C) Contaminated hair heated for 96 h at 100 ºC, without IL.

2.2.6. Process optimization

After the screening of ILs, nine promising liquids were found. The selection of one of those depended on both extraction efficiency and availability in our lab, therefore 1-hydroxyethyl-3-methyl-imidazolium tetrafluoroborate, $[C_2OHMIM][BF_4]$ was chosen. Before starting the optimization, it is important to identify first the variables to be optimized. In this case, temperature, extraction time, and amount of IL are obvious variables. However, since this particular IL is highly hygroscopic, water content was

studied as well. In order to evaluate the statistical significance and effect of each variable a two level full-factorial design was applied.

The estimated effects (main effects), interactions between variables, linear model's coefficients, Students *t* test values (for the null hypothesis that all the coefficients are zero), as well as their associated probabilities (at a level of confidence of 95%) were determined from the experimental results for the screening design of the extraction efficiencies under different conditions of temperature, time, amount of IL and water content for the two studied opiates (Table 2.3).

Table 2.3 - Estimated effects and coefficients for both morphine and 6-MAM in coded units.

	Morphine			6-MAM		
Term	**Effect**	**Coef**	**P**	**Effect**	**Coef**	**P**
Constant		35.32	0.00		25.76	0.00
Temperature	21.81	10.90	0.04	17.67	8.84	0.00
Time	2.75	1.38	0.79	18.05	9.03	0.00
IL amount	3.85	1.92	0.70	-0.13	-0.06	0.98
Water content	9.27	4.64	0.36	18.29	9.14	0.00
Temperature*Time	-5.17	-2.85	0.57	17.17	8.59	0.00
Temperature*IL amount	-6.79	-3.39	0.50	2.63	1.32	0.56
Temperature*Water content	-2.62	-1.31	0.80	-3.89	-1.94	0.39
Time*IL amount	-3.52	-1.76	0.73	7.81	3.91	0.09
Time*Water content	2.34	1.17	0.82	1.81	0.91	0.69
IL amount*Water content	9.32	4.66	0.36	-1.06	-0.53	0.81
Temperature*Time*IL amount	4.80	2.30	0.65	5.46	2.73	0.23
Temperature*Time*Water content	-1.79	-0.90	0.85	4.93	2.46	0.28
Temperature*IL amount*Water content	-1.31	-0.65	0.90	3.627	1.81	0.42
Time*IL amount*Water content	11.88	5.94	0.24	8.17	4.09	0.08
Temperature*Time*IL amount*Water content	-8.99	-4.50	0.36	1.58	0.79	0.73

The "effect" measures the change in the response (in this case the extraction efficiency) that results from alterations of variables or interactions (positive means increase and negative means decrease); the "coefficient" is the regression coefficient of a first-order model equation that describes the dependence of the response with the variables; "P" is the probability for the hypothesis of all coefficients being null for a 95% confidence level (only if $P < 0.05$ a variable or interaction will be considered significant).

Although 6-MAM is the opiate of outmost importance in this work, the analysis of the effects and statistical significance of variables and respective interactions of morphine cannot be neglected.

The screening results for 6-MAM show that the influence of the amount of IL is not statistically significant ($p \geq 0.05$) in the studied range (50-200 mg), which is not surprising since the increase of the amount of IL does not increase the liquid surface free area. The significance of the interactions between time and amount of IL, amount of IL and water content, may be attributed to the low precision of the screening based only on axial points (+1, -1).

The water content of the IL is therefore the variable with the most significant effect on the extraction efficiency for 6-MAM, though the extraction is also temperature and time-dependent. As for morphine, the extraction seems to be only temperature-dependent. This may explain why 6-MAM is more difficult to extract by this method. We must stress that a factorial design does not have a very high precision, so confirmation by a design with higher precision must be made (e.g. central composite design).

The screening design helped us identifying the significant variables for further optimization. A linear model was applied, thus the possibility of curvature in the variables effects had to be checked by means of a central composite design (CCD). In this case, all variables except the amount of IL were checked.

The application of the CCD allowed us to obtain response surface plots, which helped us to determine the region where the optimum conditions could be found. Due to the great amount of images obtained, only 6-MAM plots are shown (Figure 2.12).

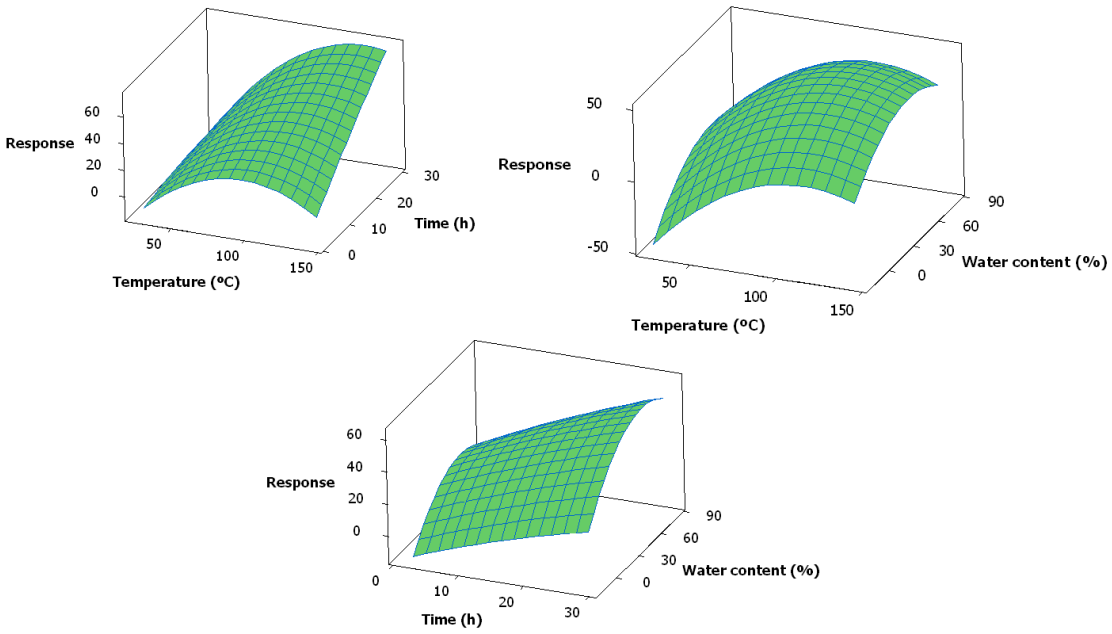

Figure 2.12 – Response surface plot of the predicted response against temperature and time, temperature and water content, time and water content for 6-MAM.

The significance of the relationship between the three studied variables of the regression model may be assessed by the value of R^2, which can be interpreted as the percentage of variation in the response explained by the regression model [8]. The obtained R^2 values (0.90 for morphine and 0.86 for 6-MAM), are not excellent (the closer to 1, the better), which can be explained by the variability (10 and 13 % for morphine and 6-MAM, respectively) of the SH0 contaminated hair samples. For both substances, all the studied variables turned to be statistically significant, though this did not happen for all interactions (Table 2.4).

Table 2.4 - Analysis of results for the applied model obtained using the central composite design for morphine (R^2 = 0.90) and for 6-MAM (R^2 = 0.86), applied to SH0 *in vitro* contaminated samples.

	Morphine			6-MAM		
Term	**Coef**	**SE Coef**	**P**	**Coef**	**SE Coef**	**P**
Constant	87.58	4.18	0.00	41.09	2.72	0.00
Temperature	22.80	3.43	0.00	11.74	1.80	0.00
Time	22.97	2.77	0.00	8.90	1.80	0.00
Water content	9.18	2.77	0.00	-8.95	2.23	0.01
Temperature*Temperature	-21.98	3.53	0.00	-0.76	1.80	0.10
Time*Time	-15.73	2.77	0.00	-7.39	1.80	0.67
Water content*Water content	-8.01	2.77	0.01	5.62	2.36	0.02
Temperature*Time	14.23	3.62	0.00	-0.97	2.36	0.68
Temperature*Water content	-3.21	3.62	0.38	1.24	2.36	0.60
Time*Water content	4.90	3.62	0.19	41.09	2.72	0.00
Source		**F**	**P**		**F**	**P**
Regression		28.83	0.000		18.59	0.00
Linear		41.30	0.000		34.55	0.00
Square		27.49	0.000		11.45	0.00
Interaction		6.01	0.003		2.04	0.13
Lack-of-Fit		8.68	0.47		8.41	0.34

In the case of morphine, the only significant second order interaction was temperature – time. This means that, despite the significant effect of the water content, it does not depend of the variations of both temperature and extraction time. Similar effect was observed in the temperature and in time relatively to the water content. For 6-MAM, the results point for second order interaction only for the pair time – water content. After performing an analysis of variance for morphine (Table 2.6), it is possible to conclude that both second order regression and interaction model are statistically significant and no lack-of-fit was observed ($p > 0.05$). In case of 6-MAM (Table 2.6), we may conclude that only the second order regression model is significant and, once more, no lack-of-fit ($p > 0.05$) was observed. The obtained coefficients were then used by the software to apply to the desirability functions (D

functions, see eq. 1.1), whose solution predicts mathematically the optimum values for each studied variable. In this specific case, since our goal was to optimize the responses of both morphine and 6-MAM, the more adequate D function, was the maximization function, with a weight of 1 for each variable. The best conditions obtained by the D function are presented in Table 2.5. It is important to remark that these conditions represent a desirability (d) of 0.805 (the closer to 1, the better).

Table 2.5 - Optimum conditions predicted by the maximization desirability function for the decontamination of SH0 samples.

	Morphine	6-MAM
Temperature (ºC)	120.0	119.9
Time (h)	16.0	16.0
Water content (%)	44.0	44.4

2.2.7. Method validation

As any new developed method, its validity must be proven through a validation procedure, though, in this particular case, there are no published guidelines for the validation of decontamination procedures. Therefore, we decided to use the procedure of Cairns et al [2] as a reference against which our method was systematically compared. Twelve negative hair samples (collected from different subjects, with different hair colors) were externally contaminated with morphine and 6-MAM. In this way the intrinsic variability of hair was taken into account, as well as the possible presence of dyes. The concentrations of the analytes in these samples, after contamination, are provided in Table 2.6).

Table 2.6 - Concentrations of the analytes (ng/mg) in the contaminated samples prior to decontamination.

Sample #	Morphine	6-MAM
1	0.04	0.65
2	0.17	0.16
3	0.25	19.20
4	1.69	16.44
5	0.70	8.65
6	1.78	11.95
7	0.21	2.91
8	0.05	0.60
9	0.17	0.78
10	0.48	7.89
11	1.57	22.95
12	0.07	0.90

Both methods (ours and that of Cairns et al.) were used to decontaminate those samples. Table 2.7 shows analyte concentrations (in pg/mg) in the hair samples (hair digests, after decontamination) and in the last washing solution.

Table 2.7 - Comparison between the Cairns *et al* washing method and our method, using contaminated samples. The IL experiments were carried at 120 ºC for 16 h and using $[C_2OHMIM][BF_4]$ containing 44% of water.

Sample #, color	Dyed	Wash fraction or hair digest	Cairns *et al.* Method				Developed method	
			Morphine (pg/mg Hair)		6-MAM (pg/mg Hair)		Morphine (pg/mg Hair)	6-MAM (pg/mg Hair)
			Wash and hair values	Hair minus (5 x LW)	Wash and hair values	Hair minus (5 x LW)	Hair values	Hair values
1, Blonde	N/D	Last wash	27		1711			
		Hair digest	37	-99	468	-8086	40	620
2, Blonde	N/D	Last wash	35		819			
		Hair digest	26	-147	655	-3993	9	101
3, Brown	D	Last wash	155		9556			
		Hair digest	112	-663	8123	-39656	190	8869
4, Brown	N/D	Last wash	903		22536			
		Hair digest	1688	-2825	13588	-99089	1369	12588
5, Brown	N/D	Last wash	58		6983			
		Hair digest	132	-159	5843	-29071	322	5147
6, Brown	N/D	Last wash	981		38412			
		Hair digest	1776	-3128	10438	-181624	1178	10844
7, Brown	D	Last wash	57		7372			
		Hair digest	106	-180	1683	-35179	101	1651
8, Black	N/D	Last wash	325		1877			
		Hair digest	41	-1585	565	-8822	5	465
9, Brown	N/D	Last wash	122		1407			
		Hair digest	7	-602	548	-6487	7	256
10, Brown	N/D	Last wash	68		10619			
		Hair digest	120	-222	5886	-47208	190	5857
11, Blonde	N/D	Last wash	2075		112353			
		Hair digest	437	-9936	7007	-554757	605	6553
12, Black	N/D	Last wash	3865		1310			
		Hair digest	17	-19310	427	-6123	10	407

As expected, and already described [2], different hair samples soaked under the same conditions, will undertake different incorporation rates of drugs. From the amount of drug present in hair digests, samples # 4, 6 and 11 (for morphine) and all samples (for

6-MAM) would be erroneously considered positive. After application of the wash criterion (descreve resumidamente da primeira vez que o referires, que acho que é esta), values < 200 pg/mg of hair were obtained, pointing out that the sample is not considered positive, despite the presence of the drug, which is probably contamination. The results illustrate well the fact that both decontamination procedures are not able to remove all the contamination. The results also show that, in the case of the application of the washing procedure of Cairns et al, if we sum the amount of drug present in both hair digests and last wash, we would get more 6-MAM that in the unwashed *in vitro* contaminated hair. Although puzzling in the beginning, one should recall that "street" heroin was used. Smith et al [9] described and quantified the spontaneous hydrolysis of heroin into 6-MAM at 23ºC in pH 6,4 phosphate buffer. According to these authors, the hydrolysis occurs at a rate of 3.0×10^{-5} min^{-1}, resulting in a conversion of 4% after 24h. Although 4% cannot be considered significant, a possible explanation for these odd results may be the fact that, at 37 ºC, the temperature used in the Cairns et al method, an exponential increase of the hydrolysis rate should be expected, thus resulting in an higher conversion degree. Comparing now with the developed and proposed method, , the occurrence of this hydrolysis was not noticed because a small amount of deionized water was used, which means that our method does not produce these kind of artifacts.

Both methods are compared in Figure 2.13, where the difference between the amounts of drug found in the hair digest (HD of Cairns et al - HD of our method.) is shown for each sample. For most of the samples, the percentage difference is less than ±12%, which is within the range of the variability expected in an hair samples, being the average difference of – 5.7 % and 11.9 % for morphine and 6-MAM, respectively.

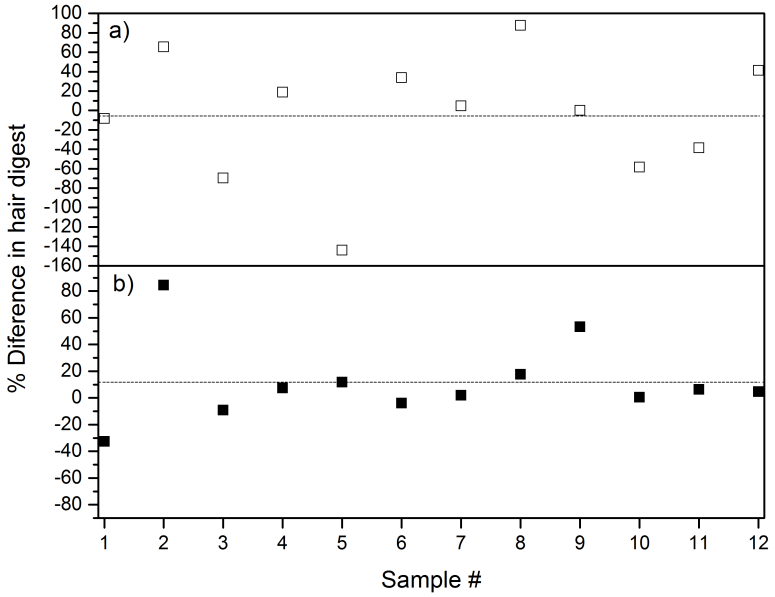

Figure 2.13 - Percentage difference in the hair digests differences between Cairns *et al* washing method and the developed method. The dashed lines represent the average difference. a) Morphine; b) 6-MAM.

Despite the low sampling (only 12 samples were tested for now), we would like to highlight the fact that the results point out to the validity of our method. Its main advantage relative to the one of Cairns et al is the possibility of achieving the same results with less steps and lower sample loss risk. In fact, as many hair samples as those that fit inside an oven may be decontaminated overnight without the need of an operator. Finally, we would like to stress that our method (a contactless procedure) preserves the integrity of hair samples, therefore a washing criterion of some sort may be developed for this method.

2.3. Conclusions

In this chapter, a novel process for the extraction of opiates from hair's surface using ILs is described. This method, which relies on the unique properties of those liquids, namely being almost non-volatile (therefore the hair is not re-contaminated) and presenting high affinity for the opiate drugs (the majority of them), is more efficient than the conventional methanolic decontamination procedure and has an efficiency superimposable to the reference method. It allows the irreversible transport of the drugs from the hair surface to the bulk of the IL, without any physical contact between the IL and the hair. Although only twelve different samples were tested so far, it seems that the developed method overcomes the problem associated to other methods (e.g. methanol washing): it does not produce any morphological changes in the hair surface which promotes the removal of external drug contamination. Although we are aware that a decontamination time of 16 h may be considered a disadvantage, it is important to remark that the presented method allows the simultaneous decontamination of many samples (possibly more than 100, depending on the size of the oven) and the process can be carried out overnight without the presence of any technician.

2.4. Experimental

2.4.1. Reagents and standards

The ILs [P(66614)][Cl], Aliquat® 336, [EMIM][$EtSO_4$], [BMIM][BF_4], [OMIM][BF_4] and [C_2OHMIM][BF_4] were kindly offered by Cytec (Ontario, Canada), Sigma Aldrich (Madrid, Spain) and Solchemar (Monte da Caparica,

Portugal), respectively. The remaining ILs were prepared in our laboratory. All ILs had purities above 98% and water contents lower than 1% (checked by Karl Fischer). Due to the number of tested ILs, complete information (name, structure and abbreviated name) is summarized in the appendix (Table A.1).

The standards of morphine and 6-monoacetylmorphine (6-MAM), as well as their tri-deuterated analogues, were supplied by Cerilliant (Round Rock, TX, USA) in methanol at 1 mg/mL. Methanol (HPLC grade), dichloromethane, n-hexane, 2-propanol, ammonium hydroxide, hydrochloric acid, and potassium dihydrogenphosphate (analytical grade) were obtained from Merck Co (Darmstadt, Germany). N-Methyl-N-(trimethylsilyl) trifluoroacetamide (MSTFA) and trimethylchlorosilane (TMS) were purchased from Macherey-Nagel (Düren, Germany). Oasis® MCX (3 mL, 60 mg) extraction cartridges were obtained from Waters (Milford, MA, USA). Working solutions at 10 and 1 μg/mL of all compounds were prepared by proper dilution of the stock solutions with methanol, and these were used for the calibrators. Additional working solutions, at 1 and 10 μg/mL, have been used to prepare the quality control samples; these solutions were prepared using different lots of the analytical standards when available. A working solution of the internal standards at 5 μg/mL was prepared also in methanol. All these solutions were stored light-protected between 2 and 8 °C.

To prepare the 0.1 M potassium dihydrogenphosphate solution, 13.61 g of potassium dihydrogenphosphate was weighed into a volumetric flask, obtaining a final volume of 1 L with deionized water.

2.4.2. Biological samples

Negative hair samples were kindly provided by laboratory staff, and were previously tested for negativity. All samples were sequentially washed with dichloromethane and water in order to remove eventual traces of sweat, sebum and hair care products.

2.4.3. Chromatographic conditions

Chromatographic analysis was performed using an HP 6890N gas chromatograph (Hewlett-Packard, Waldbronn, Germany), equipped with a model 5973 mass-selective detector (Hewlett-Packard, Waldbronn, Germany). A capillary column (30 m×0.25 mm I.D., 0.25 μm film thickness) with 5% phenylmethylsiloxane (HP-5 MS), supplied by J & W Scientific (Folsom, CA, USA), was used. Chromatographic conditions were as follows: initial oven temperature was 90 °C for 2 min, which was increased by 20 °C min^{-1} to 300 °C, held for 3 min. The temperatures of the injection port and detector were set at 220 and 280 °C, respectively. The split injection mode was used (split ratio of 1:5), and helium with a flow rate of 0.8 mL min^{-1} was used as the carrier gas. The mass spectrometer was operated with a filament current of 300 μA and electron energy of 70 eV in the electron ionization (EI) mode. Quantitation was done in the selected ion monitoring (SIM) mode, and the ions were monitored at m/z 236, *429* and 414 for morphine and at m/z *399*, 340 and 287 for 6-MAM (quantitation ions are presented in italics). For the internal standards, only one ion was monitored for each compound, at m/z 432 for morphine-d_3; and at m/z 402 for 6-MAM-d_3 [10].

2.4.4. Scanning electron microscopy (SEM)

SEM experiments of contaminated hair samples were performed on a Hitachi S2400 with a working tension of 25 kV.

2.4.5. Hair contamination procedure

For the elaboration of this work, two kinds of hair samples were prepared, hereafter designated by 'positive' hair samples (SH0) and externally contaminated hair samples.

The positive hair samples (SH0) were prepared by soaking 40 g of hair in 600 mL of 3 μg/mL solution of street heroin (containing both morphine and 6-MAM), with 15 % (v/v) of methanol, for two days at 35 ºC, under stirring. Afterwards, the hair was rinsed three times with deionized water, and allowed to dry until the next day.

For the preparation of the externally contaminated hair samples, used for the method validation, a procedure similar to the one described by Cairns et al. [2] was used. In this case, 80 mg of each hair sample were soaked in 2 mL of 1 μg/mL solution of street heroin for 1 h. Afterwards the hair was rinsed three times with 2 mL of water. After rinsing, the hair samples were transferred to clean tubes and allowed to dry until the next day.

We must stress here that the main differences between the preparation of positive and externally contaminated hair samples were the soaking time and drug concentration in the soaking solutions. Moreover, in the former case, the authors [2] who proposed the method found that drug incorporation efficiencies were very low (about 1–2%), and most of the drug remained at the hair surface and in the soaking solution. Thus, we assumed that in the latter case, the eventual contamination inside the hair matrix would be negligible, and, as such, we designated the samples as externally contaminated.

2.4.6. Decontamination experiments

The decontamination experiments were carried on a modified GC oven (Figure 2.14) coupled to a stirring motor and a magnetic bar, using customized glass flasks produced by the glassblower of Instituto Superior Técnico (Figure 2.15).

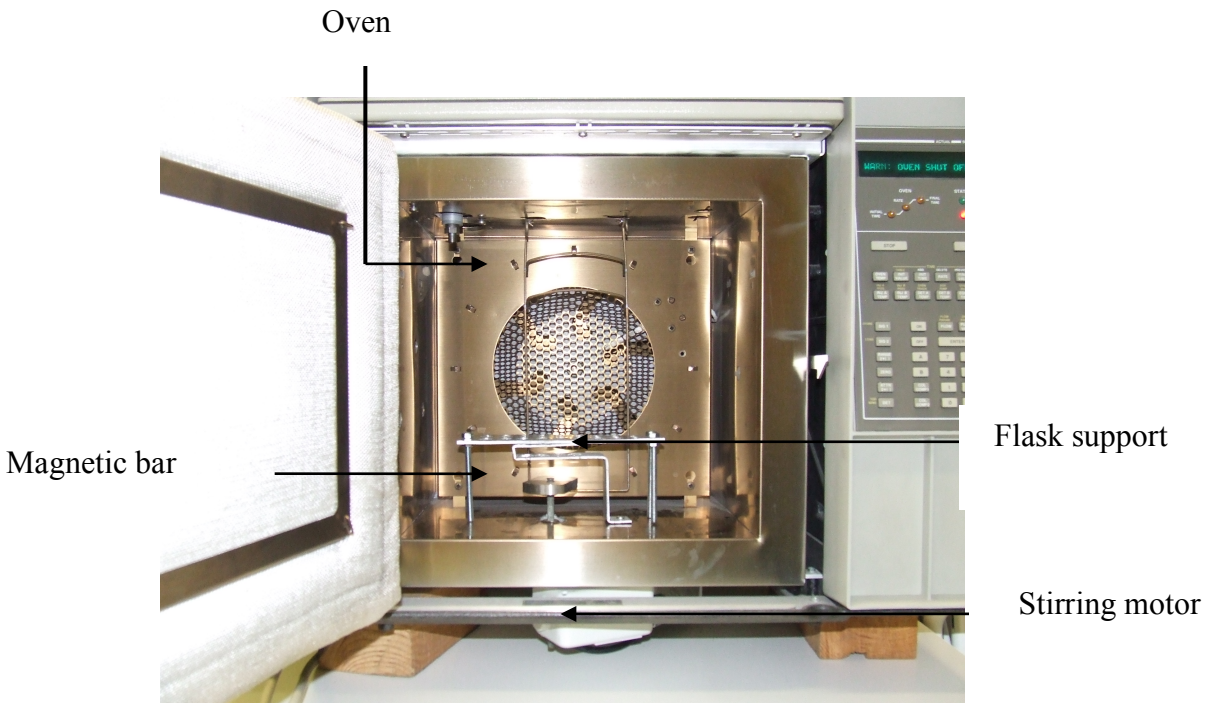

Figure 2.14 - Photograph of the apparatus used for the decontamination experiments.

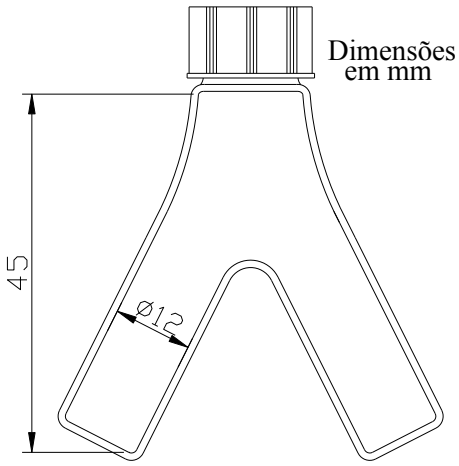

Figure 2.15 – Customized flasks used in the decontamination experiments.

.

For these experiments, a small amount of homogenized hair (c.a. 25 mg) was weighted into the flask followed by the IL (c.a. 100 mg) into the other branch of the flask. The flask was then placed in the GC oven, where it was left during the pre-determined extraction time at the chosen temperature (which were previously

optimized, see below). For the blank experiments (heat only), a similar procedure was used, though in this case no IL was used.

In order to evaluate the influence of vacuum in this process, an experimental setup similar to that used by Kulkarni *et al*. (Figure SI 3 in [11]) was used, but in this case a vial containing only about 100 mg of externally contaminated hair was used. The vial was subjected to vacuum for 72 h at 100 ºC.

In order to assess the validity of our method, hair samples were submitted to two other decontamination procedures. One is the conventional decontamination used routinely in the laboratory of Forensic Toxicology in Lisbon [10]. In this method contaminated hair samples were sequentially washed with dichloromethane, deionized water and rinsed three times with pure methanol, at room temperature.

The other method is that developed by Cairns et al [2,12] and routinely used at the for the analysis of thousands of samples every year. First, dry isopropanol (2 mL) was added to about 25 mg of hair. The tubes were shaken vigorously at 37 ºC for 15 min; after 15 min, the isopropanol was removed. Then 2 mL of 0.01 M phosphate buffer/0.01% BSA, pH6, was added to the hair samples, and the tubes were shaken vigorously for 30 min at 37 ºC, after which the buffer was removed. This 30 min wash was repeated twice more, followed by two 60 min washes using the same conditions. The last wash is then saved for analysis [2].

2.4.7. Drug extraction from hair and sample cleanup

All hair samples were analyzed according to the procedures used in the laboratory [10]. Briefly, 20 mg of hair was incubated overnight in 2 mL of methanol at 65 ºC. The methanolic extracts were transferred to polypropylene tubes, followed by the addition of 5 mL of 0.1 M potassium dihydrogenphosphate. After the addition of 25 µL of internal standard mixture (5 µg/mL), the samples were homogenized for 15 min by rotation/inversion movements. This homogenate was added to mixed-mode extraction cartridges previously conditioned with 2 mL of methanol and 2 mL of deionized water. After the samples have passed through, the cartridges were washed sequentially with 2 mL of each of the following: deionized water, 0.1 M hydrochloric

acid, methanol, and n-hexane. After drying under full vacuum for 1 min, the analytes were eluted with 2 mL of a mixture of dichloromethane: isopropanol (80:20, v/v) with 2% of ammonium hydroxide. The extracts are dried at 45 °C under a gentle nitrogen stream. Sixty five microliters of N-Methyl-N-(trimethylsilyl) trifluoroacetamide (MSTFA) with 5% of trimethylchlorosylane (TMS) was added, and after vortex mixing for 30 s, derivatization takes place at 80 °C for 25 min. The extracts were transferred to autosampler vials and a 2 μL aliquot is injected in the chromatographic system.

2.4.8. Design of Experiments (DOE) and experimental design

Using the Design of Experiments (DOE) approach as an optimization tool [8], and bearing in mind the hygroscopic properties of the ILs (1-hydroxyethyl-3-methyl-imidazolium tetrafluoroborate $[C_2OHMIM][BF_4]$ for these experiments), the process was initially optimized concerning the following variables at two levels (low – high): temperature (50 – 120 ºC), extraction time (8 – 24 h), IL amount (50 – 200 mg) and water content of the IL (0.01 – 60 %), as well as their possible interactions. These variables were screened by means of a two-level, four-factor full factorial design (2^4) [8]. Since some dispersion was expected, three replicates were performed. The independent variables, the corresponding values of the low (-1) and high (+1) levels and the matrix obtained for this screening design are shown Table 2.8). These experiments were carried out in a random order to avoid the influence of noise factors, minimizing systematic errors [13].

Table 2.8 - Design matrix for the screening experiments, expressed in uncoded units.

StdOrder	RunOrder	Temperature (ºC)	Time (h)	Amount of IL (mg)	Water content (% w/w)
13	1	50	8	200	60
1	2	50	8	50	0.01
12	3	120	24	50	60
6	4	120	8	200	0.01
9	5	50	8	50	60
10	6	120	8	50	60
3	7	50	24	50	0.01
15	8	50	24	200	60
14	9	120	8	200	60
2	10	120	8	50	0.01
11	11	50	24	50	60
5	12	50	8	200	0.01
4	13	120	24	50	0.01
7	14	50	24	200	0.01
8	15	120	24	200	0.01
16	16	120	24	200	60

The optimization of the chosen variables employed a 2^3 factorial central composite design (CCD) with a total of 20 experiments [six axial points (α=1.682), six replicates at the center points in a cube (coded as zero level) and eight cube points at the levels ±1, Table 2.9]. Therefore, each factor was evaluated at five different levels [14]. All the experiments were carried out randomly.

Table 2.9 - Design matrix for the CCD experiments, expressed in uncoded units.

StdOrder	RunOrder	Temperature (ºC)	Time (h)	Water content (% w/w)
15	1	85	2.936	30.01
18	2	85	16	78.99
16	3	85	29.064	30.01
13	4	27.85	16	30.01
20	5	85	16	30.01
17	6	85	16	-18.98
14	7	142.16	16	30.01
19	8	85	16	30.01
1	9	50	8	0.01
11	10	85	16	30.01
6	11	120	8	60
8	12	120	24	60
9	13	85	16	30.01
3	14	50	24	0.01
4	15	120	24	0.01
12	16	85	16	30.01
7	17	50	24	60
5	18	50	8	60
2	19	120	8	0.01
10	20	85	16	30.01

Both screening and optimization designs, as well as all data analysis were performed using Minitab® statistical program software, version 16.

2.5. References

[1] F. Pragst, M. a Balikova. State of the art in hair analysis for detection of drug and alcohol abuse. *Clin. Chim. Acta.*, **2006**, *370*, 17–49.

[2] T. Cairns, V. Hill, M. Schaffer, W. Thistle. Removing and identifying drug contamination in the analysis of human hair. *Forensic Sci. Int.*, **2004**, *145*, 97–108.

[3] P. S. Kulkarni, L. C. Branco, J. G. Crespo, C. A. M. Afonso. Capture of dioxins by ionic liquids. *Environ. Sci. Technol.*, **2008**, *42*, 2570–4.

[4] V. F. Monteiro, A. P. Maciel, E. Longo. Thermal analysis of caucasian human hair. *J. Therm. Anal. Calorim.*, **2005**, *79*, 289–293.

[5] L. A. Collett, M. E. Brown. BIOCHEMICAL AND BIOLOGICAL APPLICATIONS OF THERMAL ANALYSIS. *J. Therm. Anal.*, **1998**, *51*, 693–726.

[6] M. Tariq, M. G. Freire, B. Saramago, J. a P. Coutinho, J. N. C. Lopes, L. P. N. Rebelo. Surface tension of ionic liquids and ionic liquid solutions. *Chem. Soc. Rev.*, **2012**, *41*, 829–68.

[7] P. R. Stout, J. D. Ropero-Miller, M. R. Baylor, J. M. Mitchell. Morphological changes in human head hair subjected to various drug testing decontamination strategies. *Forensic Sci. Int.*, **2007**, *172*, 164–70.

[8] D. C. Montgomery. *Design and Analysis of Experiments*, John Whiley & Sons, Inc, New York, **2001**.

[9] P. T. Smith, M. Hirst, C. W. Gowdey. Spontaneous hydrolysis of heroin in buffered solution. *Can. J. Physiol. Pharmacol.*, **1978**, *56*, 665–667.

[10] M. Barroso, M. Dias, D. N. Vieira, M. López-Rivadulla, J. a Queiroz. Simultaneous quantitation of morphine, 6-acetylmorphine, codeine, 6-acetylcodeine and tramadol in hair using mixed-mode solid-phase extraction and gas chromatography-mass spectrometry. *Anal. Bioanal. Chem.*, **2010**, *396*, 3059–69.

[11] P. S. Kulkarni, L. C. Branco, J. G. Crespo, C. a M. Afonso. A comparative study on absorption and selectivity of organic vapors by using ionic liquids based on imidazolium, quaternary ammonium, and guanidinium cations. *Chem. - A Eur. J.*, **2007**, *13*, 8470–7.

[12] T. Cairns, V. Hill, M. Schaffer, W. Thistle. Levels of cocaine and its metabolites in washed hair of demonstrated cocaine users and workplace subjects. *Forensic Sci. Int.*, **2004**, *145*, 175–81.

[13] J. N. Miller, J. C. Miller. *Statistics and Chemometrics for Analytical Chemistry*, Pearson / Prentice Hall, Harlow, **2000**.

[14] M. A. Bezerra, R. E. Santelli, E. P. Oliveira, L. S. Villar, L. A. Escaleira. Response surface methodology (RSM) as a tool for optimization in analytical chemistry. *Talanta*, **2008**, *76*, 965–77.

Chapter 3 – Hair decontamination: cocaine

This chapter describes the attempt to develop and optimize a contactless hair decontamination procedure applied to cocaine.

Table of Contents

3.1. Cocaine stability

In the previous chapter, the development of a novel contactless procedure for the decontamination of hair samples was reported. According to the results presented by Gostič et al. [1], cocaine's vaporization occurs between 100 and 300 ºC. This data is quite encouraging, because it points out to the applicability of our method to this group of abused drugs. Nevertheless, it is important to remark that the major problem associated with cocaine is the spontaneous hydrolysis to its inactive metabolite benzoylecgonine (Figure 3.1) [2,3]. This spontaneous hydrolysis occurs under mild to strong alkaline conditions or in the presence of water at high temperatures.

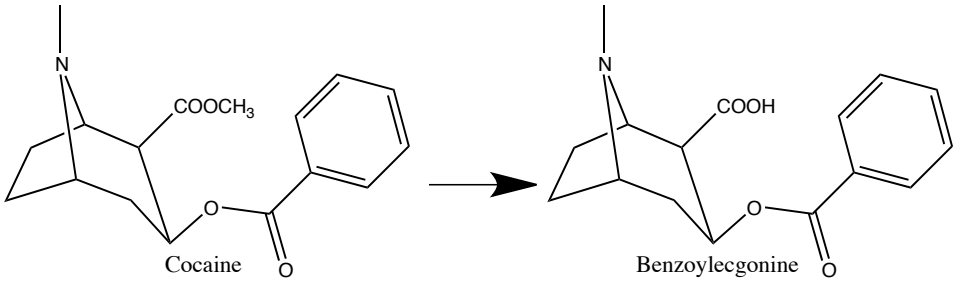

Figure 3.1 –Hydrolysis of cocaine to benzoylecgonine.

Similarly to the work described in chapter 2, a screening of ILs was performed in order to access the applicability of the process developed in the previous chapter to this specific analyte.

3.2. Results and discussion

3.2.1. Hair contamination

For the decontamination experiments, *in-vitro* contaminated hair samples were prepared by soaking, according to Barroso et al. [2]. The SHC sample, whose analyte concentrations were 4.27 $ng.mg^{-1}$ of cocaine and 3.79 $ng.mg^{-1}$ of benzoylecgonine (BZE; coefficients of variation of 8.62 and 9.96 %, respectively), was considered suitable for the decontamination experiments, since it mimics well an authentic

contamination situation (> 0.5 $ng.mg^{-1}$ of cocaine). Thus, when submitted to the wash criterion proposed by Cairns et al. [4], this sample batch was considered negative.

3.2.2. Screening of ILs

As previously mentioned, a screening of ILs was performed. In this case, fifty-two ILs were tested at 120 ºC for 24h to decontaminate the SHC samples. These experimental conditions were chosen based on the results presented in chapter 2. Negative extraction efficiencies were obtained for BZE for all the tested ionic liquids, ranging from -2 % (for [Ch][Mal]) to -439 % (for [BzTEA][DCA]). These puzzling results can be explained by the spontaneous hydrolysis of cocaine into BZE [2,3] (Figure 3.1). Both extraction temperature and residual traces of water in the IL strongly favored the hydrolysis reaction. Additionally, the extraction time (24 h) enhanced even more this reaction. So, with the hydrolysis of cocaine, the concentration of BZE increased in the samples, explaining the observed negative decontamination efficiency. The differences in the amount of cocaine converted are not directly related to the chemical characteristics of ILs, because they do not depend of their ability to absorb the drug. Nevertheless, the chemical nature of the IL will influence its hygroscopy and, therefore, the rate of cocaine conversion.

3.2.3. Heat experiments performed in the absence of ILs

Similarly to what was performed in the previous chapter, experiments were performed in the absence of IL with, and without vacuum (Table 3.1 and 3.2). Once more it is proven that, at this temperature and during this decontamination time, spontaneous hydrolysis of cocaine to benzoylecgonine occurs.

Table 3.1 – Decontamination efficiencies for *in vitro* contaminated samples obtained for the experiments, where hair was heated at 120 ºC, for 24 h, under vacuum (0.1 mBar) and without any IL (average values for three independent experiments).

	Cocaine	BZE
Efficiency (%)	67.40	- 152.43
Standard deviation	5.76	23.20
CV (%)	8.55	15.22

Table 3.2 - Decontamination efficiencies for *in vitro* contaminated samples obtained for the experiments, where hair was heated at 120 ºC, for 24 h, at atmospheric pressure and without any IL (average values for three independent experiments).

	Cocaine	BZE
Efficiency (%)	70.64	- 171.11
Standard deviation	6.01	31.5
CV (%)	8.50	18.41

3.3. Conclusions

In this chapter, the development of a novel process for the extraction of cocaine from hair's surface using ILs was attempted. Unfortunately, the experimental conditions required for the extraction are not compatible with this type of drug. Indeed, the combination of high temperature, high decontamination time and traces of water has promoted the spontaneous transformation of cocaine into its inactive metabolite BZE. For some unknown reason it was experimentally observed that the proposed method was unable to remove BZE from the hair's surface, and this feature was not subject to further optimization experiments, since the strong decontamination conditions could perhaps convert hair-incorporated cocaine to BZE, making hair analysis for those drugs worthless for forensic purposes.

3.4. Experimental

3.4.4. Reagents and standards

The ILs [P(66614)][Cl], Aliquat® 336, [EMIM][$EtSO_4$], [BMIM][BF_4], [OMIM][BF_4] and [C_2OHMIM][BF_4] were kindly offered by Cytec (Ontario, Canada)

and Sigma Aldrich (Madrid, Spain), respectively. The ILs [EMIM][$EtSO_4$], [BMIM][BF_4], [OMIM][BF_4] and [C_2OHMIM][BF_4] were purchased to Solchemar (Monte da Caparica, Portugal),. The remaining ILs were prepared in our laboratory. All ILs had purities above 98% and water contents lower than 1% (checked by Karl Fischer). Due to the number of tested ILs, complete information (name, structure and abbreviated name) is summarized in the appendix (Table A.1).

The standards of cocaine and BZE, as well as their tri-deuterated analogues, were supplied by Cerilliant (Round Rock, TX, USA) in methanol at 1 mg/mL. Methanol (HPLC grade), dichloromethane, n-hexane, 2-propanol, ammonium hydroxide, hydrochloric acid, and potassium dihydrogenphosphate (analytical grade) were obtained from Merck Co (Darmstadt, Germany). N-Methyl-N-(trimethylsilyl) trifluoroacetamide (MSTFA) and trimethylchlorosilane (TMS) were purchased from Macherey-Nagel (Düren, Germany). Oasis® MCX (3 mL, 60 mg) extraction cartridges were obtained from Waters (Milford, MA, USA). Working solutions at 10 and 1 μg/mL of all compounds were prepared by proper dilution of the stock solutions with methanol, and these were used for the calibrators. Additional working solutions, at 1 and 10 μg/mL, have been used to prepare the quality control samples; these solutions were prepared using different lots of the analytical standards when available. A working solution of the internal standards at 5 μg/mL was prepared also in methanol. All these solutions were stored light-protected between 2 and 8 °C.

To prepare the 0.1 M potassium dihydrogenphosphate solution, 13.61 g of potassium dihydrogenphosphate was weighed into a volumetric flask, obtaining a final volume of 1 L with deionized water.

3.4.5. Biological samples

Negative hair samples were kindly provided by laboratory staff, and were previously tested for negativity. All samples were sequentially washed with dichloromethane, water and methanol in order to remove eventual traces of sweat, sebum and hair care products.

3.4.6. Chromatographic conditions

Chromatographic analysis was performed using an HP 6890N gas chromatograph (Hewlett-Packard, Waldbronn, Germany), equipped with a model 5973 mass-selective detector (Hewlett-Packard, Waldbronn, Germany). A capillary column (30 m×0.25 mm I.D., 0.25 μm film thickness) with 5% phenylmethylsiloxane (HP-5 MS), supplied by J & W Scientific (Folsom, CA, USA), was used. Chromatographic conditions were as follows: initial oven temperature was 90 °C for 2 min, which was increased by 20 °C min^{-1} to 300 °C, held for 3 min. The temperatures of the injection port and detector were set at 220 and 280 °C, respectively. The split injection mode was used (split ratio of 1:5), and helium with a flow rate of 0.8 mL min^{-1} was used as the carrier gas. The mass spectrometer was operated with a filament current of 300 μA and electron energy of 70 eV in the electron ionization (EI) mode. Quantitation was done in the selected ion monitoring (SIM) mode, and the ions were monitored at m/z 82, 182 and 303 for cocaine, and at m/z 82, 240 and 361 for benzoylecgonine (quantitation ions are underlined). For the internal standards, only one ion was monitored for each compound, at m/z 185 for cocaine-d_3 and at m/z 243 for benzoylecgonine-d_3 [2].

3.4.7. Hair contamination procedure

For the elaboration of this work, *in vitro* contaminated hair samples were prepared. The contaminated samples were prepared according to Barroso et al. [2]. In this case, 4 g of hair (already cut into pieces of approximately 1 mm) was soaked in aqueous solution of both cocaine and BZE with a concentration of 100 μg/mL (solution prepared using standard solutions of 1 mg/mL of both substances), for two days at 35 ºC, under stirring.

3.4.8. Decontamination experiments

In what concerns decontamination experiments, the same procedure of that used for opiates (see chapter 2) was used, though the extraction time was reduced for 24h and the temperature increased to 120 ºC.

3.4.9. Drug extraction from hair and sample cleanup

All hair samples were analyzed according to the procedures used in the laboratory [2]. Briefly, 20 mg of hair were incubated for 3 h in 3 mL of methanol/0.1M HCl (2:1) solution at 65 ºC. The tubes were centrifuged at 3500 rpm for 5 min, after which time the supernatant was transferred to another tube and neutralized with 25 µL of a 4M sodium hydroxide solution. After addition of 25 µL of a standard mixture of both internal standards at 10 µg/mL, excess methanol was evaporated at 45 ºC under a gentle stream of N_2. Afterwards, 5 mL of 0.1M KH_2PO_4 was added, and the mixture was homogenized for 15 min by rotation/inversion movements. This homogenate was added to mixed-mode extraction cartridges previously conditioned with 2 mL of methanol and 2 mL of deionized water. After the samples passed through, the cartridges were washed sequentially with 2 mL of each of the following: deionized water, 0.1 M hydrochloric acid, dichloromethane/methanol (1:1) and n-hexane. After drying under full vacuum for 1 min, the analytes were eluted with 2 mL of a mixture of dichloromethane: isopropanol (80:20, v/v) with 2% of ammonium hydroxide. The extracts were dried at 45 °C under a gentle nitrogen stream. Sixty five microliters of N-Methyl-N-(trimethylsilyl) trifluoroacetamide (MSTFA) with 5% of trimethylchlorosylane (TMS) were added, and after vortex mixing for 30 s, derivatization takes place at 80 °C for 25 min. The extracts were transferred to autosampler vials and a 2 µL aliquot was injected in the chromatographic system.

3.5. References

[1] T. Gostič, S. Klemenc, B. Štefane. A study of the thermal decomposition of adulterated cocaine samples under optimized aerobic pyrolytic conditions. *Forensic Sci. Int.*, **2009**, *187*, 19–28.

[2] M. Barroso, M. Dias, D. N. Vieira, J. A. Queiroz, M. López-Rivadulla, M. Lo. Development and validation of an analytical method for the simultaneous determination of cocaine and its main metabolite, benzoylecgonine, in human hair by gas chromatography/mass spectrometry. *Rapid Commun. Mass Spectrom.*, **2008**, *22*, 3320–6.

[3] F. Musshoff, B. Madea. Analytical pitfalls in hair testing. *Anal. Bioanal. Chem.*, **2007**, *388*, 1475–1494.

[4] T. Cairns, V. Hill, M. Schaffer, W. Thistle. Removing and identifying drug contamination in the analysis of human hair. *Forensic Sci. Int.*, **2004**, *145*, 97–108.

Chapter 4 – Hair decontamination: cannabinoids

This chapter describes the development and optimization of a contactless hair decontamination procedure applied to cannabinoids.

The presented results are under submission for the peer-reviewed international journal Drug Testing and Analysis.

Table of contents

4.1. THC-COOH in hair as proof of cannabinoids consumption

In terms of external contamination in hair, cannabinoids are definitely the most important drugs. Since cannabinoids are smoked and due to the THC boiling point (157 ºC at normal pressure) [1], they become easily deposited at the hair surface. Although in Chapter 1 several decontamination strategies for the removal of THC from the surface were presented, according to the *Society of Hair Testing* a hair sample can only be considered positive if the metabolite 11-nor-9-carboxy-Δ^9-tetrahrydrocannabinol (THCOOH) is present at concentrations above 0.2 pg/mg [2]. The fact that THCOOH appears only in hair following active consumption allows to process hair samples without prior decontamination. Even though this situation for cannabinoids seeming almost perfect (no decontamination needed), the reality is that for detection of THC-COOH, more sensitive techniques are needed (e.g. GC-MS-MS), which are quite expensive and not available in most laboratories. Additionally, there are several publications where the authors fail to detect THCCOOH in positive hair samples, even using highly sensitive instrumentation [3–5].

4.2. Δ^9-Tetrahydrocannabinolic acid: an external contamination issue

Another problem associated to external contamination of cannabinoids is the possible presence of Δ^9-tetrahydrocannabinolic acid (THCA). THCA is the biosynthetic precursor of THC [6,7] (Figure 4.1) and it is known to be present in cannabis material at concentrations higher than those of THC. Indeed, THCA, when heated or smoked, undergoes a decarboxylation reaction, which leads to THC [8–10].

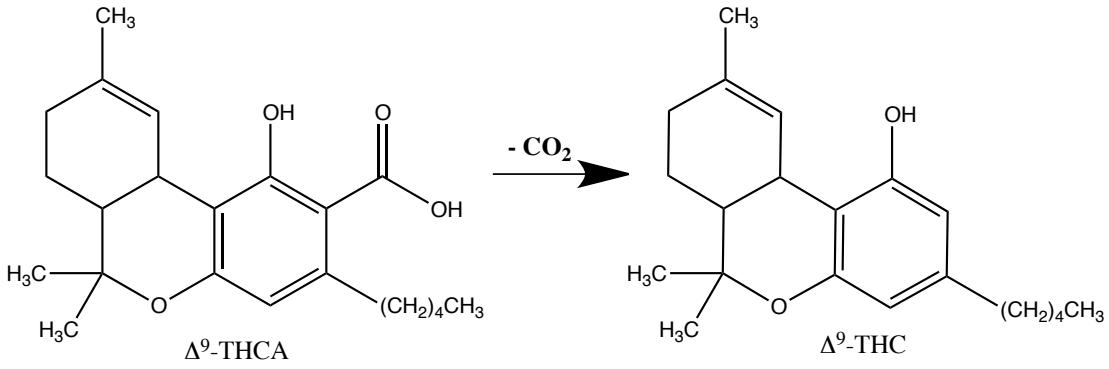

Figure 4.1 –Conversion of THCA into the active THC.

In a recent study [10], the authors demonstrated that THCA can be present at the external surface of hair in concentrations that can go up to 10 ng/mg. The authors concluded that this high concentration cannot be only explained by exposure to side stream smoke, but as well due to cannabinoid material handling. At a glance, the presence of THCA in a hair digest doesn't seem to be problematic, because the detector (MS detector) will be able to distinguish it from THC and other THC metabolites, but there is a problem related to THCA thermal stability. Dussy et al. [9] demonstrated that when THCA reaches the GC injector, the majority of it (conversion yield > 65%) is quickly converted to THC (Figure 4.1), leading to the quantification of increased concentrations.

Due to the previously mentioned reasons, the challenge to develop a decontamination process that ensures the complete removal of both THC and THCA remains and it constituted the main goal of the herein presented work.

4.3. Results and discussion

4.3.1. Hair contamination

Due to the absence of real externally contaminated hair samples, a batch of cannabinoids-free hair samples was exposed to hashish smoke for 7 h in a close environment. This sample batch presented an average THC concentration of 32 ± 7 ng/mg of hair. These samples were also submitted to the wash criterion proposed by Cairns et al. [11], and were considered negative.

4.3.2. Screening of ionic liquids

Based on the results obtained in Chapter 2, where the ability of ILs to extract the opiates in less than 24h was shown, the extraction time of 24h was chosen for the experiments of the following screening.

- **Phosphonium based ILs**

Although only two ILs were tested, it seems that the liquid containing the chloride anion has much more affinity to THC than dicyanamide (Figure 4.2).

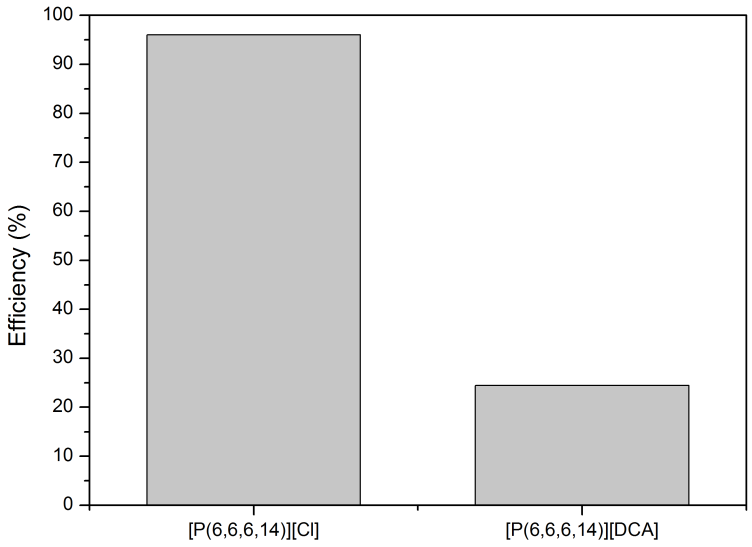

Figure 4.2 - Decontamination efficiencies obtained for the tested phosphonium based ILs. (24 h, 120 ºC).

- **1-Methyl-3-alkylimidazolium based ILs**

As already mentioned, 1-methyl-3-alkylimidazolium based ILs are the most widely studied ILs. From the results presented in Figure 4.3 it is perceptible the affinity of this group of ILs to THC (efficiency > 65%, with exception of [EMIM][$EtSO_4$]), which is a lipophilic drug. Furthermore, the increase of the alkyl chain length seems to favor the extraction. It is also important to stress the particular case of the

[C_2OHMIM] [BF_4]. Despite having a small alkyl chain, the presence of the hydroxyl group enables hydrogen-bonding interaction between the drug and the IL.

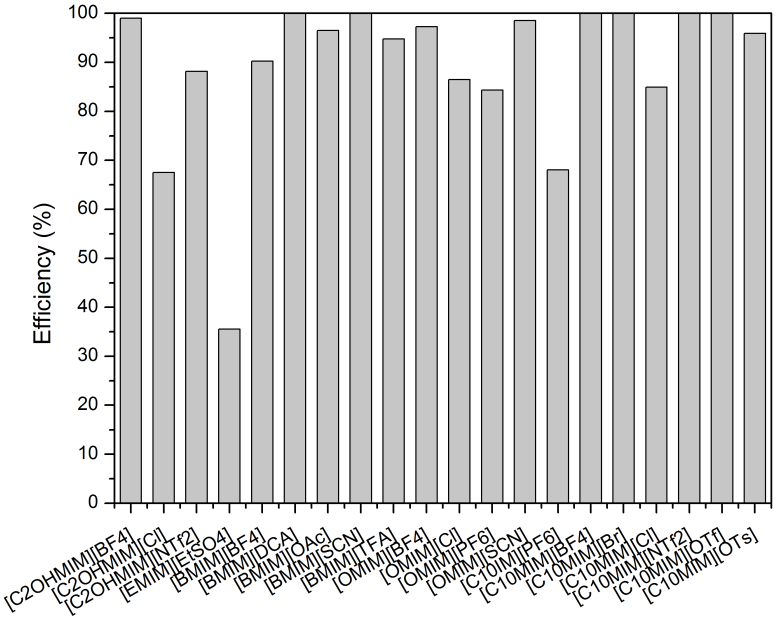

Figure 4.3 - Decontamination efficiencies obtained for the tested 1-methyl-3-alkylimidazolium based ILs (24 h, 120 ºC).

• Benzylimidazolium based ILs

In this group, both 1,3-dibenzyl and 1-methyl-3-benzylimidazolium were tested. As seen in Figure 4.4, all of them presented efficiencies above 90%.

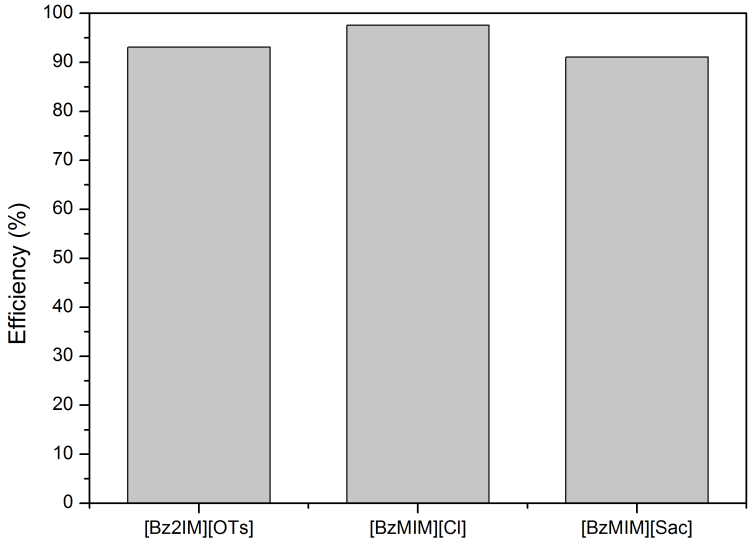

Figure 4.4 - Decontamination efficiencies obtained for the tested benzylimidazolium based ILs (24 h, 120 ºC).

• 1-Alkyl-3-methylpyridinium based ILs

In the case of 1-alkyl-3-methylpyridinium based ILs (Figure 4.5), only two ILs were tested. Once more, the IL with the smaller alkyl chain, [EMPy][$EtSO_4$], extracted poorly the THC, while [AlPy][PF_6] extracted almost 83%.

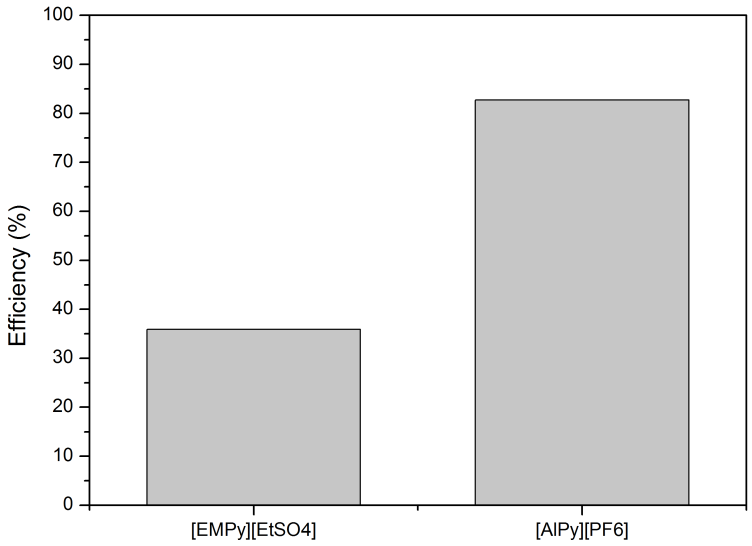

Figure 4.5 - Decontamination efficiencies obtained for the tested 1-methylpyridinium based ILs (24 h, 120 ºC).

• Quaternary ammonium based ILs

In this group, trialkylammonium, guanidinium and choline based ILs were tested. In the case of the trimethylammonium based ILs (Figure 4.6), the results obtained for [($C_{12}H_{25}$)TMA][Ots] (efficiency of 57 %) and for [($C_{16}H_{33}$)TMA][Ots] (efficiency of 99 %) seem to point again for the influence of the alkyl chain length, because its increase enhances the lipophilic character of the IL, favoring the affinity to this drug. On the other hand, for the PhTMA based ILs, the anion seems to influence the efficiency in the following increasing order: OTs < OTf < SCN < TFA < DCA.

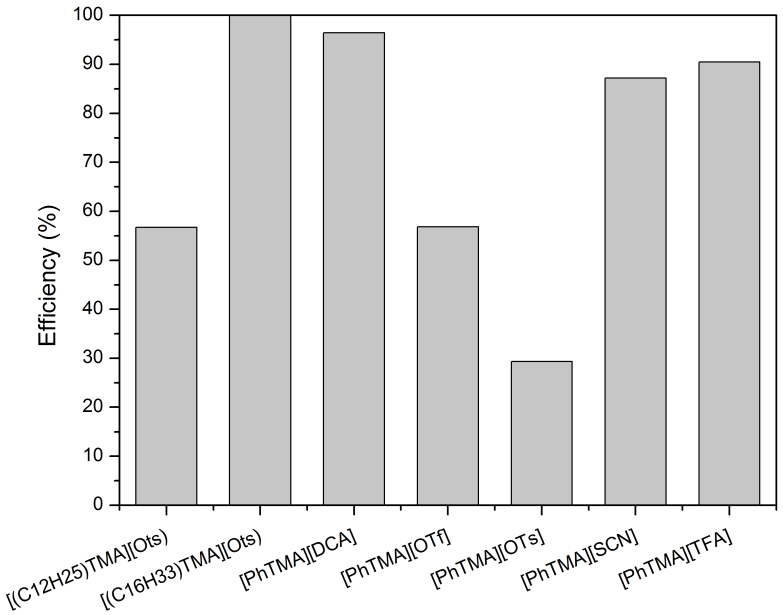

Figure 4.6 - Decontamination efficiencies obtained for the tested trimethylammonium based ILs (24 h, 120 ºC).

Regarding triethylammonium based ILs, all tested liquids present outstanding efficiencies, all above 94 % (Figure 4.7).

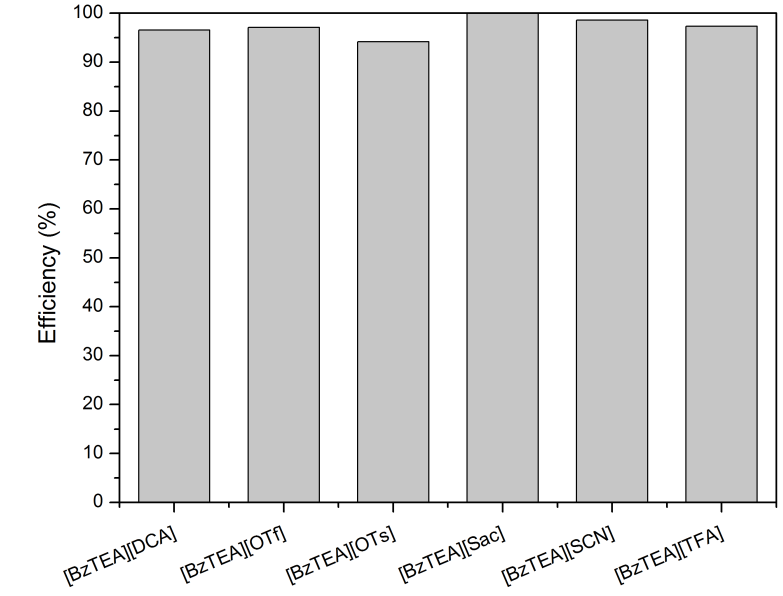

Figure 4.7 - Decontamination efficiencies obtained for the tested triethylammonium based ILs (24 h, 120 ºC).

The tested guanidinium based ILs (Figure 4.8) didn't produce very good results, with exception for [TMGC4][DCA] (efficiency of 93 %).

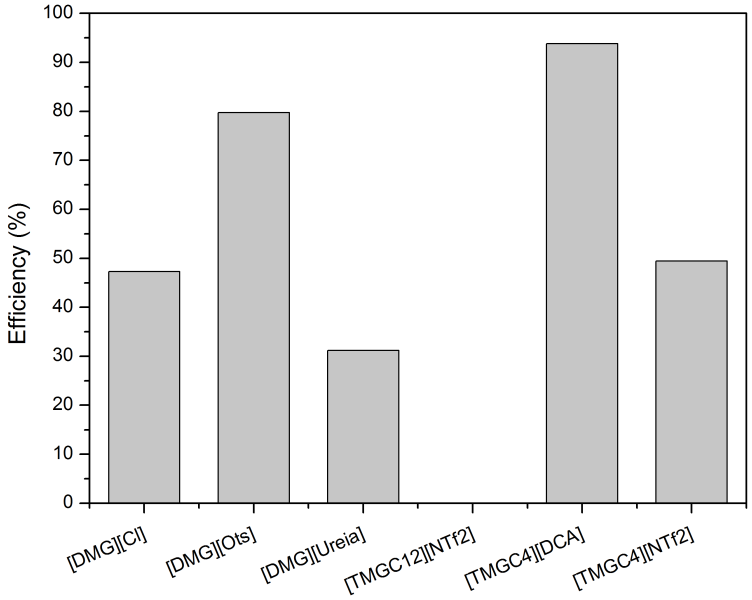

Figure 4.8 - Decontamination efficiencies obtained for the tested guanidinium based ILs (24 h, 120 ºC).

In the case of choline (Figure 4.9), choline based ILs and eutectic mixtures of choline were tested. In all cases, it seems that the increase of hydrogen-bonding donors (carbonyl groups) favors the extraction and retention of THC (malonic and tartaric acid, as well as H-maleate [Mal] (derived from malic acid), all are di-carboxylic acids).

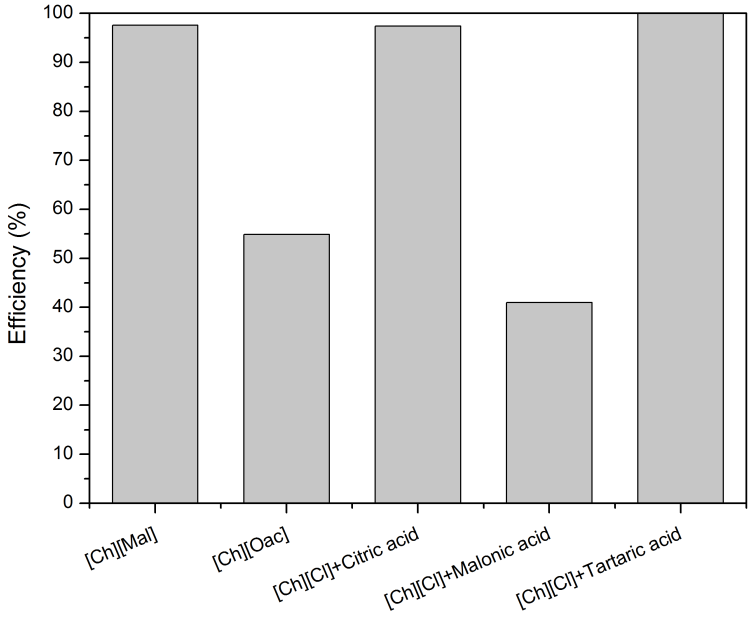

Figure 4.9 - Decontamination efficiencies obtained for the tested choline based ILs and choline eutectic mixtures (24 h, 120 ºC).

• Mixtures of ILs: Aliquat based ILs

In this part of the work, the only ILs mixtures tested were aliquat based ILs (Figure 4.10). Once more the DCA anion seems to favor the affinity of THC to the IL (efficiency of 85 %). The remaining liquids gave origin to less significant results.

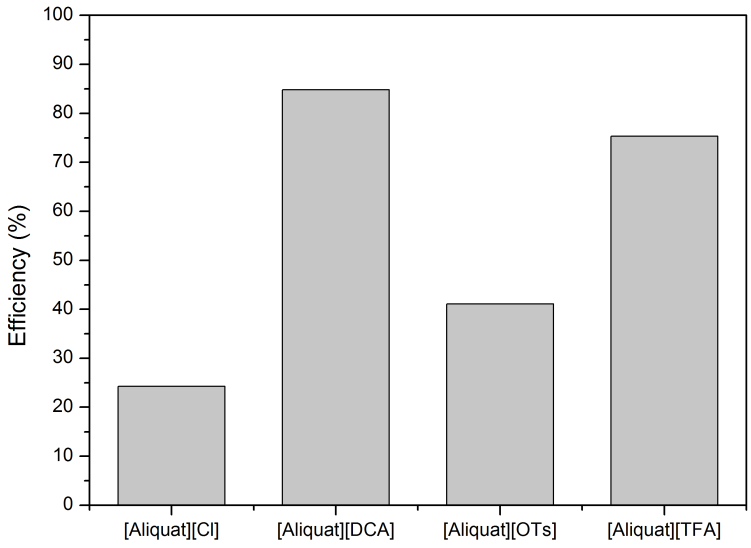

Figure 4.10 - Decontamination efficiencies obtained for the tested aliquat based ILs (24 h, 120 ºC).

4.3.3. Heat Experiments performed in the absence of ILs

Accordingly to the previous chapters, experiments performed in the absence of IL were made. In these experiments the hair was simply heated for 24 h with, and without vacuum (Table 4.1 and 4.2), and the extraction efficiencies were always below 90%.

Table 4.1 - Decontamination efficiencies for *in vitro* contaminated samples obtained for the experiments, where the hair was heated at 100 ºC, for 24 h, under vacuum (0.1 mBar) and without any IL (average values for three independent experiments).

	THC
Efficiency (%)	89.65
Standard deviation	5.32
CV (%)	5.93

Table 4.2 - Decontamination efficiencies for *in vitro* contaminated samples obtained for the experiments, where the hair was heated at 100 ºC, for 24 h, at atmospheric pressure and without any IL (average values for three independent experiments).

	THC
Efficiency (%)	61.04
Standard deviation	8.80
CV (%)	14.42

4.3.4. Screening summary

In the case of THC, the screening revealed that the large majority of the tested ILs are suitable to be applied in the decontamination of hair samples contaminated with THC. Based on the obtained screening results, and aiming at maintaining consistency, [C_2OHMIM][BF_4] was chosen. It is important to remark that this IL was already chosen in the case of opiates (high thermal stability and good capability to extract the studied opiates).

4.3.5. Process optimization

As in chapter 2, before starting optimization, it is of outmost importance to establish the variables that are supposed to influence significantly the response (in this case extraction efficiency). Therefore, the variables extraction temperature, time and amount of IL used were chosen. It is important to remark that, contrary to the case of opiates (see chapter 2), water content of the IL was not taken into account. This decision relates to relatively low boiling point of THC. Based on the screening results, we considered that the water content would have very little influence on the extraction efficiency.

In order to screen the statistical significance of the chosen variables, a two-level-full factorial design was used.

The estimated effects (main effects), interactions between variables, linear model's coefficients (Coef), Students *t*'s test values (for the null hypothesis that all the coefficients are zero; not shown), as well as their associated probabilities (*P*) (at a level of confidence of 95%) were determined from the experimental results for the screening design of the extraction efficiencies under different conditions of temperature, time and amount of IL (Table 4.3).

Table 4.3 - Estimated effects and coefficients for THC extraction.

Term	Effect	Coef	P
Constant		66.67	0.00
Temperature	23.03	11.52	0.00
Time	-10.35	-5.18	0.00
Amount IL	4.17	2.08	0.03
Temperature*Time	11.87	5.93	0,00
Temperature*Amount IL	-0.81	-0.41	0.62
Time*Amount IL	-2.53	-1.27	0.15
Temperature*Time*Amount IL	-11.22	-5.61	0,00

From the analysis of the screening results, it is possible to conclude that temperature is the one with higher effect on the response. This conclusion is in accordance with our expectations regarding this drug. The increase of temperature lead to an increase of the vapor pressure of THC present at the surface of the hair, followed by the "capture" of THC molecules at the interface of the IL. Contrary to what happened with opiates (see chapter 2), the amount of IL was statistical significant for the process, though with little effect. Besides the temperature * amount of IL interaction, all the variables and remaining interactions had statistical significance ($p < 0.05$).

As already mentioned, a linear model was applied to the screening results, thus the possibility of curvature in the variables effects had to be checked by means of a central composite design (CCD). In this case, all variables were checked.

After applying the CCD, the results allowed us to obtain response surface plots, which are very useful in determining the region where the optimum conditions can be found (Figure 4.11).

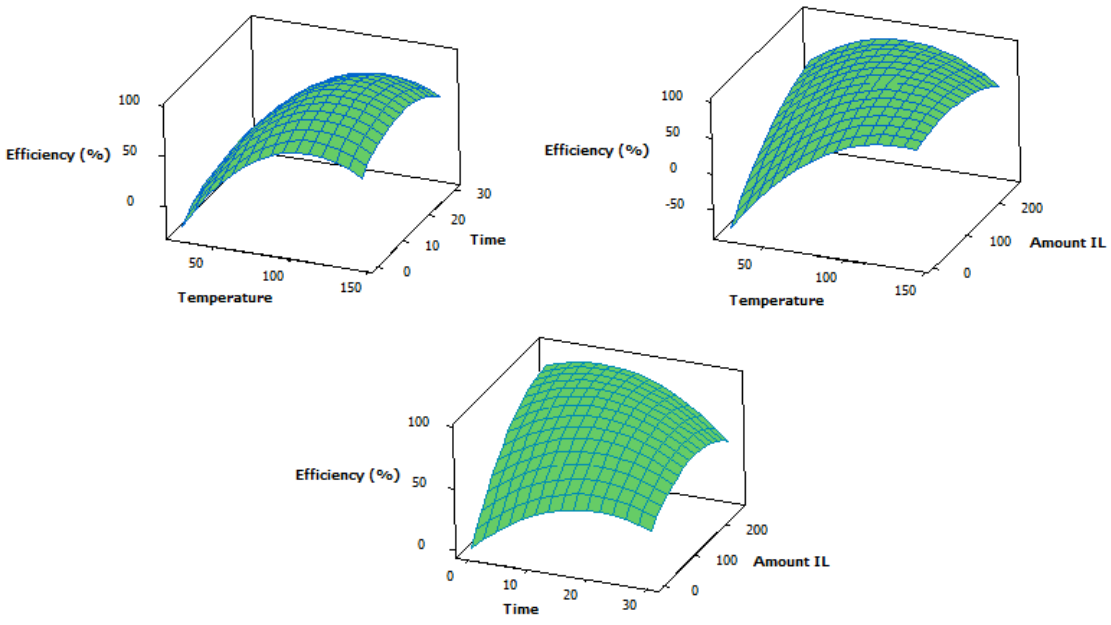

Figure 4.11 - Response surface plot of the predicted response against temperature and time, temperature and amount o IL, time and amount of IL for THC.

The R^2, given by the statistical software, is useful to obtain the percentage of variation in the response explained by the regression model [12]. In this particular case, a R^2 of 0.98 was obtained. This value means that the model can explain 98% of the variations in the response. This result is very encouraging, giving also strength to the optimized conditions.

Although the factorial design results predicted that all studied variables were statistically significant, the RSM design (higher precision) demonstrated the opposite (Table 4.4). It turned out that the extraction time (in the studied range) was not statistically significant. The same situation was observed regarding the temperature-time interaction. This means that the effect of temperature was not dependent of the extraction time.

Table 4.4 - Analysis of results for the applied model obtained using the central composite design for THC (R^2 = 0.98) to contaminated samples.

	THC		
Term	**Coef**	**SE Coef**	***p***
Constant	85.901	2.035	0.00
Temperature	23.6112	1.671	0.01
Time	-0.0265	2.307	0.99
Amount IL	14.3505	1.671	0.00
Temperature*Temperature	-16.3731	1.377	0.00
Time*Time	-8.3862	1.98	0.00
Amount IL*Amount IL	-7.2252	1.377	0.00
Temperature*Time	0.5499	2.448	0.83
Temperature*Amount IL	-12.774	2.437	0.00
Time*Amount IL	-6.6505	2.448	0.03
Source		**F**	***p***
Regression		38.39	0.00
Linear		73.52	0.01
Square		57.4	0.02
Interaction		12.26	0.03
Lack-of-Fit		0.09	0.92

The analysis of variance shows that a second order interaction model is significant for this system and no lack-of-fit is observed ($p > 0.05$).

Based on the model coefficients, presented in Table 4.6, a desirability function (D function) was applied to these results, whose solution predicts mathematically the optimum values for each studied variable. In this case, and having as goal an extraction efficiency as closest to 100 % as possible, a maximization function with a weight of 1 for each variable was chosen. The optimum conditions obtained by the D function are presented in Table 4.7. These conditions represent a desirability (D) of 0.823 (the closest to 1, the best).

Table 4.5 - Optimum conditions predicted by the maximization desirability function for the decontamination of THC contaminated hair samples.

	THC
Temperature (ºC)	101.1
Time (h)	12.7
Amount of IL (mg)	177.2

4.3.6. Method validation

Similarly to the case of opiates, we decided to compare the developed method against the method proposed by Cairns et al. [11], although these authors do not apply their decontamination to cannabinoids (since they detect and quantify the THCCOOH metabolite). Even so, we think that that method is suitable to test the validity of our approach.

Sample #	THC
1	105.10
2	335.08
3	4.15
4	180.14
5	60.60
6	12.41
7	35.43
8	56.71
9	47.51
10	684.67
11	311.48
12	230.37
13	95.57
14	77.58
15	570.37

In order to eliminate the influence of biological variability associated to hair samples, fifteen negative hair samples, collected from different subjects and with different hair colors, were externally contaminated with THC. The contamination results are presented in Table 4.8:

Table 4.6 - Concentrations of the analyte (ng/mg) in the contaminated samples prior to decontamination.

From the analysis of the previous table, it is easy to see that all samples have contamination levels very much above the cut-off (0.05 ng/mg [2]). In some cases (e.g. sample # 10), the contamination concentration is so high that it can be considered as

"unrealistic", though we think that these high contamination levels will contribute to check the strength of our method.

Both methods (ours and that of Cairns et al.) were used to decontaminate those samples. Table 4.9 shows analyte concentrations (in ng/mg) in the hair samples (hair digests, after decontamination) and in the last washing solution.

Table 4.7 - Comparison between the Cairns *et al* washing method and our method, using contaminated samples. The IL experiments were carried at 100 ºC for 13 h and using 175 mg of $[C_2OHMIM][BF_4]$.

			Cairns *et al.* Method		Developed method
Sample #, color	**Dyed**	**Wash fraction or hair digest**	**(ng/mg Hair)**		**(ng/mg Hair)**
			Wash and hair values	**Hair minus (5 x LW)**	**Hair values**
1, Blonde	N/D	Last wash	5.73		
		Hair digest	42.96	14.32	93.43
2, Blonde	N/D	Last wash	4.52		
		Hair digest	92.86	70.25	144.89
3, Brown	D	Last wash	1.54		
		Hair digest	52.59	44.87	26.59
4, Brown	N/D	Last wash	2.03		
		Hair digest	65.55	55.39	7.23
5, Black	N/D	Last wash	1.51		
		Hair digest	34.96	27.42	21.92
6, Black	N/D	Last wash	0.42		
		Hair digest	11.98	9.87	0.80
7, Black	N/D	Last wash	1.01		
		Hair digest	26.09	21.05	4.85
8, Brown	D	Last wash	1.42		
		Hair digest	57.66	50.57	18.55
9, Black	N/D	Last wash	0.66		
		Hair digest	21.57	18.29	23.96
10, Brown	N/D	Last wash	15.33		
		Hair digest	167.57	90.92	351.21
11, Blonde	N/D	Last wash	4.31		
		Hair digest	109.74	88.19	13.53
12, Black	N/D	Last wash	2.23		
		Hair digest	33.43	22.28	25.67
13, Brown	N/D	Last wash	3.90		
		Hair digest	82.33	62.83	26.19
14, Black	D	Last wash	1.83		
		Hair digest	32.77	23.62	5.16
15, Brown	N/D	Last wash	14.47		
		Hair digest	57.50	-14.85	181.85

Similar to what was observed in the case of opiates (see chapter 2), different hair samples submitted to the same contamination conditions have different contamination levels. Another important remark is that all samples are considered positive, even after washing (concentration > 0.05 ng/mg [2]). Although this observation might seem puzzling, the lipophilic character of THC may explain the obtained results. Auwärter et al. [8,13] demonstrated that THC can migrate from the surface of hair into its interior, since it can penetrate the membranes of the basal cells. Therefore, after the deposition of THC at the surface of our hair samples, part of it diffused into the interior, explaining these "positive" results.

Comparing now both decontamination methods, it is observed once more that none of them presents 100 % efficiency. Furthermore, from the analysis of Figure 4.12, where the difference between the amounts of drug found in the hair digest (HD of Cairns et al. - HD of our method.) is shown for each sample, we conclude that in most of the cases our method is more efficient. In average terms, our method is 11 % more efficient, though this difference remains in the range of the variability expected in a hair sample (20 %), resulting in lack of significance. Nevertheless, and despite the low sampling (15 samples), these results seem to point out to the validity of our method. Its main advantage relative to the one of Cairns et al. is the possibility of achieving the same results with fewer steps and lower sample loss risk and the possibility to process several samples simultaneously. Additionally, the combination of high temperature (100 ºC), 13 h and the possible traces of water in the IL will promote the full conversion of any possible THCA present in the hair samples to THC [9,14], followed by its extraction by the IL.

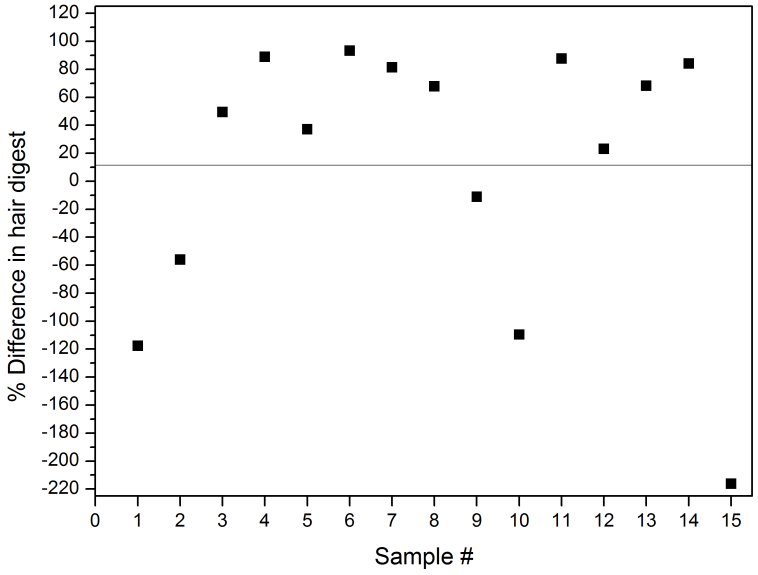

Figure 4.12 - Percentage of difference in the hair digests between Cairns *et al* washing method and the developed method. The solid line represents the average difference.

4.4. Conclusions

In this chapter, a novel process for the extraction of THC from hair's surface using ILs is described. Similarly to the case of opiates described in chapter 2, this method relies on the unique properties of ILs, namely being almost non-volatile (therefore the hair is not re-contaminated) and presenting high affinity for this drug, resulting in a contactless and efficient hair decontamination process.

Although only fifteen different samples were tested so far, it seems that the developed method is as valid as other methods (e.g. Cairns et al. method), with the advantage of overcoming the problem associated to the eventual presence of THCA contamination, because THCA is converted into THC which is then extracted (decreasing dramatically the probability of a false positive). It is also important to remark that,

although a decontamination time of 13 h may be considered a disadvantage, the method allows simultaneously decontaminating many samples (possibly more than 100, depending on the size of the oven) and the process can be carried out overnight without the presence of any technician.

4.5. Experimental

4.5.1. Reagents and standards

The ILs [P(66614)][Cl], Aliquat® 336, [EMIM][$EtSO_4$], [BMIM][BF_4], [OMIM][BF_4] and [C_2OHMIM][BF_4] were kindly offered by Cytec (Ontario, Canada) and Sigma Aldrich (Madrid, Spain), respectively. The ILs [EMIM][$EtSO_4$], [BMIM][BF_4], [OMIM][BF_4] and [C_2OHMIM][BF_4] were purchased to Solchemar (Monte da Caparica, Portugal),. The remaining ILs were prepared in our laboratory. All ILs had purities above 98% and water contents lower than 1% (checked by Karl Fischer). Due to the number of tested ILs, complete information (name, structure and abbreviated name) is summarized in the appendix (Table A.1).

The standard of THC, as well as its tri-deuterated analogue, was supplied by Cerilliant (Round Rock, TX, USA) in methanol at 1 mg/mL. Methanol (HPLC grade), dichloromethane, n-hexane, 2-propanol, sodium hydroxide, hydrochloric acid, sodium and potassium phosphate, sodium and potassium chloride (analytical grade) were obtained from Merck Co (Darmstadt, Germany). Oasis® MCX (3 mL, 60 mg) extraction cartridges were obtained from Waters (Milford, MA, USA). Working solutions at 10 and 1 μg/mL THC was prepared by proper dilution of the stock solutions with methanol, and these were used for the calibrators. Additional working solutions, at 1 and 10 μg/mL, have been used to prepare the quality control samples; these solutions were prepared using different lots of the analytical standards when available. A working solution of the internal standard at 5 μg/mL was prepared also in methanol. All these solutions were stored light-protected between 2 and 8 °C.

To prepare the phosphate buffered saline (PBS) solution, 200 mg potassium dihydrogenphosphate, 1150 mg de sodium hydrogenphosphate, 200 mg de potassium chloride and 8000 mg of sodium chloride were weighed into a volumetric flask, obtaining a final volume of 1 L with deionized water.

4.5.2. Biological samples

Negative hair samples were kindly provided by laboratory staff, and were previously tested for negativity. All samples were sequentially washed with dichloromethane and water in order to remove eventual traces of sweat, sebum and hair care products.

4.5.3. Chromatographic conditions

Chromatographic analysis was performed using an HP 6890N gas chromatograph (Hewlett-Packard, Waldbronn, Germany), equipped with a model 5973 mass-selective detector (Hewlett-Packard, Waldbronn, Germany). A capillary column (30 m×0.25 mm I.D., 0.25 μm film thickness) with 5% phenylmethylsiloxane (HP-5 MS), supplied by J & W Scientific (Folsom, CA, USA), was used. Chromatographic conditions were as follows: initial oven temperature was 150 °C for 2 min, which was increased by 20 °C min^{-1} to 300 °C, held for 6 min. The temperatures of the injection port and detector were set at 220 and 280 °C, respectively. The split injection mode was used (split ratio of 1:5), and helium with a flow rate of 0.8 mL min^{-1} was used as the carrier gas. The mass spectrometer was operated with a filament current of 300 μA and electron energy of 70 eV in the electron ionization (EI) mode. Quantitation was done in the selected ion-monitoring (SIM) mode, and the ions were monitored at m/z *314*, 299 and 271 for THC. (quantitation ion is presented in italics). For the internal standard, only one ion was monitored, at m/z 317 for THC-d_3.

4.5.4. Hair contamination procedure

For the elaboration of this work, *in vitro* contaminated hair samples were prepared. The contaminated samples were prepared by placing 20 g of hair (already cut into pieces with an approximate length of 1 mm) in contact with smoke of 150 mg of hashish electrically heated until 200 ºC (Figure 4.13) for 7 h. For the validation experiments, a similar procedure was applied, though only 1 g of each sample was used.

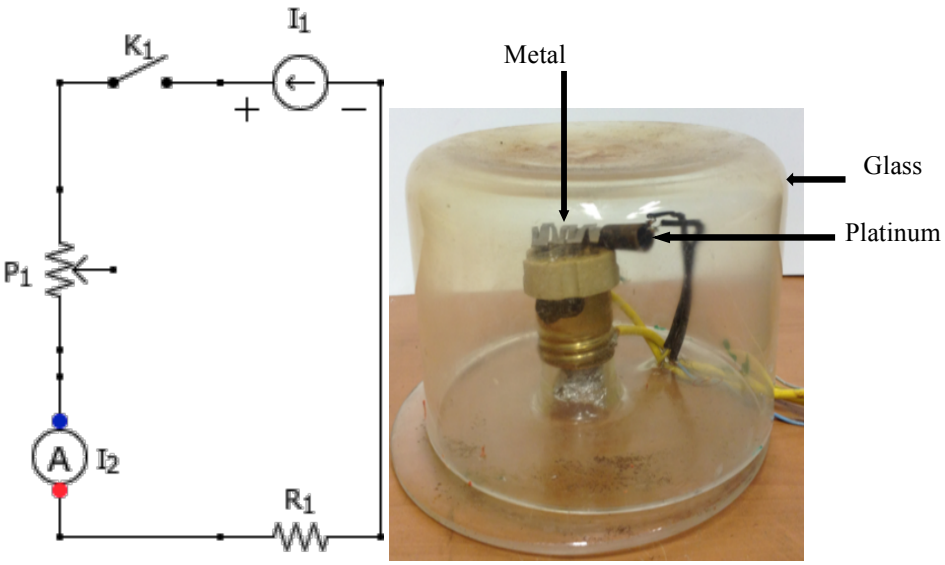

Figure 4.13 – Custom equipment used to produced THC *in vitro* contaminated hair samples.

4.5.5. Decontamination experiments

For the decontamination experiments, the same procedure of opiates (see chapter 2) was used, though the extraction time was reduced for 24h and the temperature increased to 120 ºC.

4.5.6. Drug extraction from hair and sample cleanup

All hair samples were analyzed according to the procedures used in the laboratory. Briefly, 20 mg of hair is incubated for 40 minutes in 1 mL of 1M NaOH at 50 ºC, being neutralized afterwards with 200 μL of 5M HCl. The extracts are transferred to polypropylene tubes, followed by the addition of 5 mL of PBS. After the addition of

25 µL of internal standard mixture (5 µg/mL), the samples are homogenized for 15 min by rotation/inversion movements. This homogenate is added to mixed-mode extraction cartridges previously conditioned with 2 mL of methanol and 2 mL of deionized water. After the samples pass through, the cartridges are washed sequentially with 2 mL of each of the following: 0.1 M NaOH, deionized water and n-hexane. After drying under full vacuum for 1 min, the analytes are eluted with 2 mL of a mixture of dichloromethane: isopropanol (75:25, v/v). The extracts were dried at 45 °C under a gentle nitrogen stream. Fifty microliters of methanol was added, and vortex mixed for 30 s. The extracts were transferred to autosampler vials and a 2 µL aliquot was injected in the chromatographic system.

4.5.7. Design of Experiments (DOE) and experimental design

The process was initially optimized concerning the following variables at two levels (low – high): temperature (50 – 120 ºC), extraction time (6 – 24 h) and IL amount (50 – 200 mg), as well as their possible interactions. These variables were screened by means of a two-level, four-factor full factorial design (2^3) [12]. Since some dispersion was expected, three replicates were performed. The independent variables, the corresponding values of the low (-1) and high (+1) levels and the matrix obtained for this screening design are shown in Table 4.8. These experiments were carried out in a random order to avoid the influence of noise factors, thus minimizing systematic errors [15].

Table 4.8 - Design matrix for the screening experiments, expressed in uncoded units.

StdOrder	RunOrder	Temperature (ºC)	Time (h)	Amount IL (mg)
8	1	120	24	200
12	2	120	24	50
7	3	50	24	200
10	4	120	6	50
4	5	120	24	50
5	6	50	6	200
9	7	50	6	50
15	8	50	24	200
14	9	120	6	200
2	10	120	6	50
6	11	120	6	200
11	12	50	24	50
16	13	120	24	200
1	14	50	6	50
13	15	50	6	200
3	16	50	24	50

The optimization of the chosen variables employed a 2^3 factorial central composite design (CCD) with a total of 20 experiments [six axial points (α=1.682), six replicates at the center points in a cube (coded as zero level) and eight cube points at the levels ±1, Table 4.9]. Therefore, each factor was evaluated at five different levels [16]. All the experiments were carried out randomly.

Table 4.9 - Design matrix for the CCD experiments, expressed in uncoded units.

StdOrder	RunOrder	Temperature (ºC)	Time (h)	Amount IL (mg)
9	1	26	15	125
11	2	85	0	125
1	3	50	6	50
17	4	85	15	125
18	5	85	15	125
3	6	50	24	50
12	7	85	30	125
16	8	85	15	125
6	9	120	6	200
19	10	85	15	125
14	11	85	15	251
10	12	144	15	125
4	13	120	24	50
20	14	85	15	125
7	15	50	24	200
13	16	85	15	0
2	17	120	6	50
5	18	50	6	200
8	19	120	24	200
15	20	85	15	125

Both screening and optimization designs, as well as all data analysis were performed using Minitab® statistical program software, version 16.

4.6. References

[1] J. M. McPartland, E. B. Russo. Cannabis and Cannabis Extracts. *J. Cannabis Ther.*, **2001**, *1*, 103–132.

[2] G. a a Cooper, R. Kronstrand, P. Kintz. Society of Hair Testing guidelines for drug testing in hair. *Forensic Sci. Int.*, **2012**, *218*, 20–4.

[3] M. A. Huestis, R. A. Gustafson, E. T. Moolchan, A. Barnes, J. a Bourland, S. A. Sweeney, E. F. Hayes, P. M. Carpenter, M. L. Smith. Cannabinoid concentrations in hair from documented cannabis users. *Forensic Sci. Int.*, **2007**, *169*, 129–36.

[4] T. Mieczkowski. A research note: the outcome of GC/MS/MS confirmation of hair assays on 93 cannabinoid (+) cases. *Forensic Sci. Int.*, **1995**, *70*, 83–91.

[5] H. Sachs, U. Dressler. Detection of THCCOOH in hair by MSD-NCI after HPLC clean-up. *Forensic Sci. Int.*, **2000**, *107*, 239–247.

[6] P. B. BAKER, B. J. TAYLOR, T. A. GOUGH. The tetrahydrocannabinol and tetrahydrocannabinolic acid content of cannabis products. *J. Pharm. Pharmacol.*, **1981**, *33*, 369–372.

[7] S. Sirikantaramas, S. Morimoto, Y. Shoyama, Y. Ishikawa, Y. Wada, Y. Shoyama, F. Taura. The gene controlling marijuana psychoactivity: molecular cloning and heterologous expression of Delta1-tetrahydrocannabinolic acid synthase from Cannabis sativa L. *J. Biol. Chem.*, **2004**, *279*, 39767–74.

[8] V. Auwärter, A. Wohlfarth, J. Traber, D. Thieme, W. Weinmann. Hair analysis for Delta9-tetrahydrocannabinolic acid A--new insights into the mechanism of drug incorporation of cannabinoids into hair. *Forensic Sci. Int.*, **2010**, *196*, 10–3.

[9] F. E. Dussy, C. Hamberg, M. Luginbühl, T. Schwerzmann, T. a Briellmann. Isolation of Delta9-THCA-A from hemp and analytical aspects concerning the determination of Delta9-THC in cannabis products. *Forensic Sci. Int.*, **2005**, *149*, 3–10.

[10] B. Moosmann, N. Roth, V. Auwärter. Hair analysis for THCA-A, THC and CBN after passive in vivo exposure to marijuana smoke. *Drug Test. Anal.*, **2014**, *6*, 119–25.

[11] T. Cairns, V. Hill, M. Schaffer, W. Thistle. Removing and identifying drug contamination in the analysis of human hair. *Forensic Sci. Int.*, **2004**, *145*, 97–108.

[12] D. C. Montgomery. *Design and Analysis of Experiments*, John Whiley & Sons, Inc, New York, **2001**.

[13] V. Auwärter, F. Sporkert, S. Hartwig, F. Pragst, H. Vater, A. Diefenbacher. Fatty acid ethyl esters in hair as markers of alcohol consumption. Segmental hair analysis of alcoholics, social drinkers, and teetotalers. *Clin. Chem.*, **2001**, *47*, 2114–23.

[14] H. Perrotin-Brunel, W. Buijs, J. Van Spronsen, M. J. E. Van Roosmalen, C. J. Peters, R. Verpoorte, G. J. Witkamp. Decarboxylation of Δ9-tetrahydrocannabinol: Kinetics and molecular modeling. *J. Mol. Struct.*, **2011**, *987*, 67–73.

[15] J. N. Miller, J. C. Miller. *Statistics and Chemometrics for Analytical Chemistry*, Pearson / Prentice Hall, Harlow, **2000**.

[16] M. A. Bezerra, R. E. Santelli, E. P. Oliveira, L. S. Villar, L. A. Escaleira. Response surface methodology (RSM) as a tool for optimization in analytical chemistry. *Talanta*, **2008**, *76*, 965–77.

Chapter 5 – Understanding the decontamination phenomenon: IL-water vapor interaction

This chapter describes the rationalization of the decontamination process in terms of the interaction between the water vapor and the ionic liquid.

The presented results were published in the peer-reviewed international journal Journal Physical. Chemistry. C 2013, 117, 10454−10463.

Table of Contents

5.1. Quartz crystal microbalance (QCM-D) a powerful tool for vapor detection

For many years, piezoelectric devices have been used as sensors for organic vapors [1]. Detection was based on the measurement of the frequency shifts observed when the vapor adsorbs/absorbs onto the films deposited on the surface of gold-coated quartz crystals. The recent development of high sensitivity quartz-crystal microbalances with dissipation (QCM-D) led to renewed interest in that vapor detection technique.

Ceramics, polymers, self-assembled monolayers, and organic oils were the most commonly used materials to coat the gold surface of the quartz crystals [1–4]. In principle, liquids would be attractive sensing materials because they are in thermodynamic equilibrium and they enable fast diffusion of the analytes. Ionic liquids (ILs) have the exact characteristics to be considered as excellent gas sensors. They are liquids with vanishing vapor pressure at ambient temperature, which solves the problem of liquid evaporation. On the other hand, a broad range of functionalities in the side groups of the ionic liquids may be chosen in order to ensure the wettability of the sensor surface and/or the affinity towards the specific organic vapor.

5.2. QCM as a tool to study interactions between ILs and vapors

The usage of ionic liquids as sensing materials for QCM-based vapor-sensing devices was first reported in 2002 by Liang et al [5]. They demonstrated that the responses of the ionic liquid based QCM device towards a vapor depended on the types of cations and anions present and they interpreted the frequency shifts as the result from the plasticization of the ionic liquids induced by the vapor sorption. In addition, they claimed that the mass transport rates of analytes in ionic liquids were much faster than those observed for solid inorganic or organic coatings. Goubaidoulline et al [6] used a sensor where the ionic liquid was contained in the pores of a nanoporous alumina layer, formed on the front electrode of the quartz crystal by anodization. This concept is the basis of the supported ionic liquid phase (SILP) materials which have the advantage of increasing the rate of mass transfer through the extension of the surface area of the exposed ionic liquid. Shen et al [7] studied the adsorption process of

acetone vapor into a film of 1-octyl-3 methylimidazolium bromide ([C8MIM][Br]) deposited on Y-cut langasite crystal resonators. Recently, ionic liquid films deposited on quartz crystal sensors have been used in the detection of volatile organic compounds (VOCs) [8].

Most of the above referred studies focused mainly the uptake of vapors and the affinity of various ILs for specific analytes, but a deep understanding of the behavior of IL films when the analyte molecules interact with them is still missing. In particular, knowledge of the interaction of water vapor with IL films is of special importance for this work, because in the previous chapters the presence of water was proven to be he major driver for the removal of the opiates from the surface of hair. The aim of this study was to understand the mechanism of water vapor interaction with ionic liquids. Films of a series of ionic liquids deposited by spin-coating on the gold surface of quartz crystals were exposed to the flow of saturated water vapor and the resulting changes in their viscoelastic properties were assessed using a QCM-D. The structure of the ionic liquid films was investigated by imaging with an atomic force microscope (AFM). From the time-dependence of the QCM-D data, the kinetics of the water absorption process was determined.

Two series of ionic liquids were studied, one based on the acetate anion: 1-ethyl-3-methylimidazolium acetate, [C_2mim][OAc], 1-butyl-3-methylimidazolium acetate, [C_4mim][OAc], 1-hexyl-3-methylimidazolium acetate, [C_6mim][OAc]; and the other based on the tetrafluoroborate anion:1-ethanol-3-methylimidazolium tetrafluoroborate, [C_2OHmim][BF_4], 1-octyl-3-methylimidazolium tetrafluoroborate, [C_8mim][BF_4]. In the former case the effect of the length of the alkyl R substituent on the imidazolium cation [Rmim] was addressed in a family of ionic liquids based on an halogen-free anion, while in the latter two well characterized ionic liquids with quite different polarities were investigated. The structure, solubility in water, and cation hydrophobicity parameter (defined as log $k_{0,c}$ according to reference [9]) of the studied ionic liquids are presented in Table 5.1. As expected [10], the hydrophobicity of the cation increases in the series ethyl, butyl, hexyl, octyl, while [C_2OHmim] is the most hydrophilic. Although no values of the solubility in water for the [Rmin][OAc] could be found in literature, these ionic liquids are known to form strong hydrogen bonds with water [11] which should imply a very high solubility. This means that, among the ILs investigated, only [C_8mim][BF_4] has a limited solubility in water.

Table 5.1 - Structure, solubility in water, and cation hydrophobicity parameter (log $k_{0,c}$) of the studied ionic liquids.

IL	Structure	Water Solubility % w/w	Cation hydrophobicity parameter
[C_2mim][OAc]	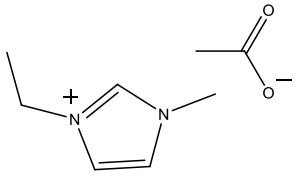	-	0.22[c]
[C_4mim][OAc]	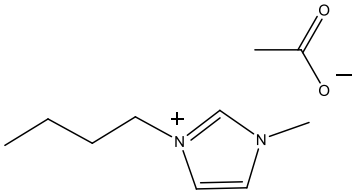	-	0.67[c]
[C_6mim][OAc]	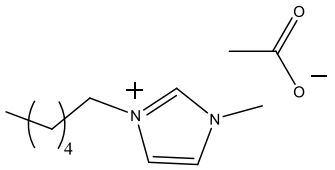	-	1.2[c]
[C_2OHmim][BF_4]	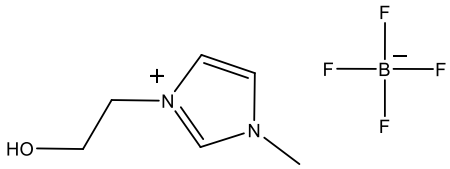	∞ [a]	-0.28[d]
[C_8mim][BF_4]	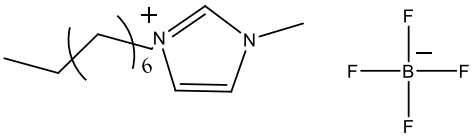	10.3[b]	1.9[c]

[a] taken from Ref [12]

[b] taken from Ref [13]

[c] taken from Ref [9]

[d] taken from Ref [14]

5.3. Results and discussion

5.3.1. Ionic liquid characterization

The densities of the ionic liquids vary linearly with the temperature according to the following equations: $\rho/g \cdot cm^{-3} = 1.5260 - 7.0\times10^{-4}T/K$ for [C_2mim][OAc], $\rho/g \cdot cm^{-3} = 1.2504 - 6.0\times10^{-4}T/K$ for [C_4mim][OAc], and $\rho/g \cdot cm^{-3} = 1.3621 - 7.0\times10^{-4}T/K$ for [C_6mim][OAc], with uncertainties of ± 0.00016 g·cm^{-3}, ± 0.00018 g·cm^{-3} and ± 0.00027 g·cm^{-3}, respectively. The densities of [C_8mim][BF_4] and [C_2OHmim][BF_4] respectively equal to: $\rho/g \cdot cm^{-3} = 1.3244 - 6.0\times10^{-4}T/K$ and $\rho/g \cdot cm^{-3} = 1.1171 - 7.0\times10^{-4}T/K$ were taken from a previous work [15].

The surface tensions and the viscosities at ambient temperature (298 K) of the ILs are shown in table 5.2: for those based on the anion acetate the values were taken from references [11,16], while the other two liquids were previously measured in our laboratory [15]. The contact angles on PTFE averaged over, at least four measurements, are also presented in the same table.

The polarity of the ILs was estimated from the surface tensions and the contact angles using the approach of Fowkes [17]. According to this approach, the surface tension, γ_i, of a solid or a liquid can be described as a sum of independent contributions each arising from the intermolecular interactions present in such phases. For practical reasons it is common to include all the non-dispersive interactions in a single term so that:

$$\gamma_i = \gamma_i^d + \gamma_i^{nd} \quad (1)$$

where subscript $i = S$ or L indicates, respectively the solid or the liquid, while superscripts *d* and *nd* stand for the dispersive and the non-dispersive terms of the surface tension. Assuming that the dispersive forces between pairs of unlike

molecules may be described by the geometric mean rule, the following relation was deduced [18]:

$$\gamma_L(1+\cos\theta) = 2\left(\gamma_S^d \cdot \gamma_L^d\right)^{1/2} \quad (2)$$

The dispersive component of the surface tension of a liquid may then be calculated from its contact angle, θ, on a purely dispersive solid, once γ_L and $\gamma_S^d = \gamma_S$ are known. The non-dispersive component is obtained using eq. (1). This assumption is valid when both phases are non-polar and may be a good estimate when only one of them is polar. The polarity fraction is then defined as the ratio between the non-dispersive component, γ_L^{nd}, (often called "polar" component) and the total surface tension. Assuming that PTFE is a purely dispersive solid with surface tension of 17.5 mJ.m^{-2} [19], the polarity fractions were calculated and are given in table 5.2.

Table 5.2 - Surface tension, contact angle on PTFE, polarity fraction (γ_L^{nd}/γ_L), and viscosity of the ionic liquids, at 298 K. The water contents of the ILs are given in parentheses.

IL	Surface tension (mJ.m^{-2})	Contact angle (°)	Polarity fraction	Viscosity (Pa.s)
[C_2mim][OAc]	41.0[a] (127 ppm)	77.5	0.39	0.162[d] (120 ppm)
[C_4mim][OAc]	39.4[a] (147 ppm)	70.2	0.30	0.485[d] (85 ppm)
[C_6mim][OAc]	36.1[a] (128 ppm)	61.9	0.22	1.710 (400 ppm)
[C_2OHmim][BF_4]	64.9[b] (800 ppm)	100.6[c]	0.38[c]	0.97[b] (800 ppm)
[C_8mim][BF_4]	32.9[b] (344 ppm)	80.4[c]	0.32[c]	0.32[b] (344 ppm)

[a] taken from Ref [11]

[b] taken from Ref [15]

[c] taken from Ref [20]

[d] taken from Ref [16]

All ionic liquids may be classified as moderately polar, with the exception of $[C_6mim][OAc]$ whose polarity is lower than the typical values of imidazolium-based ionic liquids [20]. Within the acetate-based family, polarity decreases with increasing cation hydrophobicity parameter (see table 5.1) which correlates directly with the length of the alkyl R substituent in the cation. Viscosity is strongly dependent on the anion. For the acetate-based series, viscosity increases with the alkyl chain length, but a long chain length of the cation C_8mim associated to the BF_4 anion dictates a relatively low viscosity.

5.3.2.AFM imaging

Figures 5.1a-d show AFM images of the IL films obtained after 24 h of film deposition. Images of the film obtained with $[C_2OHmim][BF_4]$ could not be acquired because in contact conditions its adhesion to the substrate was so low that the tip became readily contaminated and dragging of the liquid occurred, and in non-contact conditions the sticky behavior of the film introduces unacceptable noise in the AFM images. The surface of bare silanised gold (Fig. 5.1e) has the typical granular topography where the roundish features have average height in the order of 4 to 5 nm and an x-periodicity of the order of 50 nm. In the images of the IL films, this topography is no longer seen in between the droplets, as shown in the smaller length topographic profiles of figs 5.1.a-d. This result indicates that the thickness of the deposited films is enough to hide the underlying structure. All films exhibit the drop-on-the-layer behavior characteristic of IL films deposited from concentrated solutions (IL concentration ≥ 0.5 mg/mL) on hydrophilic substrates. Similar images were reported in a recent work involving films of $[C_8mim][BF4]$ deposited on a solid aluminum where liquid-like lamellar structures were observed [21].

However, it is possible to identify clear differences among the films obtained with the various ILs. The $[C_8mim][BF_4]$ film (Fig. 5.1d) stands out due to the very high

number of liquid drops of small and uniform dimensions. In contrast, the films obtained with the acetate-based ILs exhibit a smaller number of drops and a large distribution of drop sizes. The drops of larger height (120 nm) are found in the [C_2mim][OAc] (Fig. 5.1a). It is interesting to notice that within the series of the acetate-based IL films, those of [C_6mim][OAc] presented the lowest adhesion to the substrate which resulted in some dewetting that can be detected in the inferior left corner of the image (Fig. 5.1c). This behavior in presence of a highly hydrophilic substrate may be attributed to the low polarity fraction of this liquid (see table 5.2). In the case of [C_2OHmim][BF_4], the very small affinity to the hydrophilic substrate (average contact angle of 53º) is not consistent with its high polarity fraction, but should rather be ascribed to strong hydrogen forces between anion and cation that hinder their preferential interaction with the solid substrate.

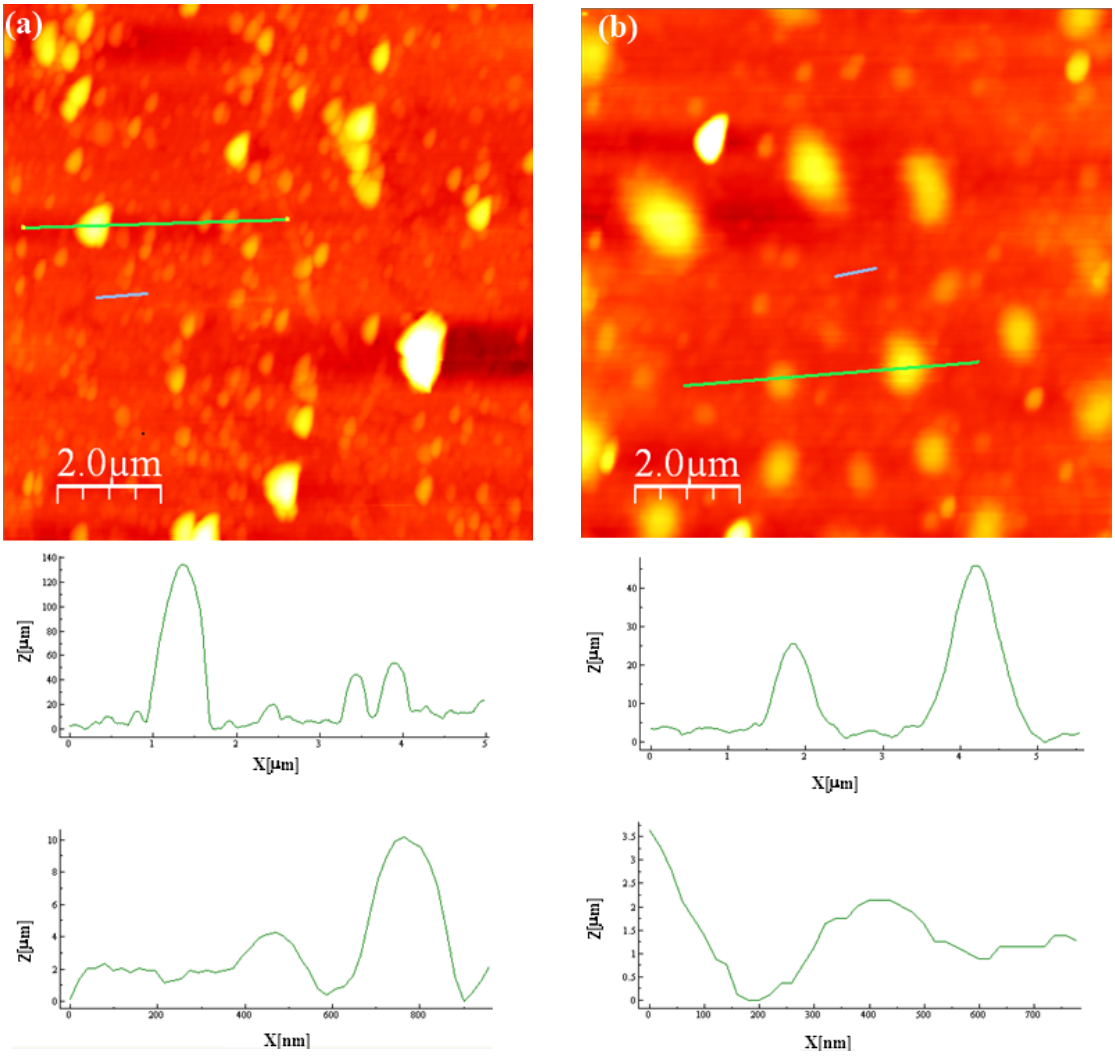
(a)
2.0μm
(b)
2.0μm
Z[μm]
X[μm]
Z[μm]
X[μm]
Z[μm]
X[nm]
Z[μm]
X[nm]

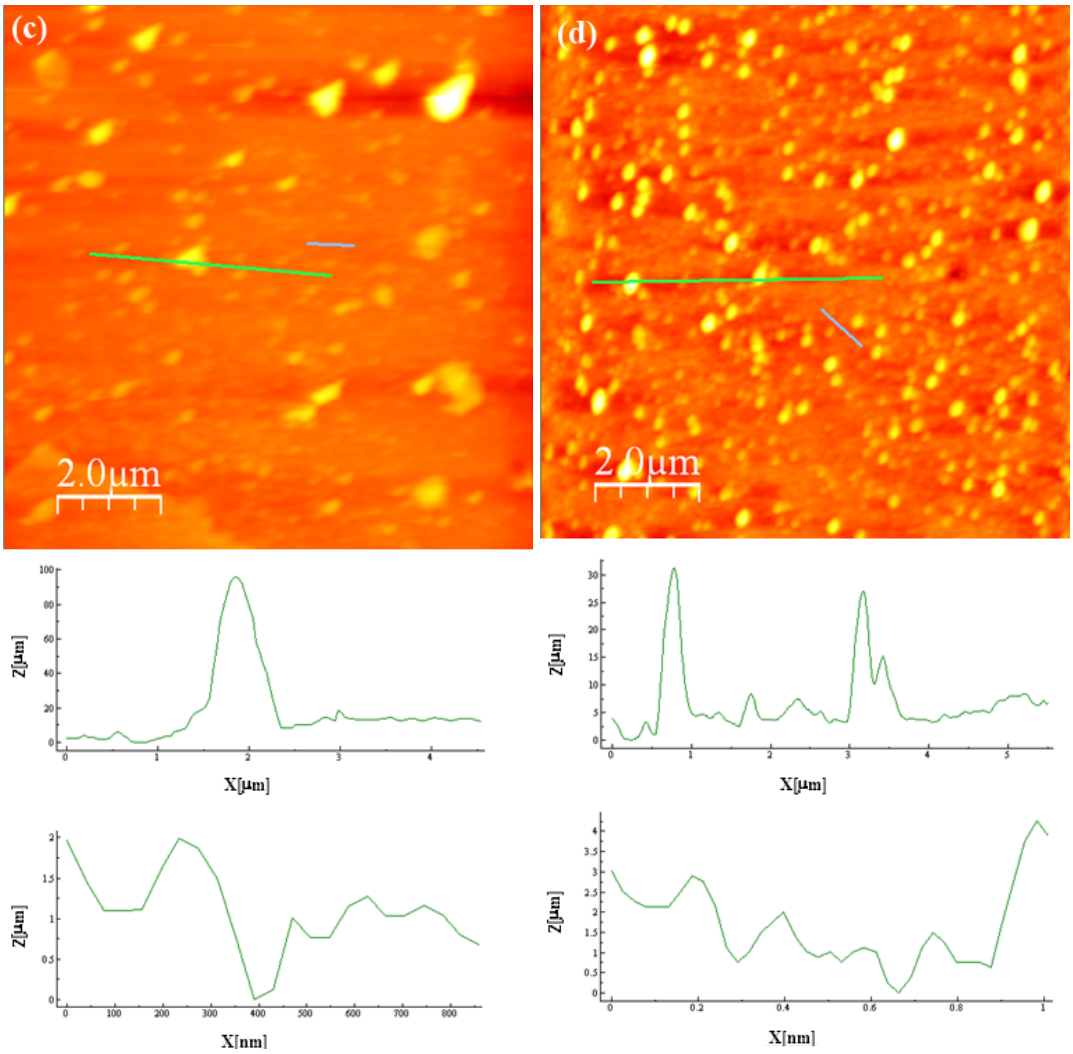
(c)
2.0µm
(d)
2.0µm
Z[µm]
X[µm]
Z[µm]
X[µm]
Z[µm]
X[nm]
Z[µm]
X[nm]

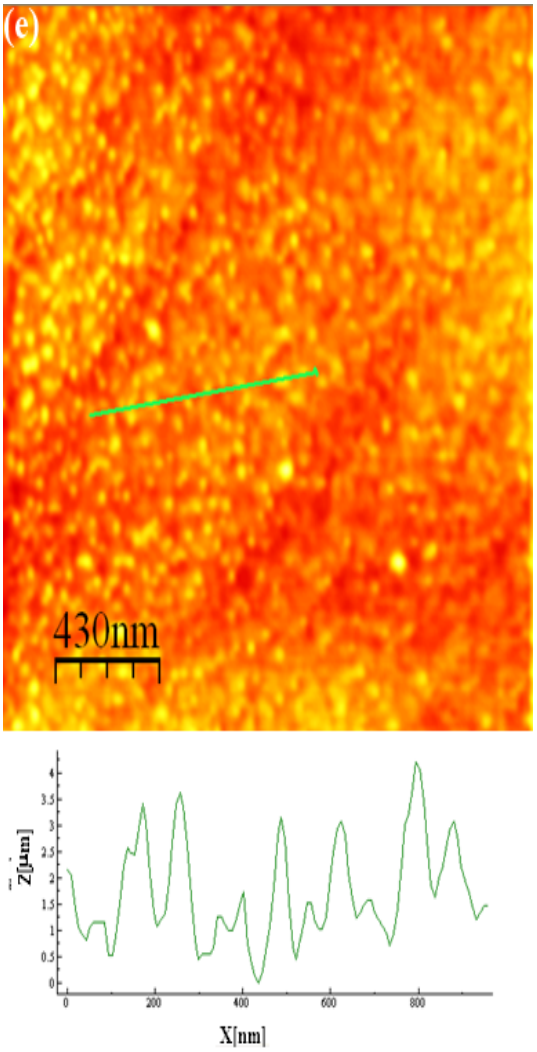

Figure 5.1 - AFM topographic images of films obtained with: [C_2mim][OAc] (a), [C_4mim][OAc] (b), [C_6mim][OAc] (c), and [C_8mim][BF_4] (d) on a silanised gold surface recorded at 24 h after film deposition. The image of the bare silanised gold surface (e) is included for comparison purposes. Height profiles are shown below each image.

5.3.3.QCM-D experiments

Figure 5.2 represents typical results of QCM-D experiments obtained with films of the five ILs tested. Taking the first addition of dry nitrogen as the baseline, the subsequent changes correspond to the interaction of the IL film deposited on the surface of the crystal with the nitrogen saturated with water vapor, followed by rinsing with the dry nitrogen.

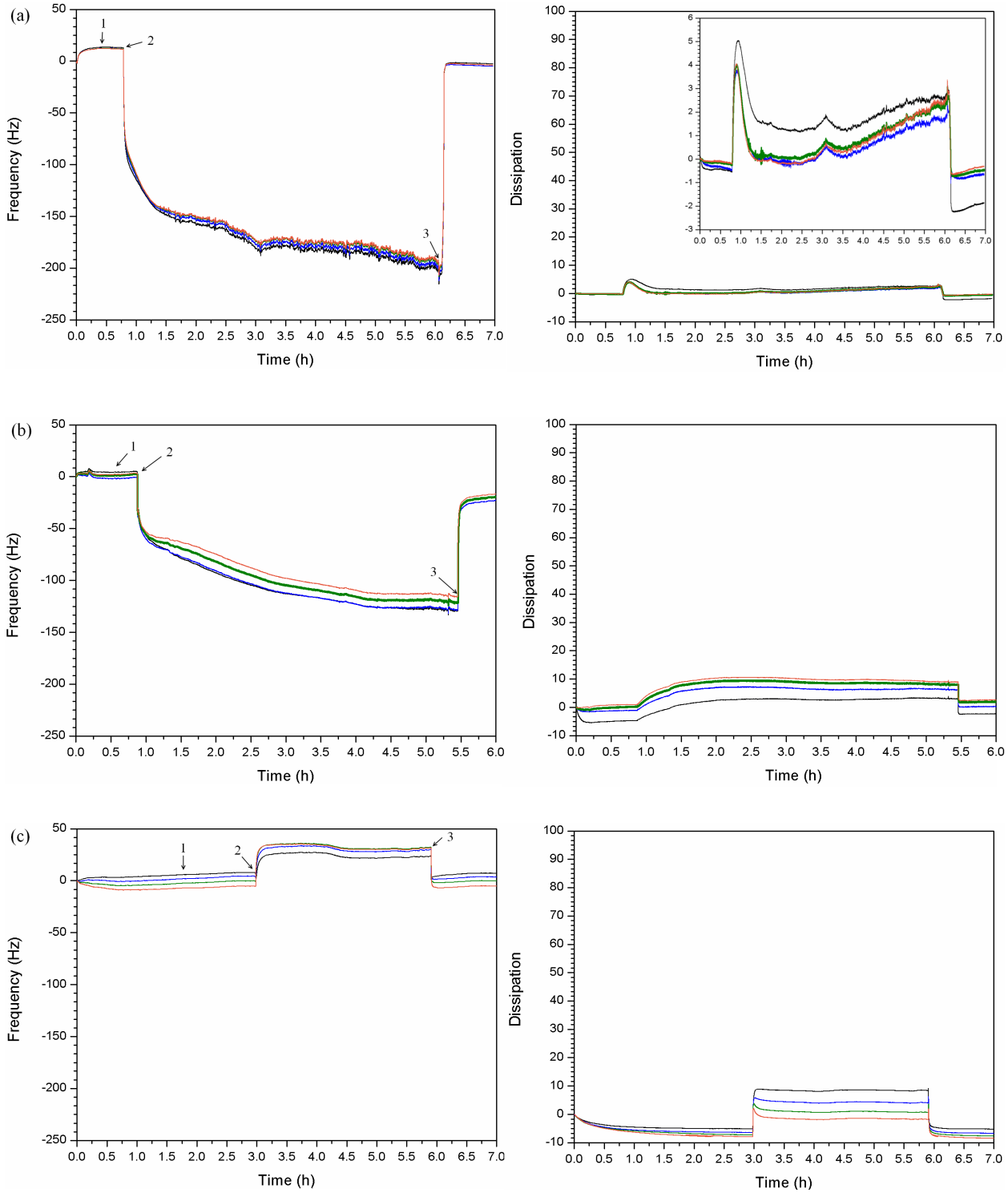
(a)
Frequency (Hz)
Time (h)
Dissipation
Time (h)
(b)
Frequency (Hz)
Time (h)
Dissipation
Time (h)
(c)
Frequency (Hz)
Time (h)
Dissipation
Time (h)

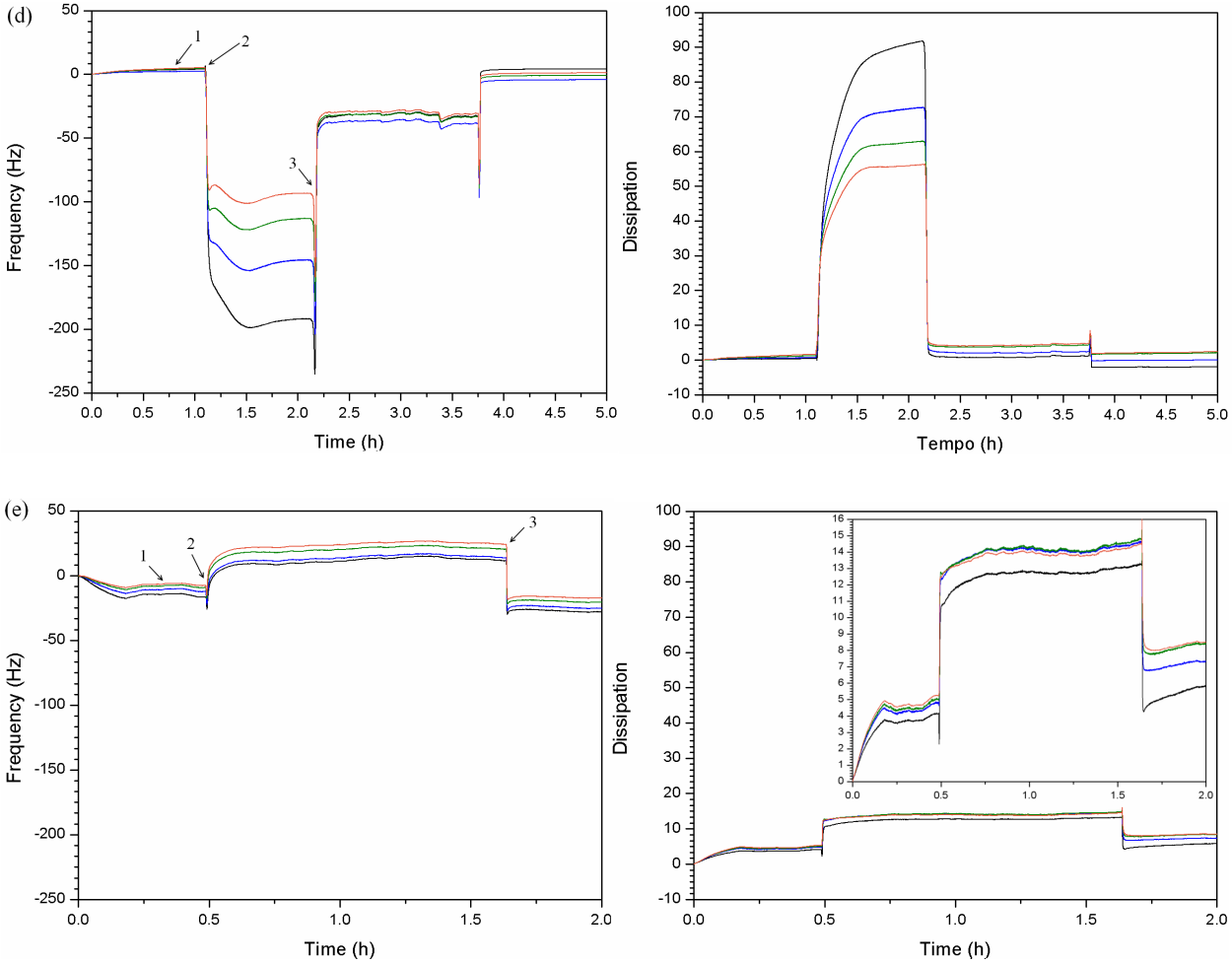

Figure 5.2 - Variation of the normalized frequency $\Delta f/n$ (left) and dissipation ΔD (right) for all harmonics of the fundamental frequency (n=3 black, n=5 blue, n=7 green, n= 9 orange) in a typical experiment consisting in: 1) contact of the IL film with dry nitrogen, 2) addition of water vapor, 3) rinsing with dry nitrogen. The ILs are: [C_2mim][OAc] (a), [C_4mim][OAc] (b), [C_6mim][OAc] (c), [C_8mim][BF_4] (d), and [C_2OHmim][BF_4] (e). Inserts with expanded views are added whenever the curves are indistinguishable.

Interpretation of QCM-D data when the resonance frequency decreases due to an increase in mass (adsorption) may be based on the Sauerbrey equation [22], if the adsorbed film is rigid, or on the modified Sauerbrey equation if the film is viscoelastic [23]. When the change in resonance frequency is associated to the variation of the medium viscosity/ density, then the equation of Kanazawa and Gordon [24] should be applied. However, in several applications the QCM-D sensor is simultaneously loaded by a rigid surface mass layer and a contacting Newtonian liquid. Martin el al. [25] solved a continuum electromechanical model to calculate the change in resonant

frequency obtained in these circumstances. When mass and liquid loading are small, the normalized change in frequency, Δf, is given by:

$$\Delta f = -\frac{2f_0^2}{(\mu_Q \rho_Q)^{1/2}}\left[\rho_f h_f + \left(\frac{\rho_L \eta_L}{4\pi f_0}\right)^{1/2}\right] \quad (3)$$

where f_0 is the frequency of the fundamental frequency of the crystal; μ_Q and ρ_Q are, respectively, the elastic modulus and the density of the quartz; ρ_f and h_f are, respectively, the density and the thickness of the surface layer; ρ_L and η_L are, respectively, the density and the viscosity of the liquid. When the mass loading is dominant, eq. 3 reduces to the first term, which is equivalent to the Sauerbrey equation; in contrast, when the mass loading is negligible in comparison with the liquid loading, eq. 3 reduces to the second term which is equivalent to the Kanazawa and Gordon equation.

For the most viscous ionic liquids, [C_6mim][OAc] and [C_2OHmim][BF_4] (Figures 5.2c and e), the interaction with water vapor led to an increase in both frequency and dissipation which may be attributed to a reduction of the damping effect associated with the decrease in the IL viscosity, η_L. In contrast, the less viscous liquids, [C_2mim][OAc] and [C_4mim][OAc] (Figures 5.2a and b), suffered a decrease in frequency (respectively, $\Delta f \sim -200$ Hz and $\Delta f \ -130$ Hz for the third harmonic) and an increase in dissipation which are consistent with the increase in mass, $\rho_f \ h_f$, due to water adsorption. The behavior of [C_8mim][BF_4] (Fig. 5.2d) is different from that observed with the pairs of ILs just referred. The frequency decreased continuously with time achieving a constant value and, after approximately one hour, increased spontaneously leading to a final constant value of $\Delta f \sim -50$Hz. Furthermore, the decrease in frequency is accompanied by a huge increase in dissipation, which is characteristic of a fluidic material and then, spontaneously decreases to very low values as the frequency increases. This strange behavior could be attributed to a two-step process where the first stage is dominated by the increase in mass followed by a decrease in viscosity. Comparison of the equilibrium frequency shifts obtained with these three ILs, shows an increase in the water uptake according to the decreasing value of hydrophobicity parameter of the cations (see table 5.1).

A deeper analysis of the QCM-D results, taking into consideration the variation of the different harmonics of the fundamental frequency, may help in the interpretation of

the results. It is known that the higher order harmonics are more sensitive to the modifications at the solid interface while those of lower order "feel" the liquid interface of the supported IL. The QCM-D results show that for [C_2mim][OAc] and [C_4mim][OAc], all harmonics have similar negative frequency shifts, and similar increases in dissipation which is consistent with the presence of a relatively rigid IL film. In contrast, for [C_8mim][BF_4] the lower order harmonic are the most affected in a first step, followed by a second step where the frequency increases, dissipation decreases, and all harmonics practically coincide. This may indicate a gradual water adsorption and diffusion through the films of [C_2mim][OAc] and [C_4mim][OAc], while in the latter, a discontinuity occurs between the formation of a water film on top of the IL which then diffuses into the bulk leading to a decrease in the film viscosity.
Further analysis of Fig. 5.2 shows that, after rinsing with the dry nitrogen, the frequency and dissipation of all ionic liquid films rapidly recover the initial values, both in the case of positive and negative frequency shifts. This means that the internal rearrangement in the IL film structure associated to the process of dissolution and removal of the water molecules is practically reversible.

5.3.4.Data correlation

In a recent publication [26] describing water absorption by anhydrous ionic liquids, the interpretation of the interaction of water vapor with IL films was done in terms of three phenomena: 1) the adsorption of water molecules on the IL surface; 2) their diffusion into the IL; 3) the formation of water-ion complexes when the IL samples have a non-negligible thickness. According to the same authors, each phenomenon depended on different IL features. Water adsorption depends on the affinity of water for the groups exposed on the IL free surface, while diffusion is largely affected by the liquid viscosity, which strongly depends on water concentration. Other authors considered the water uptake of ILs in contact the atmospheric humidity as the result of adsorption and the formation of a water film on the IL surface [27].
In general, both hydrophilic and hydrophobic ILs absorb water at a high speed but hydrophilic ILs absorb a higher amount. It is known that anions usually determine water absorption, while water solubility depends mainly on the cation, decreasing when the length of the alkyl chain on the cation increases [28]. The interactions

responsible for the solubility of water vapor in an ionic liquid are determined not only by hydrophobicity but other factors, such as stereochemistry and polarity, play a role.
The presence of [OAc] and [BF_4], water binding anions, on the IL surface favors the water adsorption and, at the same time, should reduce the rate of water diffusion inside the IL. Furthermore, it was recently demonstrated that water diffusivity inside [C_2mim][OAc] depends on the water concentration [25]. The water self-diffusivity increases at high water concentrations, probably due to the decrease in the interactions between water and the IL.
Comparison of the behavior of the less viscous ionic liquid films, [C_2mim][OAc], [C_4mim][OAc], and [C_8 mim][BF_4], suggests that water interacts with the surfaces of these films in different ways, in spite of the known water affinity to both anions. In a recent investigation on wetting films of ILs [29] some of the authors concluded that the main forces which are responsible for the stability of thin films of [C_8mim][BF_4] are dispersive interactions between the long alkyl chains of the cations segregated at the surface. In this case, the water molecules have weak affinity to the hydrophobic interface and form a liquid deposit whose viscoelastic properties are revealed by the discrepancy among the various harmonics. Only after a certain period of time, during which the ions at the surface may undergo reorientation, water molecules are able to penetrate and diffuse into the IL film. However, the amount of water absorbed is low ($\Delta f \sim -50$ Hz) due to the limited water solubility of this IL. In contrast, it is expected that, for the acetate-based ILs, hydrogen bonds between water and acetate anions are responsible for a fast adsorption and absorption process that leads to an increase in mass.
In order to further understand the mechanism of water diffusion the Fickian model, which is the easiest one for water absorption in a thin film, was applied. At short times, the relative mass increase can be written as:

$$\frac{M_t}{M_\infty} = \frac{2}{h}\sqrt{\frac{D\,t}{\pi}} \qquad (4)$$

where M_t and M_∞ are, respectively, the mass gains at time t and at equilibrium, h is the film thickness and D is the water diffusivity [4]. In the case of [C_2mim][OAc] and [C_4mim][OAc] the films present a non-viscoelastic behavior because the dissipation is low and the frequency shifts correspondent to the various harmonics almost coincide.

The mass of water absorbed on the IL film can thus be determined from the change in the resonance frequency using the Sauerbrey equation. Considering that the ratio of masses, M_t/M_∞, is equal to the ratio of frequency shifts, $\Delta f_t/\Delta f_\infty$, where Δf_t and Δf_∞ are, respectively, the frequency changes at time *t* and at equilibrium, it is possible to fit the linear part of the experimental data to eq. 4, assuming a reasonable value for the film thickness. Unfortunately we were not able to get a meaningful value for the film thickness from elipsometric measurements because an adequate model for this complex system could not be found. However, we may assume a value in the range of (150-200) nm taking into consideration that the height of the highest drops on top of the underlying layer was 120 nm (AFM images in Fig. 5.1). The experimental values of $\Delta f_t/\Delta f_\infty$ are plotted as a function of $\sqrt{t}$ in Figure 5.3.

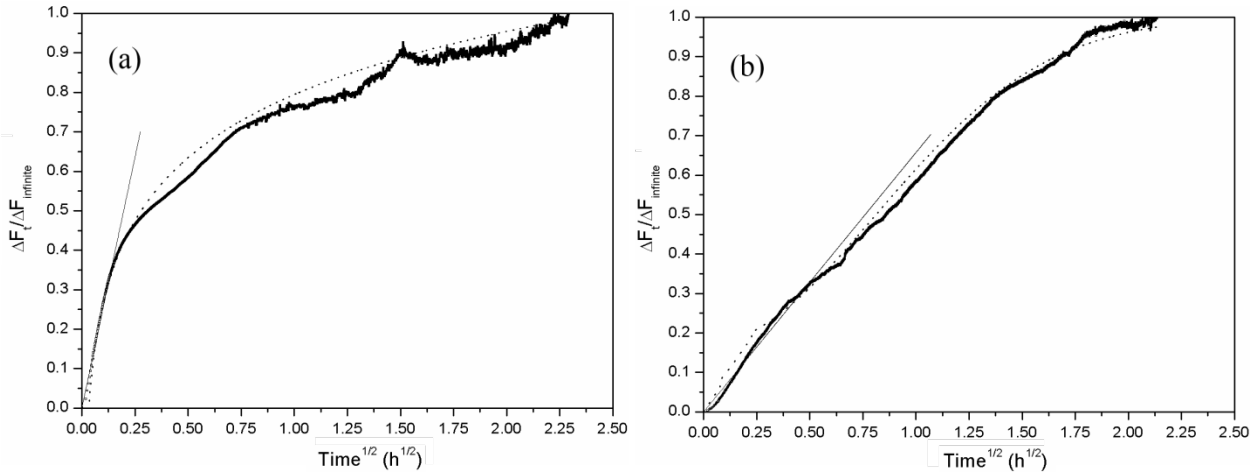

Figure 5.3 - Relative mass increase of the [C_2mim][OAc] (a) and [C_4mim][OAc] (b) films due to water absorption (thick lines resulting from the superposition of a great number of experimental points). Data were fitted to the Fickian model (thin line) and to variable-surface concentration two-step model (dashed line).

The mass of the film increases rapidly in the first minutes, followed by a slower pace that continues until equilibrium. The initial slope has a Fickian behavior, which allows the calculation of the film thicknesses and of the diffusion coefficients of water in [C_2mim][OAc] and in [C_4mim][OAc]. The values of these parameters (respectively, *h* and *D*) resulting from the linear fittings are shown in table 5.3. The second stage exhibits a non-Fickian behavior, which is not diffusion controlled. Several theoretical models have been proposed to describe two step absorption processes [30]. The variable-surface concentration model proposed by the Long and Richman has been

successfully applied to fit experimental data. According to this model [30], the absorption process results from two independent contributions: a diffusion controlled part (governed by Fick's law) and a relaxation controlled part. Assuming only a first-order relaxation process, the fractional mass uptake at time *t* can be described as the linear superposition of both contributions (eq 5):

$$\frac{M_t}{M_\infty} = \phi\left[1 - \frac{8}{\pi^2}\sum_{n=0}^{\infty}\frac{e^{\left(\frac{-(2n+1)^2\pi^2\theta}{4}\right)}}{(2n+1)^2}\right] + (1-\phi)\left[1 - \frac{tan\sqrt{\psi}e^{-\psi\theta}}{\sqrt{\psi}} - \frac{8}{\pi^2}\sum_{n=0}^{\infty}\frac{e^{\left(\frac{-(2n+1)^2\pi^2\theta}{4}\right)}}{(2n+1)^2\left(1-\frac{(2n+1)^2\pi^2}{4\psi}\right)}\right] \quad (5)$$

where $\phi = \frac{C_0}{C_\infty}$, $\theta = \frac{Dt}{h^2}$, $\psi = \frac{kh^2}{D}$ and k is the rate constant of the relaxation process. The dimensionless number ϕ represents the ratio of the water concentration at the film surface immediately after contacting the vapor, C_0, to the final concentration, C_∞, and the dimensionless number ψ is the ratio between the characteristic diffusion time and the characteristic relaxation time.

It is important to remark that this model has the advantage of having only four parameters to fit, where two of them (*h* and *D)* can be obtained from the initial slope using eq. 4. Starting with the values of *h* and *D* previously determined, the data were fitted to eq. 5 and the resulting curves are shown in Figure 5.3 while parameters ϕ and ψ are given in table 5.3. Small values of ψ mean that the relaxation time is larger than the diffusion time which is the case in the [C_2mim][OAc] films but not in the [C_4mim][OAc] films. In both cases the values of ϕ are very small meaning that the amount of relaxation controlled absorption is very large.

Table 5.3 - Fitting parameters: film thickness, *h*, and water diffusion coefficient, *D*, were obtained with eq. 4; dimensionless numbers ϕ and ψ were determined using eq. 5. The quadratic correlation coefficients, R^2, characterize the fittings to both equations.

IL	*h* (nm)	*D* ($m^2 \cdot s^{-1}$)	R^2(eq.4)	ϕ	ψ	R^2(eq.5)
[C_2mim][OAc]	180	4.70×10^{-17}	0.9897	7.5×10^{-4}	0.09	0.9930
[C_4mim][OAc]	180	3.05×10^{-18}	0.9767	2.8×10^{-4}	2.39	0.9915

Although we could not find in the literature any values for the diffusion coefficient of water in ionic liquid films, we may compare our results with the bulk diffusion coefficients of water in [C_2mim][OAc] recently reported by Shi et al.[28]. These values varied between $5\times10^{-11}m^2s^{-1}$and $1\times10^{-10}m^2s^{-1}$ depending on the water mole fraction. The difference in the order of magnitude between this set of values and those presented in table 5.3 may be explained by the effect of liquid confinement. Although this issue is controversial, several authors [4,31] claimed that water mobility in films decreases in relation to their bulk values. Namely, Vogt et al. [4] found a decrease in the diffusion coefficient of water in polyelectrolyte films from $3\times10^{-17}m^2s^{-1}$ to $5\times10^{-21}m^2s^{-1}$ when the film thickness decreased from 200 to 2 nm The lower value of the diffusion coefficient for [C_4mim][OAc] in comparison with that of [C_2mim][OAc] may be attributed to the longer length of the alkyl substituent of the former cation which is responsible for its higher hydrophobicity.

Finally, we should remark that the most viscous ionic liquids, [C_6mim][OAc] and [C_2OHmim][BF_4], formed films with low adhesion to the substrate surface. While good quality AFM images of the latter could not be obtained for this reason, the films of the former revealed non-coated areas on the gold surface. These heterogeneous films may experience a large damping effect, which is characteristic of a viscoelastic medium.

5.4. Conclusions

Films of several imidazolium-based ILs were deposited on quartz in order to study the water vapor interaction with the IL. Two distinct behaviors were observed upon interaction with water vapor: for the films of the most viscous ILs, such as [C_2OHmim][BF_4] and [C_6mim][OAc], the decrease in viscosity was the dominant

effect, while for the others, C_8mim][BF_4], [C_2mim][OAc] and [C_4mim][OAc], the mass loading effect predominates.

Analysis of the changes of the different harmonics of the fundamental frequency obtained with the less viscous liquids seems to indicate a gradual water adsorption and diffusion through the films of [C_2mim][OAc] and [C_4mim][OAc], while for [C_8mim][BF_4] a discontinuity occurs between the formation of a water film on top of the IL which then diffuses into the bulk leading to a decrease in the film viscosity.

Application of the Fickian model to water absorption at short times allowed the calculation of water diffusion coefficients in the films of [C_2mim][OAc] and [C_4mim][OAc]. These values are much smaller than the bulk values which may be attributed to the effect of liquid confinement. Further analysis of the kinetics of water absorption was done using the Long and Richman variable-surface concentration model which considers two stages: diffusion controlled (governed by Fick's law) and relaxation controlled. According to this model, the relaxation time is larger than the diffusion time in the case of [C_2mim][OAc] and smaller, for [C_4mim][OAc].

5.5. Experimental

5.5.1. Materials

The ionic liquids 1-alkyl-3-methylimidazolium acetate, [$C_n$mim][OAc], with n = 2, 4 and 6, 1-ethanol-3-methylimidazolium tetrafluoroborate, [C_2OHmim][BF_4], and 1-octyl-3-methylimidazolium tetrafluoroborate, [C_8mim][BF_4], were purchased from Solchemar (Portugal) with purity >98%. The purity of the ionic liquids was checked by NMR after the synthesis. The water content, checked by Karl-Fisher, was ≈ 600 ppm for [C_2mim][OAc], 300 ppm for [C_4mim][OAc], 400 ppm for [C_6mim][OAc], 344 ppm for [C_8mim][BF_4], and 800 ppm for [C_2OHmim][BF_4]. The chlorine content, determined with a selective Cl-electrode, was < 50 ppm. Toluene and acetone were from Panreac, ethanol from AGA and (3-aminopropyl) triethoxysilane, from Fluka. Milli-Q water was used in all experiments.

The AT-cut 5 MHz piezoelectric quartz crystals (14 mm in diameter) coated with gold were supplied by Q-Sense (Gothenburg, Sweden). For the contact angle measurements substrates of poly-(tetrafluoroethylene) (PTFE) sheet with 1 mm thickness (Goodfellow) were used.

5.5.2. Methods

The contact angle measurements were carried out by the sessile drop method using the ADSA-P software (Axisymetric Drop Shape Analysis, Applied Surface Thermodynamics Research Associates, Toronto, Canada) for image analysis. During the experiments, the chamber was flushed with pure, dry nitrogen. Further experimental details may be found in ref. [15]. The contact angles were measured at room temperature. The contact angle evolution over time was recorded, for time intervals ranging from 10 to 60 min, depending on the liquid spreading kinetics. When a plateau is achieved, the so-called static contact angle is recorded. The density values, which are necessary for the experimental determination of the surface tension, were measured with an Anton-Paar DMA 5000 vibrating-tube densimeter in the temperature range of (298-363) K. All reported density data were corrected for the effect of viscosity using the internal calibration of the densimeter. To prevent the effect of air bubbles, each measurement was repeated twice. The viscosity was measured with an automated SVM 3000 Anton Paar rotational Stabinger viscometer-densimeter. The temperature uncertainty is ±0.02 K, while the precision of the dynamic viscosity measurements is ± 0.5 %. The overall uncertainty of the measurements was reported to be 2% [32].

A Q-Sense quartz crystal microbalance with dissipation (model E4) was used to assess the adsorption/absorption of the water vapor on the IL films. The experiments were done at 25ºC and the results are averages of, at least, four independent measurements. Prior to the measurements, all the QCM-D balance parts were sonicated 5 min in a 10% alkaline cleaning solution of Extran and then twice in Milli-Q water, followed by blow dry with nitrogen. The quartz crystals were carefully cleaned according to the same protocol and finally dried during 2 h inside a vacuum oven at room temperature. After drying, the crystals were submitted to two successive

10 min UV/ozone treatments, separated by rinsing with Milli-Q water. To achieve complete spreading of the ionic liquids, polar surfaces were prepared with a silane containing amino groups, according to the procedure described by Batchelor et al. [33] The crystals were then submersed in 10 mL of 5% (w/w) toluene solution of (3-aminopropyl) triethoxysilane and stored at room temperature overnight. After completion of the reactions, the crystals were isolated and rinsed sequentially with toluene, acetone and water, blown with nitrogen, and dried during 2 h inside a vacuum oven. The only sample which did not wet the silanised gold surface was $[C_2OHmim][BF_4]$. The amine-terminated surface was further used to prepare a surface with trimethylammonium groups but complete spreading was not achieved. In this case, the best solution was to use the UV/ozone treated gold substrate where the contact angle of $[C_2OHmim][BF_4]$ was 53º, still much higher than the contact angles of the other ILs on silanised gold (e. g. 19º for $[C_8mim][BF_4]$).

The wetting films of ILs were deposited by spin-coating, at 2000 rpm during 40 s, from ethanol (99.5 % purity grade) solutions with concentration of 2.5 mg/mL on freshly prepared silanised quartz crystals. After deposition, the samples were kept under vacuum until being imaged. The IL films were studied at 24 h after film production due to the known time dependence of the film structure [21].

Figure 5.4 shows a scheme of the experimental arrangement for water vapor adsorption on the IL film. A saturated water vapor stream was obtained by passing dry nitrogen through a liquid water reservoir. The inlet QCM tubes are connected via a three-way valve to allow admission of dry nitrogen or water-saturated nitrogen. A typical QCM-D experiment consists in the following steps: (1) injection of a constant dry nitrogen flow (850 / mm^3s^{-1} measured with a flow meter Omega FL5511g) into the measuring cells; (2) replacement of dry nitrogen by the same flow of nitrogen saturated with water vapor, (3) final rinsing with dry nitrogen. Each step is performed until stabilization of the frequency shift is achieved. The normalized frequency shift, Δf, (change in frequency divided by the harmonic number) and the dissipation, ΔD, are recorded for the *n* harmonics of the fundamental frequency (*n* = 3, 5, 7, 9, and 11) against time.

A Veeco DI CPII atomic force microscope (AFM) was used for the visualization of the ionic films. The AFM was operated in contact mode using Si tips with a spring constant of 0.9 N/m at a constant contact force of 100 nN. These conditions were the

only ones that enable to obtain AFM images with an acceptable level of noise in all of the observed samples. To guaranty that visualization in contact mode does not interfere with the film topography, successive scans at increasing lengths were made. Topographic images were recorded only if no changes in the successive scans were detected, either in topography or in lateral force mode.

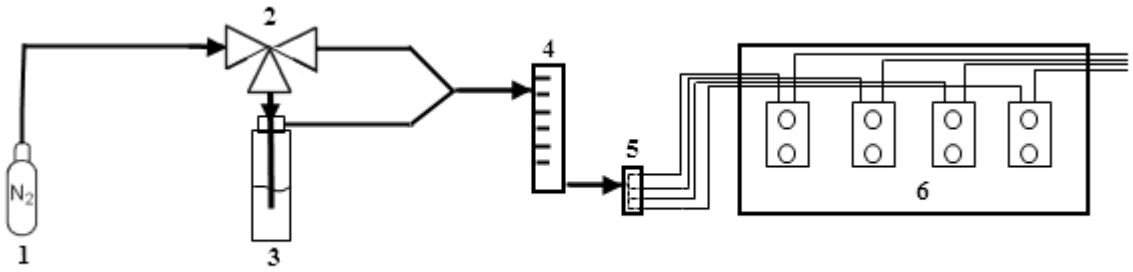

Figure 5.4 - Experimental setup for the QCM-D gas sensing experiments: 1 – Nitrogen cylinder; 2 – Three-way valve; 3 – Water container; 4 – Flow meter; 5 – Tubing distributor; 6 – Q-Sense stage.

5.6. References

[1] J. W. Grate. Acoustic Wave Microsensor Arrays for Vapor Sensing. *Chem. Rev.*, **2000**, *100*, 2627–2648.

[2] A. J. Ricco, R. M. Crooks, G. C. Osbourn. Surface Acoustic Wave Chemical Sensor Arrays: New Chemically Sensitive Interfaces Combined with Novel Cluster Analysis To Detect Volatile Organic Compounds and Mixtures. *Acc. Chem. Res.*, **1998**, *31*, 289–296.

[3] A. Mirmohseni, V. Hassanzadeh. Application of polymer-coated quartz crystal microbalance (QCM) as a sensor for BTEX compounds vapors. *J. Appl. Polym. Sci.*, **2001**, *79*, 1062–1066.

[4] B. D. Vogt, C. L. Soles, H.-J. Lee, E. K. Lin, W. Wu. Moisture Absorption and Absorption Kinetics in Polyelectrolyte Films: Influence of Film Thickness. *Langmuir*, **2004**, *20*, 1453–1458.

[5] C. Liang, C.-Y. Yuan, R. J. Warmack, C. E. Barnes, S. Dai. Ionic Liquids: A New Class of Sensing Materials for Detection of Organic Vapors Based on the Use of a Quartz Crystal Microbalance. *Anal. Chem.*, **2002**, *74*, 2172–2176.

[6] I. Goubaidoulline, G. Vidrich, D. Johannsmann. Organic vapor sensing with ionic liquids entrapped in alumina nanopores on quartz crystal resonators. *Anal. Chem.*, **2005**, *77*, 615–9.

[7] D. Shen, X. Li, Q. Kang, H. Zhang, Y. Qi. Monitor adsorption of acetone vapor to a room temperature ionic liquid 1-octyl-3-methylimidazolium bromide by a langasite crystal resonator. *Anal. Chim. Acta*, **2006**, *566*, 19–28.

[8] A. Rehman, A. Hamilton, A. Chung, G. A. Baker, Z. Wang, X. Zeng. Differential solute gas response in ionic-liquid-based QCM arrays: elucidating design factors responsible for discriminative explosive gas sensing. *Anal. Chem.*, **2011**, *83*, 7823–33.

[9] J. Ranke, A. Müller, U. Bottin-Weber, F. Stock, S. Stolte, J. Arning, R. Störmann, B. Jastorff. Lipophilicity parameters for ionic liquid cations and their correlation to in vitro cytotoxicity. *Ecotoxicol. Environ. Saf.*, **2007**, *67*, 430–8.

[10] J. G. Huddleston, A. E. Visser, W. M. Reichert, H. D. Willauer, G. A. Broker, R. D. Rogers. Characterization and comparison of hydrophilic and hydrophobic room temperature ionic liquids incorporating the imidazolium cation. *Green Chem.*, **2001**, *3*, 156–164.

[11] W. Guan, X.-X. Ma, L. Li, J. Tong, D.-W. Fang, J.-Z. Yang. Ionic parachor and its application in acetic acid ionic liquid homologue 1-alkyl-3-methylimidazolium acetate {[C(n)mim][OAc](n = 2,3,4,5,6)}. *J. Phys. Chem. B*, **2011**, *115*, 12915–20.

[12] L. C. Branco, J. N. Rosa, J. J. Moura Ramos, C. a M. Afonso. Preparation and characterization of new room temperature ionic liquids. *Chemistry*, **2002**, *8*, 3671–7.

[13] J. Vila, P. Ginés, J. M. Pico, C. Franjo, E. Jiménez, L. M. Varela, O. Cabeza. Temperature dependence of the electrical conductivity in EMIM-based ionic liquids. *Fluid Phase Equilib.*, **2006**, *242*, 141–146.

[14] S. Stolte, J. Arning, U. Bottin-Weber, A. Miller, W.-R. Pitner, U. Welz-Biermann, B. Jastorff, J. Ranke. Effects of different head groups and functionalised side chains on the cytotoxicity of ionic liquids. *Green Chem.*, **2007**, *9*, 760.

[15] J. Restolho, A. P. Serro, J. L. Mata, B. Saramago. Viscosity and Surface Tension of 1-Ethanol-3-methylimidazolium Tetrafluoroborate and 1-Methyl-3-octylimidazolium Tetrafluoroborate over a Wide Temperature Range. *J. Chem. Eng. Data*, **2009**, *54*, 950–955.

[16] S. Fendt, S. Padmanabhan, H. W. Blanch, J. M. Prausnitz. Viscosities of Acetate or Chloride-Based Ionic Liquids and Some of Their Mixtures with Water or Other Common Solvents. *J. Chem. Eng. Data*, **2011**, *56*, 31–34.

[17] F. M. Fowkes. Attractive forces at interfaces. *Ind. Eng. Chem.*, **1964**, *56*, 40–52.

[18] N. T. Correia, J. J. M. Ramos, B. J. V. Saramago, J. C. G. Calado. Estimation of the Surface Tension of a Solid: Application to a Liquid Crystalline Polymer. *J. Colloid Interface Sci.*, **1997**, *189*, 361–369.

[19] F. Liu, W. Shen. Forced wetting and dewetting of liquids on solid surfaces and their roles in offset printing. *Colloids Surfaces A Physicochem. Eng. Asp.*, **2008**, *316*, 62–69.

[20] J. Restolho, J. L. Mata, B. Saramago. On the interfacial behavior of ionic liquids: surface tensions and contact angles. *J. Colloid Interface Sci.*, **2009**, *340*, 82–86.

[21] R. Köhler, J. Restolho, R. Krastev, K. Shimizu, J. N. Canongia Lopes, B. Saramago. Liquid- or solid-like behavior of [omim][BF4] at a solid interface? *J. Phys. Chem. Lett.*, **2011**, *2*, 1551–1555.

[22] G. Sauerbrey. Verwendung von Schwingquarzen zur Wägung dünner Schichten und zur Mikrowägung. *Zeitschrift für Phys.*, **1959**, *155*, 206–222.

[23] J. Lukkari, M. Salomäki, T. Ääritalo, K. Loikas, T. Laiho, J. Kankare. Preparation of Multilayers Containing Conjugated Thiophene-Based Polyelectrolytes. Layer-by-Layer Assembly and Viscoelastic Properties. *Langmuir*, **2002**, *18*, 8496–8502.

[24] K. Keiji Kanazawa, J. G. Gordon. The oscillation frequency of a quartz resonator in contact with liquid. *Anal. Chim. Acta*, **1985**, *175*, 99–105.

[25] S. J. Martin, V. E. Granstaff, G. C. Frye. Characterization of a quartz crystal microbalance with simultaneous mass and liquid loading. *Anal. Chem.*, **1991**, *63*, 2272–2281.

[26] F. Di Francesco, N. Calisi, M. Creatini, B. Melai, P. Salvo, C. Chiappe. Water sorption by anhydrous ionic liquids. *Green Chem.*, **2011**, *13*, 1712.

[27] S. Cuadrado-Prado, M. Domínguez-Pérez, E. Rilo, S. García-Garabal, L. Segade, C. Franjo, O. Cabeza. Experimental measurement of the hygroscopic grade on eight imidazolium based ionic liquids. *Fluid Phase Equilib.*, **2009**, *278*, 36–40.

[28] W. Shi, K. Damodaran, H. B. Nulwala, D. R. Luebke. Theoretical and experimental studies of water interaction in acetate based ionic liquids. *Phys. Chem. Chem. Phys.*, **2012**, *14*, 15897–908.

[29] J. Restolho, J. L. Mata, K. Shimizu, J. N. Canongia Lopes, B. Saramago. Wetting Films of Two Ionic Liquids: [C 8 mim][BF4] and [C 2 OHmim][BF 4]. *J. Phys. Chem. C*, **2011**, *115*, 16116–16123.

[30] Y.-M. Sun. Sorption/desorption properties of water vapour in poly(2-hydroxyethyl methacrylate): 2. Two-stage sorption models. *Polymer (Guildf).*, **1996**, *37*, 3921–3928.

[31] B. Schwarz, M. Schönhoff. Surface Potential Driven Swelling of Polyelectrolyte Multilayers. *Langmuir*, **2002**, *18*, 2964–2966.

[32] M. Tariq, P. J. Carvalho, J. A. P. Coutinho, I. M. Marrucho, J. N. C. Lopes, L. P. N. Rebelo. Viscosity of (C2–C14) 1-alkyl-3-methylimidazolium bis(trifluoromethylsulfonyl)amide ionic liquids in an extended temperature range. *Fluid Phase Equilib.*, **2011**, *301*, 22–32.

[33] T. Batchelor, J. Cunder, A. Y. Fadeev. Wetting study of imidazolium ionic liquids. *J. Colloid Interface Sci.*, **2009**, *330*, 415–20.

Chapter 6 – Understanding the decontamination phenomenon: the influence of polarity

This chapter describes the rationalization of the decontamination process in terms of polarities.

The presented results were published in the peer-reviewed international journal Journal of Solution. Chemistry. DOI: 0.1007/s10953-014-0272-2,(article in press).

Table of contents

6.1. The mechanism of drug capture: an assumption

In Chapter 2 a novel hair decontamination procedure is described for opiate drugs. In the wide range of tested ILs, different behaviours were observed: some of the tested ILs yielded high extraction efficiencies for both analytes while others presented analyte-selectivity. The analytes morphine and 6-monoacetylmorphine, (6-MAM), one of the major metabolites of heroin, were considered as representatives of opiates. Since these drugs have low volatility, they were chosen as model to study the influence of polarity in their capture by the ILs.

The mechanism of drug capture may be assumed to involve three steps: transport of drug molecules to the IL surface, adsorption onto the IL free surface and absorption in the bulk IL. The first step seems to be dependent on the water content of the IL through the contribution of the water vapor to transport the drugs from the hair to the liquid. Since the interaction of the water vapor with the IL was already studied in the previous chapter, here we focus our attention on the two other steps. The adsorption of the drugs was assessed through IL surface tension measurements in presence of the vaporized opiate drugs, under the same conditions as those used in the drug extraction. Absorption of the drugs was rationalized in terms of the IL polarity. However, in the case of ILs, a single polarity parameter is not sufficient because two different ionic liquids with identical polarity can behave quite differently as solvents [1]. Crowhurst et al [2] proposed the set of solvent polarity parameters defined by Kamlet and Taft to explain the interactions of ionic liquids with specific solutes. Other authors [3,4] used these parameters to predict the efficacy of ionic liquids in the lignocellulose treatment. In this work, we look for a correlation between the drug extraction capacity and the ILs polarity characterized by their Kamlet and Taft parameters, reported in the literature.

6.2. Kamlet-Taft polarity parameters

The Kamlet–Taft parameters quantify the hydrogen bond acidity (α), hydrogen bond basicity (β), and polarizability (π*) and may be used to predict the solubility properties of many ionic liquids from data acquired with a limited number. The α values are mainly determined by the nature of the cation, especially the presence of

hydrogen-bond donor groups, while the β values are dominated by the nature of the anion. The polarizability is usually high and varies with both anion and cation. According to Crowhurst et al [2], the ability of ILs to interact with a solute molecule through the formation of hydrogen bonds is controlled by the hydrogen bond acceptor ability of its anion and the hydrogen bond donor ability of its cation. In other words, the stronger the hydrogen bond between anion and cation, then the weaker the hydrogen bond to the solute will be.

Correlations between the efficiency of drug extraction from hair and the water content, surface tension and polarity of the ionic liquids were proposed. The efficiency of the process of drug extraction was found to increase with the IL water content, although different curve shapes were observed for each specific pair IL/drug. The higher the efficiency, the larger was the decrease in the IL surface tension observed during the process of drug extraction. Efficiency was high for ionic liquids of high acidity and low basicity ($[C_2OHmim][BF_4]$) and low for liquids of low acidity and high basicity [Hmim][OAc].

6.3. Results and discussion

6.3.1. Drug extraction results

The efficiency of drug extraction, defined as the ratio between the difference in drug concentration in hair before and after the treatment divided by the drug concentration in the contaminated hair (see Chapter 2):

$$Efficiency\ (\%) = \frac{[contaminated\ hair] - [decontaminated\ hair]}{[contaminated\ hair]} \times 100 \quad (1)$$

is presented in Figure 6.1 for the six tested ILs. The reported efficiencies are average values obtained from three independent experiments. The high values of the standard deviation (SD ≤ 6%) are typical of the contamination processes of hair samples. Although the efficiencies depend on the drug, overall, the most efficient IL is $[C_2OHmim][BF_4]$ while the least efficient is [Hmim][OAc].

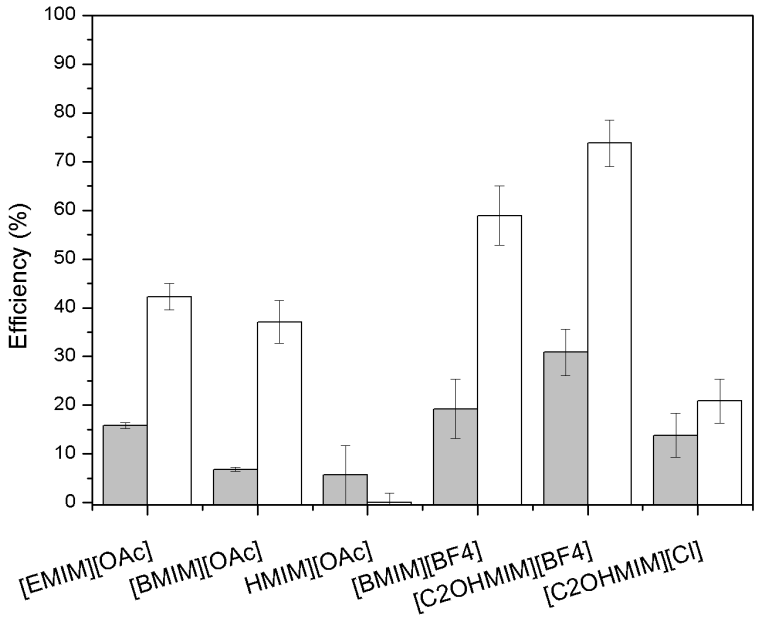

Figure 6.1 - Drug extraction efficiencies of the six ILs tested: 6-MAM (white bars); morphine (grey bars) for 100 ºC, 24 h and dry ILs. The error bars represent the SDs.

6.3.2. Effect of water content

The water content of the ILs is known to have a significant effect on their physical properties, namely, viscosity, density and surface tension. The influence of the IL water content on the extraction efficiency was compared for two ILs with quite different efficiencies: $[C_2OHmim][BF_4]$ and [Hmim][OAc]. The results depicted in Figure 6.2 show that the dependence of the extraction efficiency on the water fraction varies according to the nature of the IL, even for high water contents.

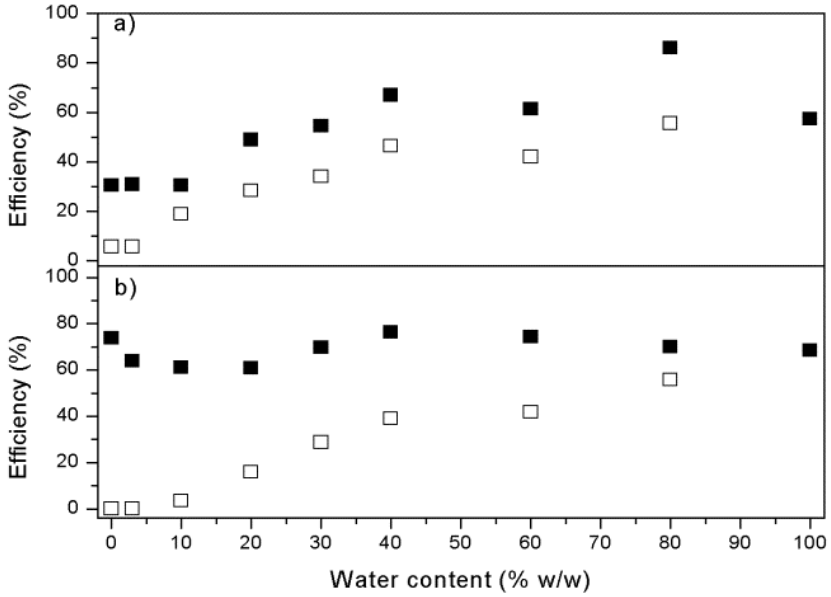

Figure 6.2 - Comparison of extraction efficiencies at different water contents for two ILs: [C2OHmim][BF4] (■), [Hmim] [OAc] (□) and two drugs: a) Morphine; b) 6-MAM; at 100 ºC for 24 h. Error bars are not included for the sake of clarity but efficiency SD ≤ 6%.

The first observation is that the effect of the water is visible only for water content ≥ 10% w/w in all systems. For the less efficient [Hmim][OAc], the efficiencies of 6-MAM and morphine extraction increase almost monotonically with the water content from a very small value characteristic of the IL (water content < 10% w/w) up to the efficiency of pure water, demonstrating that water was the main responsible for the drug extraction. In contrast, the efficiency of morphine extraction by $[C_2OHmim][BF_4]$ increases with the water content up to values above the efficiency of the pure components, while that of 6-MAM remains practically constant. These results may be correlated with the conclusions of a recent molecular dynamics simulation study on the influence of water content upon the structural and diffusion properties of imidazolium-based IL−water mixtures [5]. The authors found that, at low to intermediate water concentrations, the IL behavior is slightly affected by the presence of water, but for high concentrations the system transforms into an IL aqueous solution due to great solvation around the IL cations and anions. This may explain why water has no effect for concentrations < 10 % w/w (x_{water}= 43 % in the case of $[C_2OHmim][BF_4]$).

Thus, the presence of water enhances the extraction efficiency, especially in the case of the less efficient ILs. The following question is to rationalize this dependence: may the water present in the IL act as the means of transport for the drug molecules?

To answer this question, we used a simple distillation setup with pure water in the heating vessel in which the water vapor was forced to pass through highly contaminated hair. The average values of the efficiencies of this extraction obtained from two independent experiments, together with the standard deviations, are 91 ±10 (%) for 6-MAM and 43±4 (%) for morphine.

The results clearly show the ability of the water vapor to solubilize the opiates, which favors the hypothesis of the water contained in the IL contributing to the transport of the molecules during the extraction process. However, the extraction process occurs even in vacuum (see Chapter 2). At this point, it must be stressed that, although the efficiency of the use of pure water is high, ionic liquids have the great advantage of being low volatile. This characteristic allows the use of minute quantities of ILs imbibed in solid support which is not possible with water. Furthermore, the intensive use of water may lead to undesired extraction of drugs from the hair matrix [6], since protic solvents are known to promote the swelling of the hair.

6.3.3. Surface tension behaviour

As previously referred, the amount of IL did not influence the extraction efficiency, which suggests that the IL free surface plays an important role in the process of drug capture.

Adsorption of the drugs was assessed through IL surface tension measurements in presence of the vaporized opiate drugs, under the same conditions as those used in the drug extraction. The surface tension of the pure IL was compared to that of the IL exposed to the vaporized drugs. The surface tension of both samples was monitored along 24 hours at 100 ºC and the difference between the average values obtained during the last 18 hours of the experiment is designated as $\Delta\gamma$ (surface tension of the pure IL – surface tension of the contaminated IL). This time interval was chosen to ensure the stability of the measurements since a long equilibration time was needed (at least 5 hours).

The extraction efficiencies for both drugs are plotted as a function of Δγ for five tested ILs in Figure 6.3. Data for [C_2OHmim][Cl] are missing due to experimental difficulties derived from its very high melting temperature. Although data interpretation has to be made with care due to the high standard deviations of both plotted values, it is possible to identify a clear tendency for a higher efficiency being associated with a higher drop in the value of the surface tension. These results show that the adsorption of the drug molecules on the surface of the liquid drops may be detected whenever the drug extraction efficiency is high enough to allow for a measurable decrease in the surface tension. Thus, adsorption of the target molecules may be considered as the second step of the extraction mechanism.

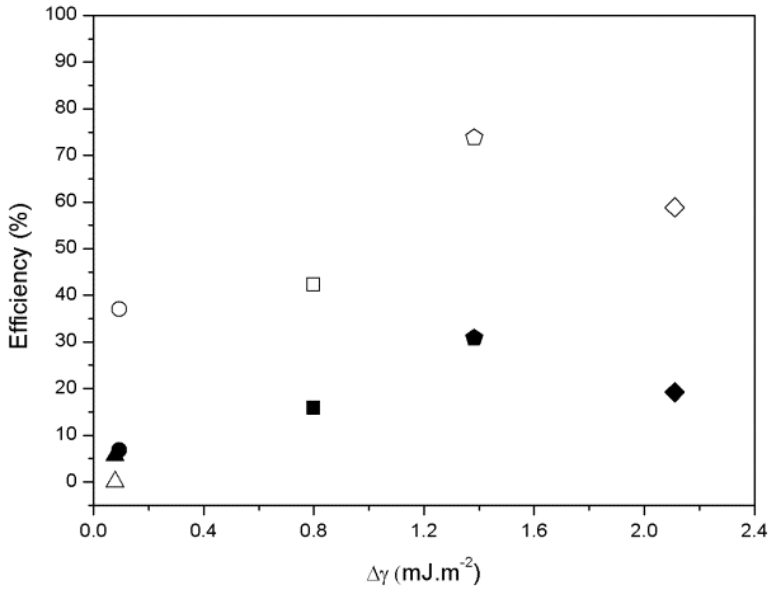

Figure 6.3 - Drug extraction efficiency as a function of Δγ (surface tension of the pure IL –surface tension of the contaminated IL). The open symbols refer to 6-MAM and the closed symbols to morphine. Triangle: [Hmim] [OAc]; Circle: [Bmim] [OAc]; Square: [Emim] [OAc]; Pentagon: [C_2OHmim][BF_4]: Diamond: [Bmim][BF_4]. Error bars are not included for the sake of clarity but efficiency SD ≤ 6%.

6.3.4. Drug–IL interactions correlated with the Kamlet–Taft parameters

The use of Kamlet–Taft approach to interpret the solvent behavior of molecular solvents has long been established. In a recent review, the Kamlet–Taft parameters for

a large set of ILs were collected [7]. According to these authors, there is a great deal of inconsistency among the values presented in different papers. Keeping this in mind, we chose the Kamlet–Taft parameters for the six ILs studied preferentially from the same bibliographic source. The Kamlet–Taft parameters which characterize the hydrogen bond donor capacity (α), the hydrogen bond acceptor capacity (β), and polarizability (π*) are presented in table 6.1.

Table 6.1 - Kamlet–Taft parameters α, β, and π* for the studied ILs.

IL	α	β	π*
[Hmim] [OAc]	-	-	-
[Bmim] [OAc][8]	0.48	1.2	0.96
[Emim] [OAc][8]	0.57	1.06	0.97
[Bmim][BF_4][8]	0.63	0.37	1.05
[C_2OHmim][BF_4][9]	1.05	0.22	1.16
[C_2OHmim][Cl][9]	0.73	0.68	1.16

Although we could not find the Kamlet–Taft parameters for [Hmim][OAc], we may predict that its acidity is the lowest in the acetate based series. In fact, assuming that the α value is only slightly affected by the nature of the anion[2] and considering the sequence of α values for series of ILs based on 1-alkyl-3-methylimidazolium, [$C_n$mim] cations, (eg for: α = 0.705, 0.617 and 0.259 for [Emim] [$(CF_3SO_2)_2N$], [Bmim] [$(CF_3SO_2)_2N$] and [Hmim] [$(CF_3SO_2)_2N$, respectively[10], we may conclude that acidity decreases with the increase in the chain length.

Analysis of the values in table 6.1 shows that the higher hydrogen bond acidity (α), the lower the hydrogen bond basicity (β), with the exception of [C_2OHmim][Cl] which presents both moderately high acidity and basicity. The polarizability (π*) is similar for all the ILs. The three imidazolium ring protons are known to be acidic and it is expected that hydrogen bonding occurs mainly between those protons and the anions. However, the presence of OH in [C_2OHmim] makes it a better hydrogen bond donor cation.

In Figures 6.4 a) and b) the Kamlet–Taft parameters α and β of the studied ILs are plotted together with the extraction efficiency for morphine and 6-MAM, respectively.

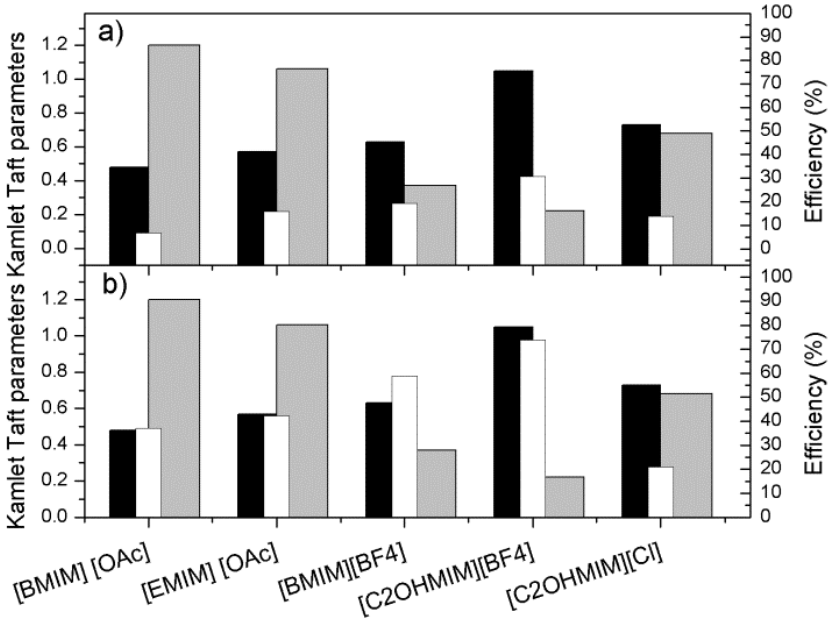

Figure 6.4 - Kamlet–Taft parameters α (black bars) and β (grey bars) and extraction efficiency (white bars) of the studied ILs for morphine a) and 6-MAM b).

According to Crowhurst et al [2], the ability of ILs to form a hydrogen bond with a solute molecule appears to derive from the competition between the interactions cation-anion and cation-solute. Thus, it is expected that the interaction between hydrogen bond donor cation and the solute would be important in the absence of hydrogen bond accepting anions. For ILs with the same cation ([Bmim]) and different anions ([OAc] and $[BF_4]$), when the anion becomes less basic, the hydrogen bond donor ability of the ionic liquid should increase. This is in agreement with the higher efficiency of [Bmim][BF_4] when compared to that of [Bmim][OAc]. [C_2OHmim][BF_4] has the highest acidity and lowest basicity which means that it is able to form strong hydrogen bonding to solutes. In contrast, the behavior of [C_2OHmim][Cl] stands out from the general trend because the strength of the cation-anion, due to relatively high α and β parameters, hinders a significant interaction with the drugs.

The higher extraction efficiency of all ILs for 6-MAM than for morphine may be ascribed to the presence of the acetate group in 6-MAM. In fact, the difference in the

structures between both molecules derives from the substitution of one of the two –OH groups in morphine by one acetate group in 6-MAM. This acetate group is able to coordinate more strongly than the –OH group with hydrogen bond donor cations.

The effect of water content on the drug extraction may also be interpreted in terms of the Kamlet-Taft parameters. The parameters α, β, and π* of water are reported to be 1.02–1.17, 0.14-0.18, and 1.09, respectively. The addition of water to ILs is known to have the highest impact on the β parameter, for example in the case of [Bmim][OAc], it dropped 17% upon the addition of 10 % w/w of water [3]. This means that water addition decreases the basicity of the anions and, in consequence, weakens their interaction with the cations which become more available to interact with the solute.

Absorption of the drug molecules which constitute the last step of the extraction mechanism seems to be determinant since the correlation between the extraction efficiencies and the IL-solute interaction are the most striking.

6.4. Conclusions

In this chapter, the aim of the experiments was to understand the special affinity of specific combinations cation/anion towards morphine and 6-monoacetylmorphine and the ability of a set of imidazolium-based ILs ([Bmim][BF_4], [C_2OHmim][BF_4], [C_2OHmim][Cl], [Emim][OAc], [Bmim][OAc] and [Hmim][OAc]) to extract morphine and 6-MAM from contaminated hair samples, without any morphological change of the hair surface, was demonstrated. Comparison of the drug extraction efficiencies showed that different ILs led to a wide range of values. The most efficient IL was [C_2OHmim][BF_4], while [Hmim][OAc] was the worst. The effect of the IL water content was assessed: the presence of water enhances the extraction efficiency, especially in the case of the less efficient ILs.

An interpretation for the process of drug capture was done in terms of a three-step mechanism: transport of drug molecules, adsorption onto the liquid free surface and absorption in the bulk liquid. The transport of the drug appears to be strongly related with the water content of the IL. Although this transport process occurs even in vacuum, the presence of water vapor facilitates the transfer due to the solubilization of the opiates. Adsorption of the drugs was demonstrated by the surface tension decrease

observed for the most efficient ILs in presence of the vaporized opiate drugs. Absorption of the drugs was rationalized in terms of the IL Kamlet-Taft parameters: ILs with the highest acidity and lowest basicity parameters ([C_2OHmim][BF_4] and [Bmim][BF_4]) are the most efficient in the removal of the drugs from hair. This may be explained by the increased availability of the cation to form hydrogen bonds with the solute when its interaction with the anion is not so strong. Extraction efficiency of all ILs was higher for 6-monoacetylmorphine than that of morphine, probably due to a stronger hydrogen bonding between the cation and the acetate group in 6-MAM.

6.5. Experimental

6.5.1. Reagents and standards

The ILs [Bmim][BF_4], [C_2OHmim][BF_4], [C_2OHmim][Cl], [Emim][OAc], [Bmim][OAc] and [Hmim][OAc], were supplied by Solchemar (Monte da Caparica, Portugal). All ILs had purities above 98% and water contents lower than 1% (checked by Karl Fischer). These ILs are designated as dry ILs. The standards of morphine and 6-monoacetylmorphine (6-MAM), as well as their tri-deuterated analogues, were supplied by Ceriliant (Round Rock, TX, USA), in solution at a concentration of 1 mg/mL. Methanol (HPLC grade), dichloromethane, *n*-hexane, 2-propanol, ammonium hydroxide, hydrochloric acid, and potassium dihydrogenphosphate (analytical grade) were obtained from Merck Co (Darmstadt, Germany). *N*-Methyl-*N*-*(*trimethylsilyl) trifluoroacetamide (MSTFA) and chlorotrimethylsilane (TMSCl) were purchased from Macherey-Nagel (Düren, Germany). Oasis® MCX (3 mL, 60 mg) extraction cartridges were obtained from Waters (Milford, MA, USA). Working solutions of concentrations 1 μg/mL and 10 μg/mL of both morphine and 6-MAM were prepared by proper dilution of the stock solutions with methanol, and these were used for the calibrators. Working solutions of the tri-deuterated analogues (internal standards) of concentration 5μg/mL were prepared also in methanol. All these solutions were stored light-protected between 2 and 8 °C.

6.5.2. Hair contamination and decontamination procedures

The externally contaminated hair samples were produced according with the procedure described in Chapter 2. A more externally contaminated hair sample, SH1, was prepared using 600 mL of an aqueous solution of methanol (15% v/v) containing 10 mg of each standard (morphine and 6-MAM) and 2 g amounts of hair. The SH1 samples were used for the distillation with water. The hair was soaked in this solution for two days at 35 ºC, under stirring. It is important to remark that, according to Cairns et al [11], with this contamination procedure most of the drug remains on the hair surface and in the soaking solution.

The drug content in the hair samples was determined according to the procedures used in the Laboratory of Forensic Toxicology [12]. Both drug content in the hair samples and decontamination procedures were already described in the experimental section of Chapter 2.

The capability of water vapour to dissolve the opiates present in the contaminated hair samples was assessed using a simple distillation setup (Figure 6.5) with c.a. 10 mL of distilled and deionised water to produce the vapour. About 100 mg of the contaminated hair sample was entrapped between two pieces of cotton. The extraction was carried out until the water ran out, and the distillate was collected and analysed according to the previously mentioned procedure [12].

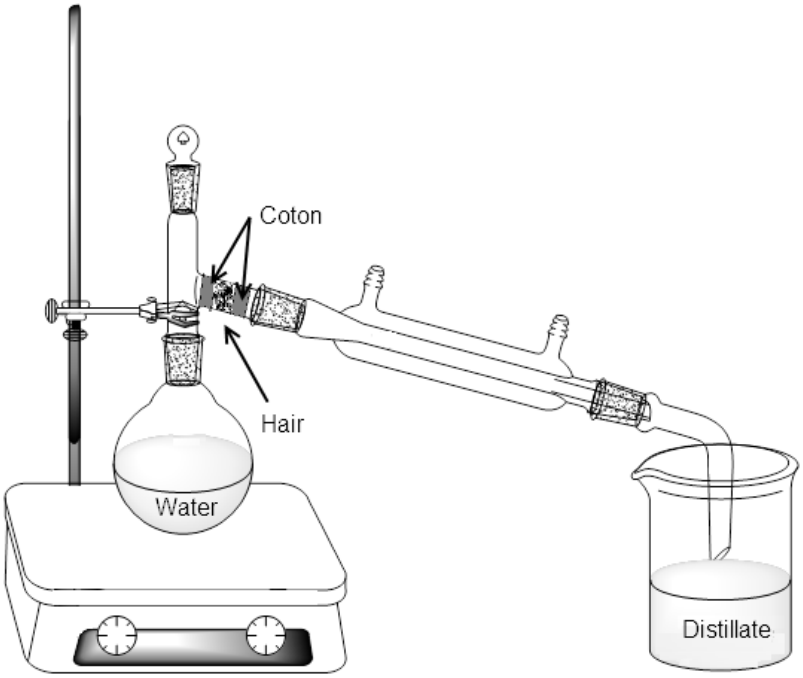

Figure 6.5 -Experimental setup for the water vapour extraction experience

6.5.3. Surface tension measurements

The surface tension measurements were carried out by the pendant drop method, using a Video Camera (jAi CV-A50) mounted on a Wild M3Z microscope to record the drop image. The video signal was transmitted to a frame grabber (Data Translation model DT3155), with the image acquisition and analysis performed on a computer, running the ADSA-P software (Axisymetric Drop Shape Analysis, Applied Surface Thermodynamics Research Associates, Toronto, Canada).

The liquid drop was generated with a gastight syringe (Hamilton) and kept inside a modified ambient chamber (Ramé-Hart) at constant temperature, 100 ± 0.05ºC, during 24 hours, to simulate the drug decontamination conditions. Further details on the apparatus may be found in a previous publication [13]. The ambient chamber was flushed with pure nitrogen. To check the effect of the drug vapor, surface tension measurements were done only in the presence of nitrogen (pure IL) and in the presence of 100 mg of contaminated hair placed inside the ambient chamber

(contaminated IL). The standard deviations (SD) corrected with the Student parameter (95%) ranged from 0.3 to 2.6 $mJ \cdot m^2$.

6.6. References

[1] J. L. Anderson, J. Ding, T. Welton, D. W. Armstrong. Characterizing ionic liquids on the basis of multiple solvation interactions. *J. Am. Chem. Soc.*, **2002**, *124*, 14247–54.

[2] L. Crowhurst, P. R. Mawdsley, J. M. Perez-Arlandis, P. A. Salter, T. Welton. Solvent-solute interactions in ionic liquids. *Phys. Chem. Chem. Phys.*, **2003**, *5*, 2790–2794.

[3] T. V Doherty, M. Mora-Pale, S. E. Foley, R. J. Linhardt, J. S. Dordick. Ionic liquid solvent properties as predictors of lignocellulose pretreatment efficacy. *Green Chem.*, **2010**, *12*, 1967–1975.

[4] A. M. da Costa Lopes, K. G. João, A. R. C. Morais, E. Bogel-Łukasik, R. Bogel-Łukasik. Ionic liquids as a tool for lignocellulosic biomass fractionation. *Sustain. Chem. Process.*, **2013**, *1*, 3.

[5] A. A. Niazi, B. D. Rabideau, A. E. Ismail. Effects of Water Concentration on the Structural and Diffusion Properties of Imidazolium-Based Ionic Liquid–Water Mixtures. *J. Phys. Chem. B*, **2013**, *117*, 1378–1388.

[6] F. Pragst, M. A. Balikova. State of the art in hair analysis for detection of drug and alcohol abuse. *Clin. Chim. Acta.*, **2006**, *370*, 17–49.

[7] P. G. Jessop, D. A. Jessop, D. Fu, L. Phan. Solvatochromic parameters for solvents of interest in green chemistry. *Green Chem.*, **2012**, *14*, 1245–1259.

[8] M. A. Ab Rani, A. Brant, L. Crowhurst, A. Dolan, M. Lui, N. H. Hassan, J. P. Hallett, P. A. Hunt, H. Niedermeyer, J. M. Perez-Arlandis, M. Schrems, T. Welton, R. Wilding. Understanding the polarity of ionic liquids. *Phys. Chem. Chem. Phys.*, **2011**, *13*, 16831–40.

[9] S. Zhang, X. Qi, X. Ma, L. Lu, Q. Zhang, Y. Deng. Investigation of cation–anion interaction in 1-(2-hydroxyethyl)-3-methylimidazolium-based ion pairs by density functional theory calculations and experiments. *J. Phys. Org. Chem.*, **2012**, *25*, 248–257.

[10] T. Welton. Electrodeposition from Ionic Liquids. Edited by Frank Endres, Andrew P. Abbott, and Douglas R. MacFarlane. *Angew. Chemie Int. Ed.*, **2008**, *47*, 4468–4468.

[11] T. Cairns, V. Hill, M. Schaffer, W. Thistle. Removing and identifying drug contamination in the analysis of human hair. *Forensic Sci. Int.*, **2004**, *145*, 97–108.

[12] M. Barroso, M. Dias, D. N. Vieira, M. López-Rivadulla, J. a Queiroz. Simultaneous quantitation of morphine, 6-acetylmorphine, codeine, 6-acetylcodeine and tramadol in hair using mixed-mode solid-phase extraction and gas chromatography-mass spectrometry. *Anal. Bioanal. Chem.*, **2010**, *396*, 3059–69.

[13] J. Restolho, A. P. Serro, J. L. Mata, B. Saramago. Viscosity and Surface Tension of 1-Ethanol-3-methylimidazolium Tetrafluoroborate and 1-Methyl-3-octylimidazolium Tetrafluoroborate over a Wide Temperature Range. *J. Chem. Eng. Data*, **2009**, *54*, 950–955.

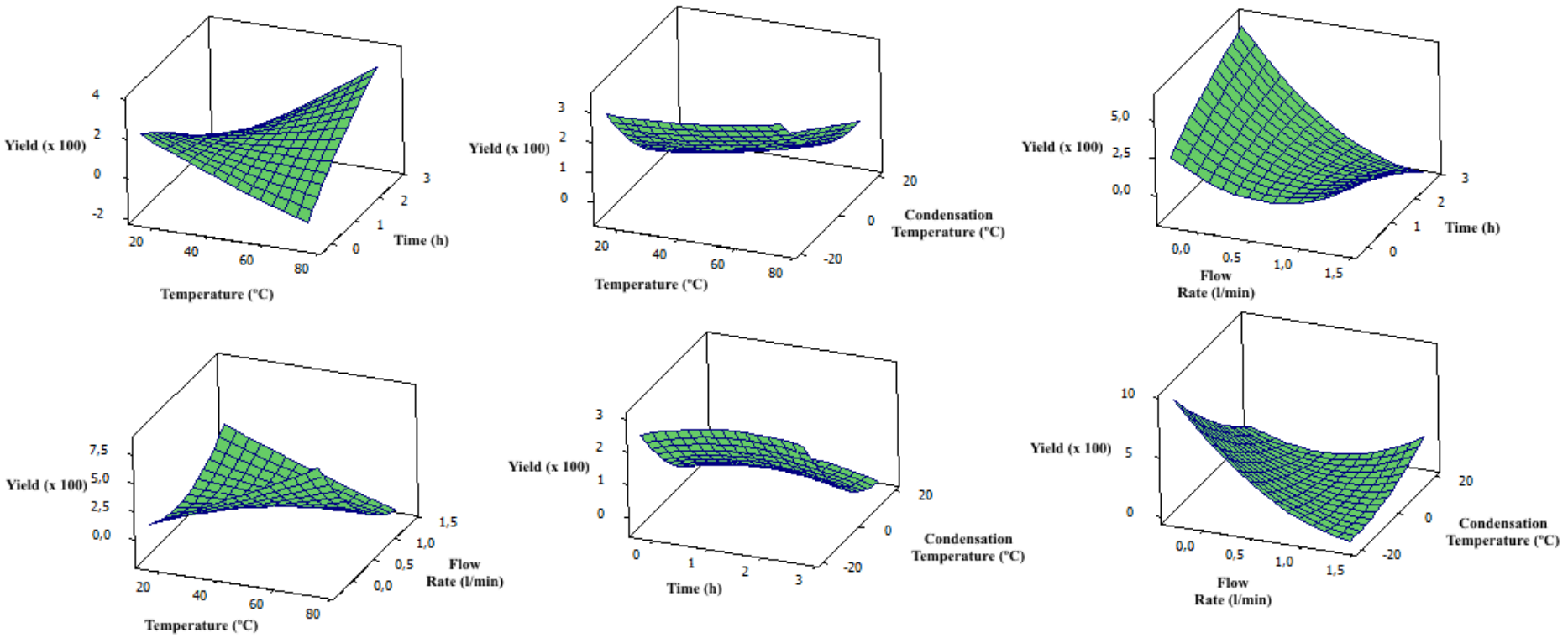

Figure 7.4 - Response surface plot of the predicted response.

An analysis of variance was performed (Table 7.2), and it was possible to conclude that both second order regression and interaction models were statistically significant and no lack-of-fit was observed ($p > 0.05$). The obtained coefficients were then used by the software to apply to the desirability functions (D functions, see eq. 1.1), whose solution predicts mathematically the optimum values for each studied variable. In this specific case, since our goal was to optimize the response (maximizing the extraction yield), the more adequate D function was the maximization function, with an weight of 1 for each variable. The best conditions obtained by the D function are presented in Table 7.3). It is important to remark that these conditions represented desirability (d) of 0.966 (the closer to 1, the better).

Table 7.3 - Optimum conditions predicted by maximizing the desirability function for this system.

Temperature (ºC)	50.00
Flow rate (l/min)	0.15
Time (h)	2.36
Condensation Temperature (ºC)	-10.00

With these conditions and with the proposed extraction method, we have obtained an essential oil with a relative composition of 1,8-Cineole of 96 % (almost pure) and with an extraction yield of 6.11 ± 0.08 % (w/w), which is much higher than that obtained by hydrodistillation (0.18 % w/w) for this compound [1].

7.3.3. Lavender and rosemary

In order to test our method, we decided to apply it to other plants using the previously optimized conditions (previous section): lavender (*Lavandula dentata*) and rosemary (*Rosmarinus officinalis* L.).

In the following tables (Table 7.4 e 7.5) we present a comparison between the composition of oils obtained by hydrodistillation and by our contactless extraction method, for both plants. JOSÉ PÕE TAMBÉM OS CROMATOGRAMAS

Table 7.4 - Comparison between the compositions of lavender essential oil obtained by hydrodistillation and by our contactless extraction method.

			Relative composition (%)	
RT (min)	**Compound**	**Probability (%)**	**Hydrodestillation**	**Contactless**
13.978	α-Pinene	97	0.83	0.00
14.709	3-Trimethylcyclohexene	71	0.05	0.03
16.147	β-Pinene	96	2.74	0.02
16.645	1-Octen-3-ol	82	0.10	0.20
17.087	Myrcene	98	0.99	0.04
17.51	α-Phellandrene	72	0.03	0.05
18.564	β-Phellandrene	91	2.03	0.08
18.755	1.8-Cineole	98	76.65	52.07
19.095	Ocimene	93	0.33	0.21
19.815	γ-Terpinene	91	0.13	0.17
20.122	Linalyl acetate	88	0.26	4.17
21.415	Linalool	89	0.19	0.98
22.717	Pincarveol	87	0.21	1.16
22.873	Camphor	98	1.97	3.62
23.622	Pinocarvone	83	0.18	0.13
23.884	Borneol	94	1.51	14.34
24.33	4-Terpineol	91	0.42	1.14
24.977	α-Terpineol	95	1.64	15.85
25.138	Myrtenal	85	0.20	0.00
48.608	Trans-β-Farnesene	91	2.86	0.00

Table 7.5 - Comparison between the compositions of rosemary essential oil obtained by hydrodistillation and by our contactless extraction method.

			Relative composition (%)	
RT (min)	**Compound**	**Probability (%)**	**Hydrodestillation**	**Contactless**
13.977	α-Pinene	96	0.27	0.76
14.708	Camphene	96	0.26	0.50
16.147	β-Pinene	89	0.06	0.77
16.633	3-Octen-2-ol	91	0.41	1.72
16.869	3-Octanone	96	0.20	0.45
17.085	Myrcene	94	0.15	0.83
17.512	α-Phellandrene	88	0.08	0.91
18.068	α-Terpinene	89	0.07	0.00
18.408	*p*-Cymene	94	0.53	3.60
18.747	1,8-Cineole	97	37.57	0.22
19.095	Trans-Ocimene	82	0.05	2.03
19.815	γ-Terpinene	93	0.15	2.74
20.128	Trans-sabinene hydrate	81	0.05	3.73
20.932	Terpinolene	83	0.10	2.44
21.484	Linalool	94	2.84	20.19
23.027	Camphor	97	31.88	4.17
23.64	Pinocarvone	87	0.28	0.87
23.899	Borneol	97	5.76	1.00
24.146	3-Pinanone	89	0.82	0.00
24.398	4-Terpineol	94	4.42	0.00
25.061	α-Terpineol	94	6.10	0.00
25.848	Verbenone	94	0.98	0.00

The results show that our method leads to different extractions rates of the same compound from different botanicals. The explanation for this phenomenon should lie

in the way through which the compound is bound inside the plant. Even though the extraction is mostly from the aerial parts of the plant, the plants have different mechanisms to avoid their unnecessary evaporation.

Another interesting conclusion regards the method's selectivity. In both plants our method selectively removed the more volatile compounds, leaving the less volatile behind (mostly sesquiterpenes), as expected. Furthermore, the obtained yields for both plants (7.23 ± 0.63 % and 4.28 ± 0.33 %, for lavender and rosemary, respectively) are once more much higher than the values reported in the literature (1.41% and 0.35%, for both lavender and rosemary, respectively [3,4]).

Analyzing now in more detail each plant, we see that in the case of lavender, although the majority of the compounds appear in low percentage, the compounds responsible for the characteristic scent of the plant (in this case linalool, linalyl acetate, camphor and borneol) appear at much higher concentrations. Another interesting fact is the high concentration of α-terpineol, which is quite used in the cosmetic industry.

In the case of rosemary, a behavior similar to that of lavender was observed. Once more, the compounds responsible for the characteristic scent (pinenes, camphor, linalool, etc) were extracted at much higher levels, while the less volatile ones (e.g. verbenone) were not extracted.

7.4. Conclusion

In this chapter, a new essential oil isolation technique was developed. This method is based on the principle of the vapor pressure equilibrium of every compound and it relies only on the extraction temperature and in the presence of a gentle nitrogen flow. *Eucalyptus globulus* was used as a model and the method was optimized by means of experimental design. The optimized method was further applied to other two botanicals: lavender and rosemary. In all cases, when compared to the more commonly used isolation method (hydrodistillation), the extraction yields were always higher for the most representative compounds. Regarding the chemical composition of the obtained essential oils, they were characterized by the higher

concentration of the more volatile compounds, when compared with the ones obtained by hydrodistillation.

We believe that our contactless method might represent a significant breakthrough in terms of essential oils isolation, particularly for the cosmetic industry, where selectivity and yields are of outmost importance. Additionally, our extraction method requires less energy than hydrodistillation.

7.5. Experimental

7.5.1. Plants

The leafs of *Eucalyptus globulus*, *Lavandula dentata* and *Rosmarinus officinalis* were freshly harvested and allowed to dry at room temperature for two weeks in the absence of light.

7.5.2. Essential oil isolation by hydrodistillation

The dried leafs were submitted to hydrodistillation for 3 h using a Clevenger type apparatus (Figure 7.5), according to the European Pharmacopoeia [5]. Briefly, the plant was immersed in water and heated to boiling, after which the essential oil was evaporated together with the water and collected in the condenser. The essential oil was dissolved in dichloromethane and injected in the GC-MS.

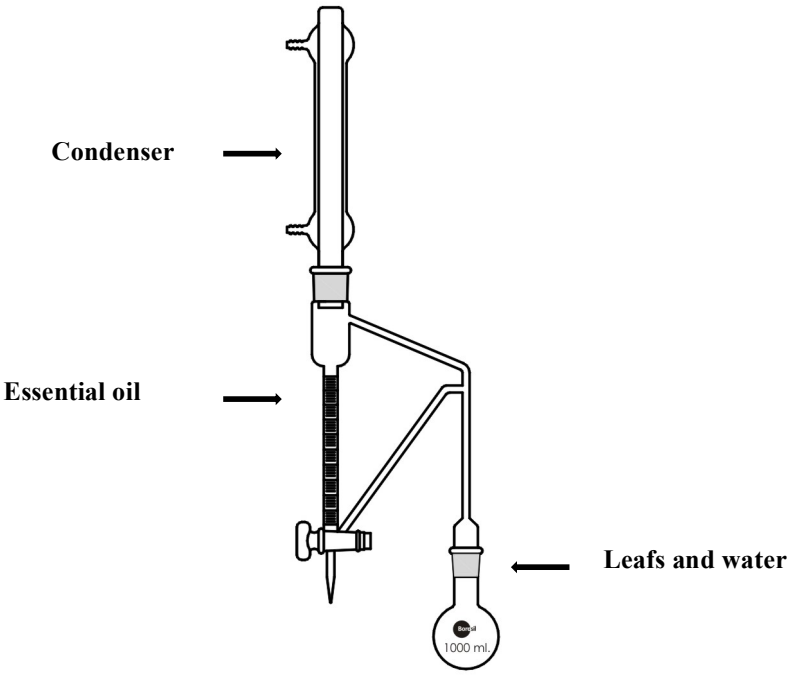

Figure 7.5 - Schematic representation of a Clevenger type apparatus.

7.5.3. Essential oil isolation by contactless extraction

For the extraction of the essential oils by the contactless technique, 4 g of grinded leafs were placed inside the custom glass reactor (Figure 7.6). Leafs were maintained at constant temperature (through circulation of a thermostatic fluid) and the nitrogen was forced to pass through the leafs and afterwards it was cooled down, in order to promote the condensation of the essential oil. The nitrogen flow was monitored by a flowmeter from Omega Engineering (Connecticut USA). Afterwards, the essential oil was dissolved in dichloromethane and injected in the GC-MS.

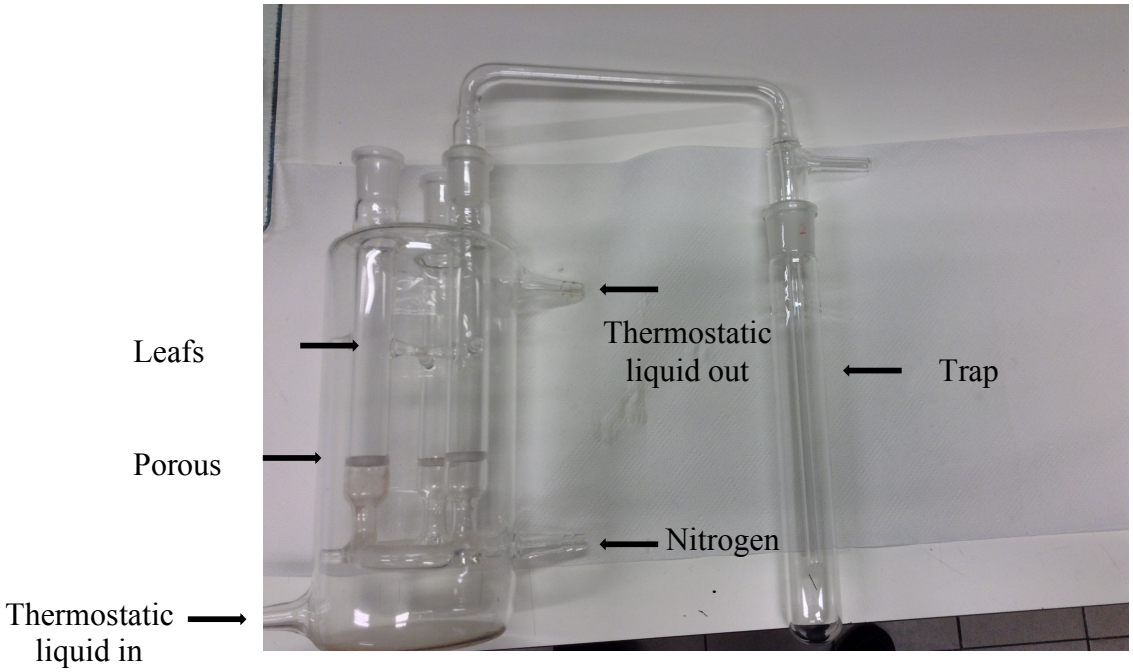

Figure 7.6 – Custom glass reactor used for the contactless extraction of essential oils.

7.5.4. Chromatographic conditions

Chromatographic analysis was performed using a Shimadzu GC2010 gas chromatograph (Shimadzu, Kyoto, Japan), equipped with a model GCMS-QP2010S mass-selective detector (Shimadzu, Kyoto, Japan). A capillary column (30 m×0.25 mm I.D., 0.25 μm film thickness) with 5% phenylmethylsiloxane (TRB-5MS), supplied by Teknokroma (Barcelona, Spain), was used. Chromatographic conditions were as follows: initial oven temperature was 40 °C for 10 min, which was increased by 5 °C min^{-1} to 100 °C, held for 10 min, followed by an increase of 10 °C min^{-1} until 250 ºC and held for 5 min. The temperatures of the injection port and detector were set at 250 and 280 °C, respectively. The split injection mode was used (split ratio of 1:5), and helium with a flow rate of 1.36 mL min^{-1} was used as the carrier gas. The mass spectrometer was operated with a filament current of 300 μA and electron energy of 70 eV in the electron ionization (EI) mode.

7.6. References

[1] A. Song, Y. Wang, Y. Liu. Study on the chemical constituents of the essential oil of the leaves of Eucalyptus globulus Labill from China. *Asian J. Tradic. Med.*, **2009**, *4*, 134–140.

[2] D. C. Montgomery. *Design and Analysis of Experiments*, John Whiley & Sons, Inc, New York, **2001**.

[3] R. A. Mothana, M. S. Alsaid, S. S. Hasoon, N. M. Al-mosaiyb, A. J. Al-rehaily, M. A. Al-yahya. Antimicrobial and antioxidant activities and gas chromatography mass spectrometry (GC / MS) analysis of the essential oils of Ajuga bracteosa Wall . ex Benth . and Lavandula dentata L . growing wild in Yemen. *J. Med. Plants Res.*, **2012**, *6*, 3066–3071.

[4] M. Lo Presti, S. Ragusa, A. Trozzi, P. Dugo, F. Visinoni, A. Fazio, G. Dugo, L. Mondello. A comparison between different techniques for the isolation of rosemary essential oil. *J. Sep. Sci.*, **2005**, *28*, 273–80.

[5] C. of Europe. *European Pharmacopoeia*, Strasbourg, **2014**.

Chapter 7 – Natural compounds extraction: a contactless approach

This chapter describes the development of a contactless method for the extraction of natural essential oils.

Table of Contents

7.1. *Eucalyptus Globulus*: a model for process development

Eucalyptus globulus is a fast-growing species from the family of *Myrtaceae.* Although this tree is native from Australia, it is widely distributed across Portugal. Its essential oil is composed mainly by oxygenated monoterpenes [1,8-cineole (72.71 %), α-terpineol (2.54 %), terpinen-4-ol (0.34 %), and linalool (0.24 %)], monoterpenes [α-pinene (9.22 %), and β-pinene (0.4 %)] and oxygenated sesquiterpenes [α-eudesmol (0.39 %), (-)-globulol (2.77 %), and epiglobulol (0.44 %)] [1]. The major presence of volatile compounds in this essential oil (e.g. 1,8-cineole), as well as its availability, makes it an excellent candidate to be used as a model plant for the development of a new procedure for the extraction of its essential oil .

7.2. Contactless process for extracting essential oils: hypothesis

It is generally accepted that, at a certain temperature and pressure, the equilibrium between the solid phase and the vapor phase is reached. This equilibrium (dynamic) means that the number of molecules in the vapor phase is constant, as long as this system remains undisturbed. When an external force removes the molecules from the vapor phase, more molecules are needed in order to re-establish the equilibrium, and this is the physical explanation of sublimation. On the other hand, in the previous chapters (see chapters 2 to 7) it was proven that it is actually possible to remove compounds (either volatile or non-volatile; water vapor is needed to solubilize the latter) from a solid substrate simply by increasing their vapor pressure (this is achieved by increasing temperature). It is important to remark that this behavior is well explained by thermodynamics. When the temperature increases, the vapor pressure of all compounds will also increase, though the increase rate is higher for the more volatile compounds. Bearing those considerations in mind, the following question may arise:

> *Would it be possible to continuously remove molecules from the vapor phase directly from a solid substrate (e.g. plant leafs), to condense them and to collect the condensate?*

Although this idea seems trivial, the fact is that we didn't find any published material on this matter. Therefore, the aim of this part of the work was to develop a contactless extraction procedure (Figure 7.1) for natural essential oils, using *Eucalyptus globulus* leafs as a model. Since it is expected that only the more volatile compounds are extracted, it might be an interesting approach for the extraction of natural volatile compounds to be used in the cosmetic industry.

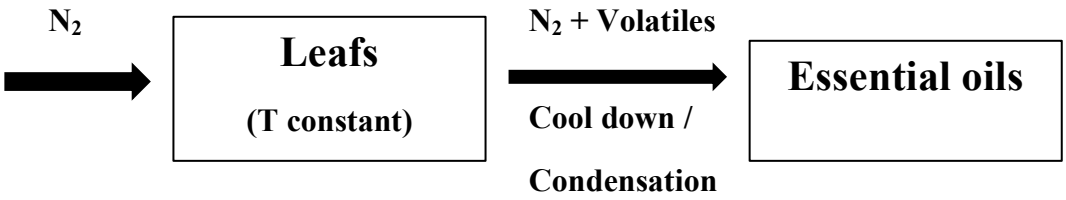

Figure 7.1 - Schematic representation of the contactless extraction method

7.3. Results and discussion

7.3.1. *Eucalyptus globulus* essential oil characterization

In order to enable the evaluation of the new extraction method, the chemical composition of the essential oil, obtained from eucalyptus leaves by hydrodistillation, was studied (Figure 7.2 and Table 7.1):

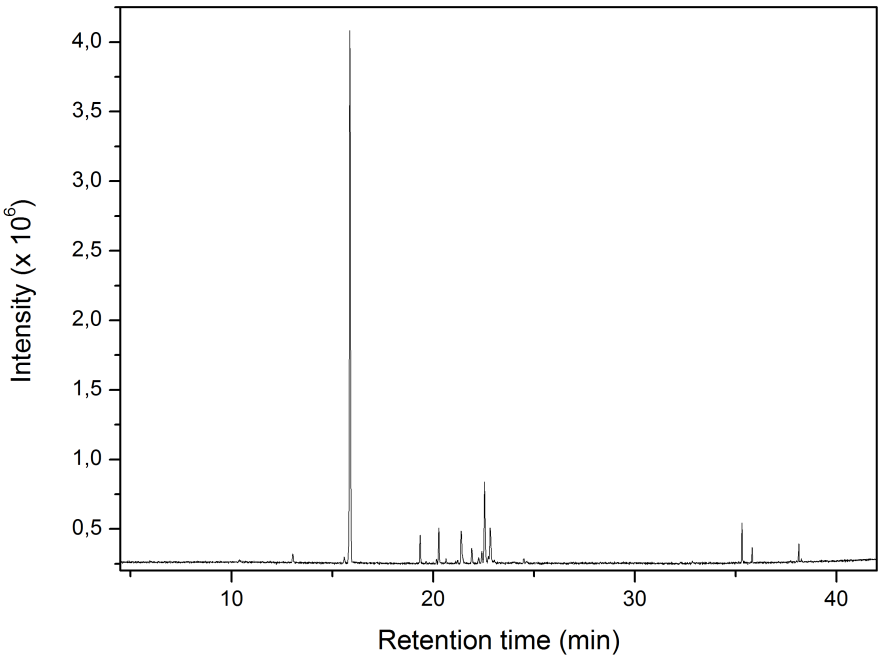

Figure 7.2 - Eucalyptus essential oil GC-MS chromatogram.

Table 7.1 - Compound identification of the eucalyptus essential oil, obtained by hydrodistillation.

Retention time (RT, min)	Compound	Probability (%)	Relative content (%)
16.07	1,8-Cineole	94	68.00
21.97	Terpen-4-ol	87	0.41
22.09	α-Terpineol	89	1.78

From the obtained results, we were only able to identify the major constituents of the essential oil, which are 1,8-cineole, terpen-4-ol and α-terpineol, as expected.

From this starting point, the proposed technique was applied, using a working temperature of 40 ºC (to promote the increase of the vapor pressure of the compounds and to facilitate their extraction from leafs' cells) and a nitrogen flow of 0.100 L/min. In Figure 7.3 it is depicted the chromatogram of the essential oil obtained with the proposed method.

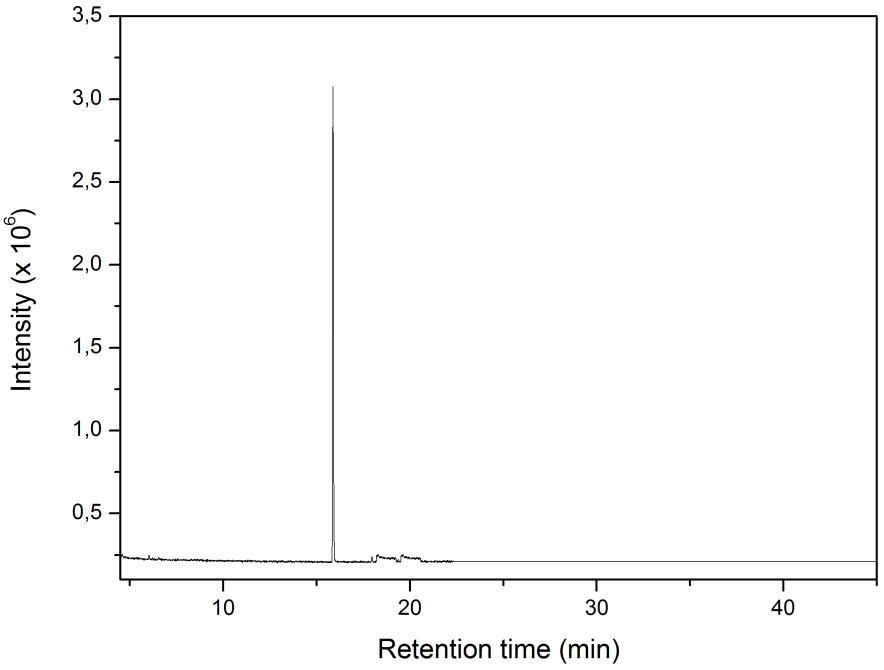

Figure 7.3 – Chromatogram of the eucalyptus essential oil obtained by the contactless extraction method (η = 1.9 % (w/w)).

From the analysis of the previous figure, it becomes clear that the proposed method seems to enable the selective extraction of the more volatile compounds (in this case only 1,8-cineole). Although the proof of concept was achieved, further optimization was deemed necessary.

7.3.2. Contactless essential extraction method optimization

Once more, design of experiment appeared as the best tool for process optimization. The use of a factorial screening was discarded in this situation, because high dispersion on the responses (extraction yield) was expected. Therefore, the response surface method would overcome more efficiently this problem, through using an higher number of replicates (six)at the center point. In this case a central composite design (CCD) was used, and four variables were studied: extraction and condensation temperatures, extraction time and nitrogen flow rate (Figure 7.4).

During the application of CCD, a regression model was fitted to the results. This model was considered suitable, for it could explain 96 % of all response variations (R^2 = 0.96) [2] . Except for the extraction time, all studied variables were considered as statistically significant, as well as the majority of their interactions ($p < 0.05$ for a confidence level of 95 %; Table 7.2).

Table 7.2 - Analysis of results for the applied model, obtained using the central composite design (R^2 = 0.96).

Term	**Coef**	**SE Coef**	**P**
Constant	0.77	0.19	0.00
Temperature	0.27	0.13	0.08
Flow rate	-1.02	0.13	0.00
Time	0.03	0.11	0.79
Condensation T	-0.73	0.10	0.00
Temperature*Temperature	0.04	0.12	0.75
Flow rate*Flow rate	0.46	0.12	0.00
Time*Time	-0.08	0.09	0.40
Condensation T*Condensation T	0.18	0.09	0.07
Temperature*flow rate	-0.78	0.13	0.00
Temperature*Time	0.52	0.13	0.00
Temperature*Condensation T	0.06	0.14	0.67
Flow rate*Time	-0.48	0.13	0.00
Flow rate*Condensation T	0.69	0.14	0.00
Time*Condensation T	-0.04	0.14	0.78
Source		**F**	**P**
Regression		18.71	0.00
Linear		28.25	0.00
Square		5.09	0.02
Interaction		12.92	0.00
Lack-of-Fit		0.24	0.94

Chapter 8 – Conclusions

This chapter summarizes the conclusions of the presented work.

In this thesis, the main aim was the development of new extraction methods of volatile compounds, applied to both forensic toxicology and natural aromas. The novelty of the proposed methods is the possibility of extraction without any physical contact with the samples.

Concerning the application in the field of forensic toxicology, the problematic of external contamination of hair samples by drugs (mainly smoked drugs) was addressed. Ionic liquids allowed us to develop a contactless method to remove the contamination from the surface of the hair without any physical contact. The process was developed for both opiates and cannabinoids. Unfortunately, its application to cocaine was not successful and we were not able to envisage the reason for this failure. Although the developed method is more time consuming, it can be carried out overnight and allows the simultaneous decontamination of many samples as the ones that can fit inside the a modified GC oven (possibly more than 100). This way we promote the increase of sample throughput in the lab.

The efficiency of this decontamination process was found to vary substantially among the large range of tested ionic liquids. In order to further understand the special affinity of specific combinations cation/anion towards the opiate drugs, other studies were performed. A three-step mechanism was proposed to rationalize the decontamination process: transport of drug molecules, adsorption onto the liquid free surface and absorption in the bulk liquid. The transport of the drug appears to be strongly related with the water content of the IL, while adsorption of the drugs was demonstrated by the surface tension decrease. Absorption of the drugs in the IL bulk was found to be correlated with the Kamlet-Taft parameters: liquids with the highest acidity and the lowest basicity are the most efficient due to the increased availability of the cation to form hydrogen bonds with the solute.

To better understand the role of water on the decontamination process, an investigation on the mechanism of water absorption on thin films of ILs deposited on quartz crystal sensors was done. For the most viscous ILs, the decrease in viscosity was the dominant effect, while for the others, the mass loading effect predominated. The water diffusion coefficients in some of those IL films were much smaller than the bulk values showing the effect of liquid confinement.

In the case of the essential oils extraction, the new method is based on the principle of the vapor pressure equilibrium of the different compounds present in the plant leafs. The developed method relies on the increase of the vapor pressure through a mild increase in temperature and the use of a dragging nitrogen flow. This method was applied to eucalyptus, lavender and rosemary. In these cases, it was demonstrated the capability to selectively extract the more volatile compounds. Furthermore, comparing the results with those obtained by the most commonly used extraction method (hydrodistillation), we conclude that our method achieves always higher yields.

Although two new technologies were successfully developed, there is always much more to do. In the future, the work must be focused in the development of new applications, such as the detection of exposure to harmful compounds (in the hair) or the search of new application for our contactless extraction of essential oils.

Appendix

Table A. 1 Name, abbreviation and structure of the ILs used in this work.

Name	Abbreviation	Structure
Aliquat® 336 (Sigma Aldrich)	-	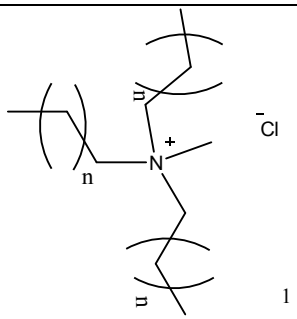 [1]
Cyphos IL 101 (Cytec)	P(66614)Cl	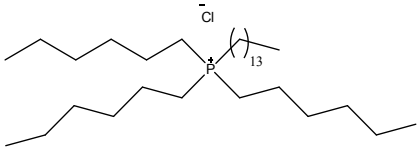
1-Ethyl-3-methylimidazolium ethylsulphate (Solchemar)	[EMIM][$EtSO_4$]	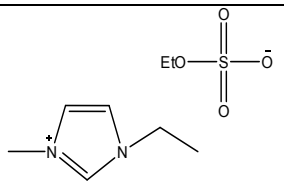
1-Butyl-3-methylimidazolium tetrafluoroborate (Solchemar)	[BMIM][BF_4]	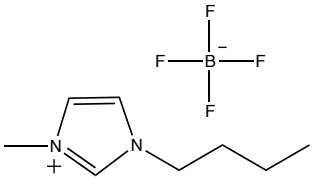
1-Butyl-3-methylimidazolium dicyanamide (*)	[BMIM][DCA]	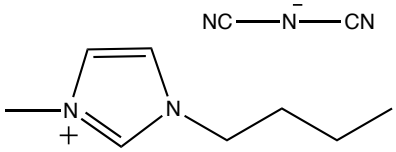
1-Butyl-3-methylimidazolium thiocyanate (*)	[BMIM][SCN]	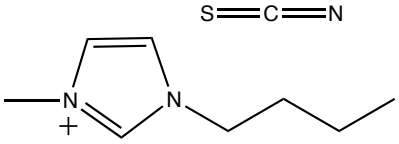

[1] n = 7, 8 and 10. Aliquat® is composed of a mixture of these three compounds, being the n=7 the major one.

1-Butyl-3-methylimidazolium trifluoroacetate (*)	[BMIM][TFA]	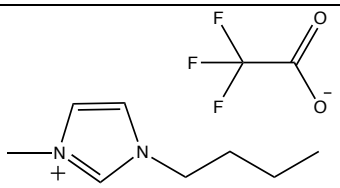
1-Octyl-3-methylimidazolium tetrafluoroborate (Solchemar)	[OMIM][BF_4]	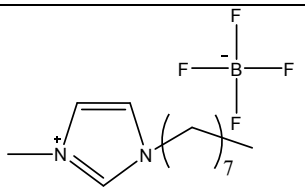
1-Octyl-3-methylimidazolium hexafluorophosphate (*)	[OMIM][PF_6]	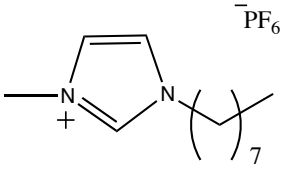
1-Octyl-3-methylimidazolium thiocyanate (*)	[OMIM][SCN]	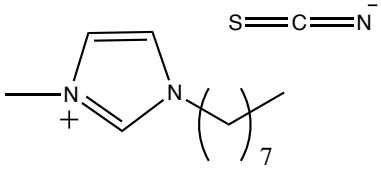
1-Ethanol-3-methylimidazolium bis(trifluoromethanosulphonyl)imide (*)	[C_2OHMIM] [NTf_2]	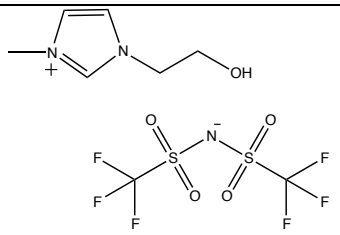
1-Ethanol-3-methylimidazolium tetrafluoroborate (Solchemar)	[C_2OHMIM] [BF_4]	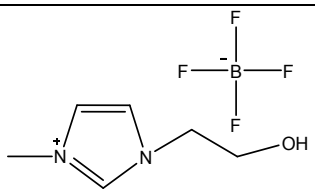
1-Ethyl-3-methylpyridinium ethylsulphate (Solchemar)	[EMPy] [$EtSO_4$]	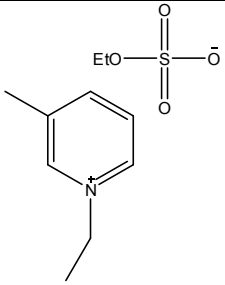

1-Allylpyridinium hexafluorophosphate (*)	[AlPy][PF_6]	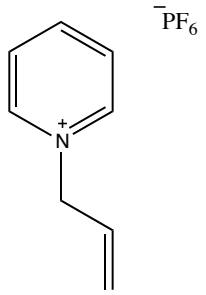
1-octyl-3-methylimidazolium chloride (*)	[OMIM] [Cl]	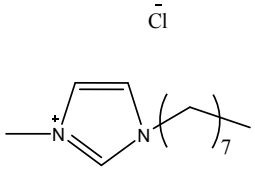
1-ethanol-3-methylimidazolium chloride (*)	[C_2OHMIM] [Cl]	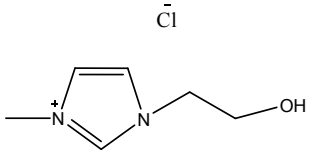
Bis(dihexyl)dimethylguanidinum chloride (*)	[dHDMG][Cl]	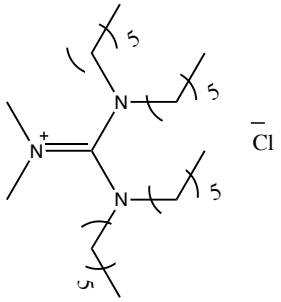
Bis(dihexyl)dimethylguanidinum tosylate (*)	[dHDMG] [OTs]	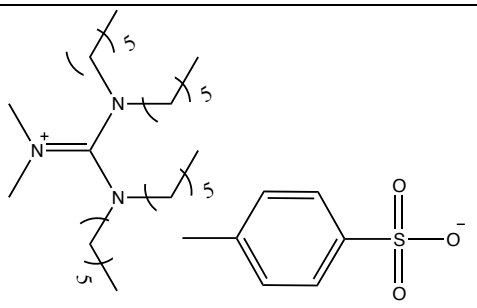
1-decyl-3-methylimidazolium chloride (*)	[C_{10}MIM][Cl]	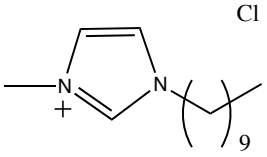

1-decyl-3-methylimidazolium bromide (*)	$[C_{10}MIM][Br]$	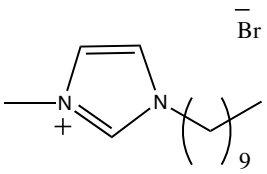
1-decyl-3-methylimidazolium tetrafluoroborate (*)	$[C_{10}MIM]$ $[BF_4]$	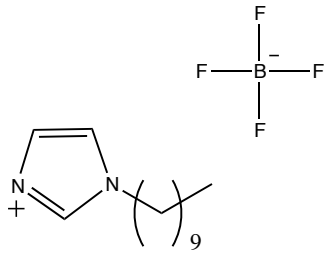
1-decyl-3-methylimidazolium bis(trifluoromethanosulphonyl)imide (*)	$[C_{10}MIM]$ $[NTf_2]$	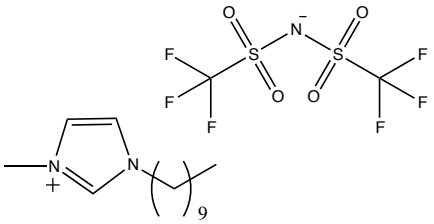
1-decyl-3-methylimidazolium triflate (*)	$[C_{10}MIM]$ [OTf]	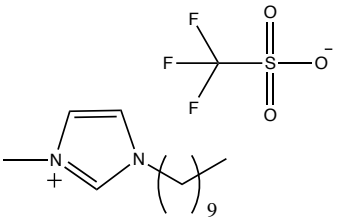
1-decyl-3-methylimidazolium tosylate	$[C_{10}MIM]$ [OTs]	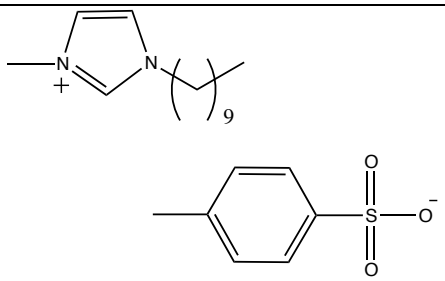
Choline chloride (*)	[Ch][Cl]	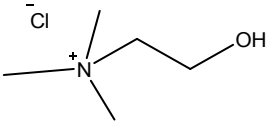
Choline acetate (*)	[Ch][OAc]	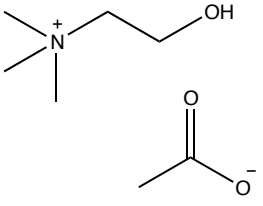

Choline H-maleate	[Ch][H-Mal]	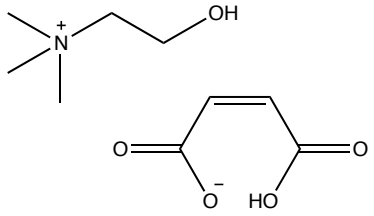
Bis(dimethyl)dibutylguanidinium dicyanamide (*)	[$TMGC_4$] [DCA]	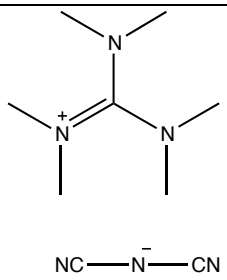
Bis(dimethyl)dibutylguanidinium bis(trifluoromethanosulphonyl)imide (*)	[$TMGC_4$] [NTf_2]	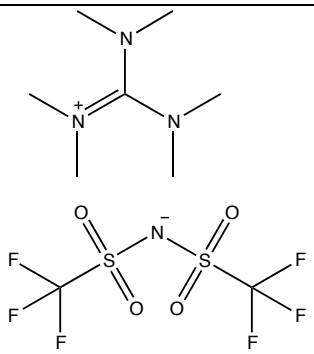
1-Butyl-3-methylimidazolium acetate (*)	[BMIM] [OAc]	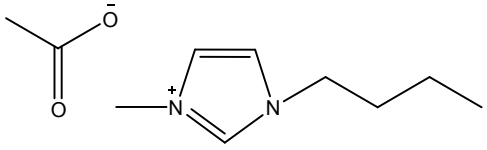
Bis(dihexyl)dimethylguanidinium acetate (*)	[dHDMG] [OAc]	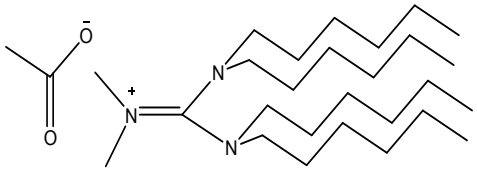
Bis(dihexyl)dimethylguanidinium dicyanamide (*)	[dHDMG] [DCA]	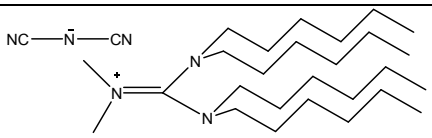

Bis(dimethyl)didodecylguanidinium bis(trifluoromethanosulphonyl)imide (*)	[$TMGC_{12}$] [NTf_2]	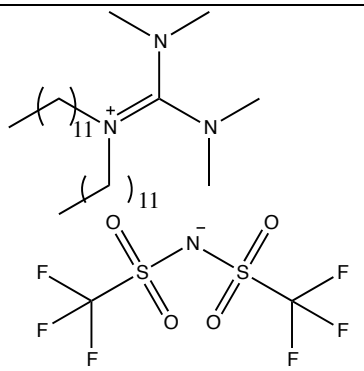
1-Methyl-3-benzylimidazolium chloride (*)	[BzMIM] [Cl]	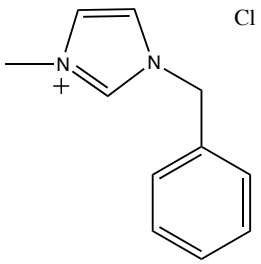
1,3-Dibenzylimidazolium triflate (*)	[Bz_2IM] [OTf]	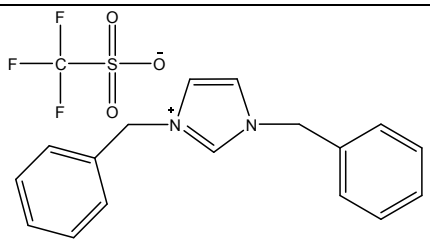
Phenyltrimethylammonium triflate (*)	[PhTMA] [OTf]	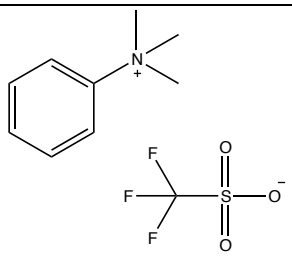
Phenyltrimethylammonium dicyanamide (*)	[PhTMA] [DCA]	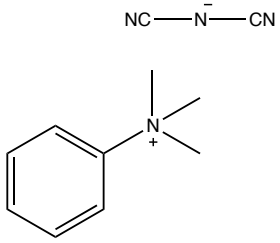

Phenyltrimethylammonium tosylate (*)	[PhTMA] [OTs]	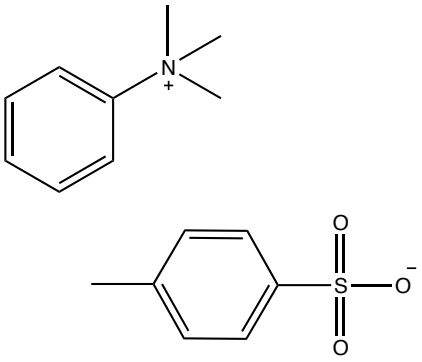
Phenyltrimethylammonium thiocyanate (*)	[PhTMA] [SCN]	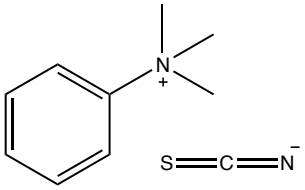
Phenyltrimethylammonium trifluoroacetate (*)	[PhTMA] [TFA]	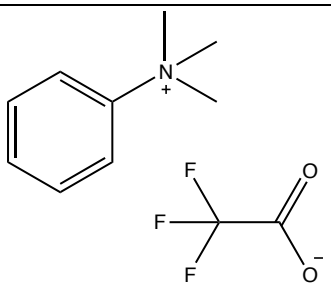
Benzyltriethylammonium thiocyanate (*)	[BzTEA] [SCN]	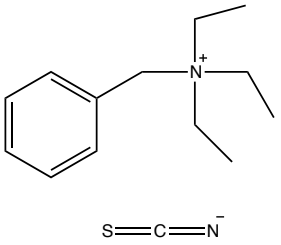
Benzyltriethylammonium dicyanamide (*)	[BzTEA] [DCA]	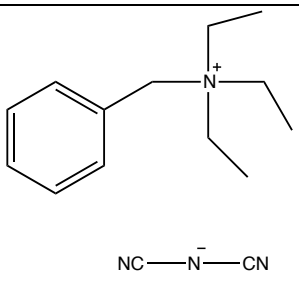

Benzyltriethylammonium triflate (*)	[BzTEA] [OTf]	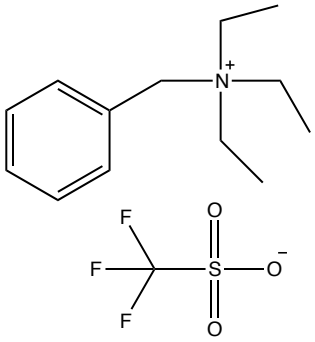
Benzyltriethylammonium saccharin (*)	[BzTEA] [SAC]	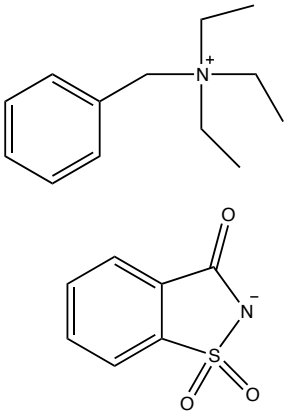
Benzyltriethylammonium trifluoroacetate (*)	[BzTEA] [TFA]	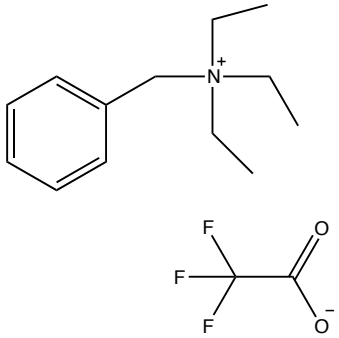
Benzyltriethylammonium tosylate (*)	[BzTEA] [OTs]	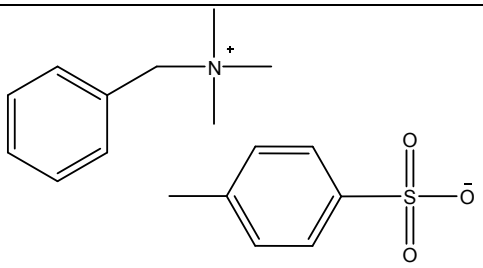
1-Benzyl-3-methylimidazolium saccharin (*)	[BzMIM] [SAC]	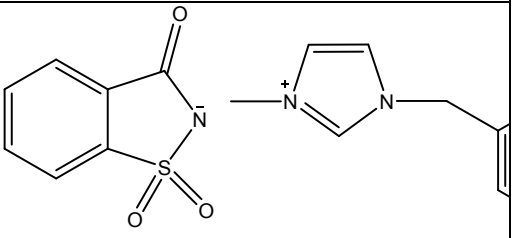

Trihexyl(tetradecyl)phosphonium dicyanamide (*)	[P(66614)] [DCA]